ABSTRACT

DUDUIT, JAMES ROBERT. Coordinated Transcriptional Regulation of the Carotenoid Biosynthesis Pathway Genes Contributes to Fruit Lycopene Content in High-Lycopene Tomato Cultigens. (Under the direction of Dr. Wusheng Liu).

Lycopene content in tomato fruit is largely under genetic control and varies greatly among genotypes. Little is known about the molecular mechanisms regulating fruit lycopene content in high-lycopene tomatoes. In the present study, 42 potential high-lycopene tomato cultigens with different genetic backgrounds were collected worldwide. High performance liquid chromatography (HPLC) analysis was used to quantify fruit carotenoid (lycopene, phytofluene, prolycopene, and beta-carotene) contents at four fruit developmental stages (i.e., breaker, orange, pink, and ripe) of each cultigen. Real-time RT-PCR was used to quantify the relative expression levels of all the 25 pathway genes individually at the breaker and ripe stages. In these cultigens, we found *i*) a general trend of strong expression of upstream genes prior to lycopene biosynthesis and weak expression of most downstream genes at both stages; *ii*) significant higher expression in 7 upstream genes and 8 downstream genes at the breaker or both stages than in the negative control cultigen Moneymaker; and *iii*) significant higher phytofluene, lycopene and beta-carotene contents during fruit ripening than in Moneymaker. Thus, coordinated transcriptional regulation of the pathway genes contributed to significantly higher metabolic flux flow into the pathway in these cultigens than in Moneymaker, leading to higher fruit lycopene content. This was the first systematic investigation of the role of the complete carotenoid biosynthesis pathway genes in fruit lycopene content across many high-lycopene cultigens, which will enable tomato breeding and gene editing for improved fruit lycopene content.

Coordinated Transcriptional Regulation of the Carotenoid Biosynthesis Pathway Genes Contributes to Fruit Lycopene Content in High-Lycopene Tomato Cultigens

by
James Robert Duduit

A thesis submitted to the Graduate Faculty of
North Carolina State University
in partial fulfillment of the
requirements for the degree of
Master of Science

Horticultural Science

Raleigh, North Carolina
2020

APPROVED BY:

_____	_____
Dr. Wusheng Liu Committee Chair	Dr. Penelope Perkins-Veazie

_____
Dr. Thomas Ranney

BIOGRAPHY

Plants have been one of my main interests and passions in life since I was young. I was heavily involved with boy scouts which gave me the beginning tools and knowledge to better understand and explore my local environment. This included learning about which plants are important to humans and what features they have; that kickstarted my interest in hiking and foraging which furthered my dedication to learning about plants. My passion and goal in life is to continue studying and developing knowledge of plants which humans use for health and well-being by focusing on molecular mechanisms that can be improved or better understood for more efficient exploitation.

Through my main master's project and time in this department I have been able to develop skills and gain experiences in critical molecular biology, communication, and problem-solving skills. My main project has been focused on the gene expression analysis of the carotenoid biosynthetic pathway genes in high lycopene tomato breeding lines. This lycopene project has been a large-scale project with 42 pototential high-lycopene cultigens where 6 fruit growth stages were collected. Breaker and Ripe Red fruit maturity stages are the main focus of this project where biological replicates were tested for all 25 carotenoid biosynthetic genes, upstream and downstream of lycopene, with 3 carotenoid products' concentration determined via HPLC to correlate gene expression with metabolite production. I have also been working on a secondary project to overexpress a potential *Ralstonia solanacearum* bacterial wilt resistance gene in tomatoes. Through these projects I have gained the ability to work on and better communicate techniques such as real-time RT-PCR, cloning, HPLC, tissue culture, and plant transformation.

DEDICATION

To my parents, grandparents, and wife who have helped and supported me throughout my entire education. And to Dr. Tom Kozel who helped and pushed me beyond my own boundaries.

ACKNOWLEDGMENTS

The authors thank the USDA National Institute of Food and Agriculture Hatch project 02685, North Carolina State University for the startup funds, and the North Carolina Tomato Growth Association funds to the Liu laboratory. The authors also thank Jack Lotito for growing the tomato plants in the Kannapolis greenhouse, and Liwei Gao, Xianlian Chen, Yonghui Wu, and Kaitlin Duduit for assistance with tomato sample collection. We also thank Dr. Branko Lovic at United Genetics for providing Lycobol, Lycomech, and Nemacrimson; Alicia Suits at Sakata for providing Amai; Dr. Chunxiao Jiang at HM Clause for providing CXD277 and HM9905; Richard Blakey at Paramount Seeds and Dr. Massimiliano Beretta at ISI Sementi for providing Sevance; Francesco Pacini at Akira Seeds for providing AK-TC 035; M. Ballardini at Esasem for providing Crispino F1, Crispino Plum, and Kalvert F1; Dr. Rich Ozminkowski at KraftHeinz for providing H1311, H1657, H7204, H9997, and H1175; Randy Cummings at Johnny's for providing Valentine F1; and Drs. Tong Geon Lee and Samuel Hutton at University of Florida for providing Tasti-Lee, Fla. 7907B and Fla. 8059.

TABLE OF CONTENTS

LIST OF TABLES

LIST OF FIGURES

Introduction

Tomato (*Solanum lycopersicum* L.) is the most economically important horticultural commodity crop in the U.S., and the second only to potato in dietary consumption worldwide (FAOSTAT, 2020; Foolad et al., 2008). Tomato fruit is rich in vitamins A and C, fiber, essential minerals, and carotenoids that are the colorless and colored (yellow, orange, red, etc.) secondary metabolites (Burton-Freeman and Sesso, 2014; Rao and Rao, 2007). Lycopene is the primary carotenoid that gives tomato fruit a red color at the ripe stage (Yoo et al., 2017). Lycopene functions primarily as a photoprotective compound in tomato fruit to protect cells from UV damage since it is the most significant quencher of singlet oxygen produced by UV lights (Mascio et al., 1989; Islamian et al., 2015). Lycopene also functions as a dietary antioxidant for human health, which can reduce risk of diabetes, cardiovascular diseases, and cancer (Burton-Freeman and Sesso, 2014; Rao and Rao, 2007). The red color of lycopene is one of the most significant factors when customers select desirable fresh tomatoes for consumption (Oltman et al., 2014). Thus, 85% of the lycopene consumed in the American diet comes from tomato fruit (Rao and Agarwal, 1999), while the remaining lycopene consumption may come from many fruits and vegetables such as watermelon, papaya, autumn olive, pink grapefruit, pink guava, etc.

Lycopene begins to accumulate at the breaker stage and reaches maximal content at the ripe stage in tomato fruit. Fruit lycopene content is largely genetically controlled and varies among tomato genotypes (Ilahy et al., 2018). Lycopene is an intermediate metabolite in the carotenoid biosynthesis pathway which occurs in plastids. The carotenoid biosynthesis pathway uses the isopentenyl diphosphate (IPP) from the methylerythritol 4-phosphate (MEP) pathway to make phytofluene and then lycopene, while lycopene is the substrate to make other carotenoids including beta-carotene, lutein and neoxanthin (Cazzonelli et al., 2010; Namitha et al., 2011;

Walter et al., 2011; Figure 1). Most of these biosynthesis genes are single copied and a few are multiple copied (Gallagher et al., 2004; Ronen et al., 2000; Walter et al., 2011). Starting from the breaker stage, expression of most of the biosynthesis genes upstream and downstream of lycopene biosynthesis is naturally increased and dramatically decreased, respectively, leading to the significant increase in lycopene content in the fruit of many low-lycopene tomato cultigens and two high-lycopene tomato cultigens (Ailsa Craig and Red Setter) (Table 1; Fantini et al., 2013; Isaacson et al., 2002; Namitha et al., 2011; Pandurangaiah et al., 2016; Ronen et al., 1999; 2000; Stigliani et al., 2011; Yuan et al., 2015). For example, geranylgeranyl pyrophosphate synthase 1 (*GGPPS1*) was found to be downregulated at all fruit maturity stages but *GGPPS2* and *GGPPS3* were upregulated across all fruit maturity stages in low-lycopene tomato cultigen MP1 (Zhou et al., 2020). The phytoene synthase 1 (*PSY1*), phytoene desaturase (*PDS*), and ζ-carotene desaturase (*ZDS*) genes had been shown to be highly expressed at the breaker stage, which decreased at the ripe stage in Ailsa Craig, Moneymaker, Arka Ahuti, IIHR-249-1, IIHR-2866, VF36, and Red Setter (Bramley, 2002; Fantini et al., 2013; Fraser et al., 1999; Namitha et al., 2011; Pandurangaiah et al., 2016; Pecker et al., 1996; Stigliani et al., 2011). *PSY2* became downregulated after the fruit entered into the breaker stage in Ailsa Craig (Fraser et al., 1999; Bramley, 2002), but was slightly upregulated at ripe stage in Red Setter (Stigliani et al., 2011). In Moneymaker and Alisa Craig, *PSY3* had a low expression at all fruit stages, ζ-carotene isomerase (*Z-ISO*) had high expression at the breaker stage that lowered at the ripe stage, and *ZDS*, carotenoid isomerase (*CrtISO*), *CrtISO-like 1* (*CrtISO-L1*) and *CrtISO-L2* had high expression at the breaker and ripe stages (Fantini et al., 2013). In contrast, the downstream genes ε-lycopene cyclase (*ε-LCY*), *β-LCY2*, *CYP97A29*, *CYP97C11*, *β*-carotene hydroxylase 1 (*BCH1*), *BCH2*, zeaxanthin epoxidase (*ZEP*), violaxanthin desaturase (*VDE*), and neoxanthin synthase (*NSY*) had

low expression at the breaker and ripe stages in Red Setter (Stigliani et al., 2011) and Arka Ahuti (Namitha et al., 2011), and *β-LCY1* had low expression at the breaker and ripe stages in VF36 and Red Setter (Pecker et al., 1996; Stigliani et al., 2011).

Since tomato's original domestication in Latin America and Mesoamerica, conventional tomato breeding efforts have largely focused on agronomic traits such as fruit size, increased shelf-life, and disease resistance rather than red fruit color pigmentation which decreased in content as domestication progressed (Bai et al., 2007; Razifard et al., 2020). Several spontaneous mutations in the carotenoid biosynthesis pathway (*yellow-flesh*, *tangerine*, *delta*, *old-gold*, and *old-gold-crimson*, *beta*, and *hp-3*) have been identified, which impact tomato fruit lycopene content (for review, Liu et al., 2015). The *yellow-flesh* and *tangerine* mutants have loss-of-function mutations in *PSY1* (Cazzonelli et al., 2010; Kachanovsky et al., 2012; Yoo et al., 2017) and *CrtISO* (Isaacson et al., 2002; Kachanovsky et al., 2012; Yoo et al., 2017), respectively, while the *delta* and *beta* mutants overexpressed *ε-LCY* (Ronen et al., 1999) and *β-LCY2* (Ronen et al., 2000), respectively. Each of these four mutants caused decreased fruit lycopene content. Conversely, *old-gold* / *old-gold-crimson* and *high pigment (hp)-3* are mutations in the carotenoid enzymatic *β-LCY2* (Ronen et al., 2000) and *ZEP* (Galpaz et al., 2007) genes, respectively, leading to increased lycopene content in tomato fruit. These *og* and *hp* mutations have been used in conventional breeding for the generation and release of high-lycopene cultigens across a wide range of genetic backgrounds worldwide (Ilahy et al., 2018; Table 1). The fruit lycopene content in these cultigens varies from 22.7 µg/g fresh weight (FW) (cultigen Fla. 47; Djidonou et al., 2016) to 303.8 µg/g FW (cultigen Ha-3518; Armendariz et al., 2006). The variation in fruit lycopene content among tomato genotypes suggests the existence of genetic factors at play that affect the difference in fruit lycopene content, as demonstrated in molecular breeding using

genetic engineering and genome editing (Li et al., 2018; McQuinn et al., 2018; Rothan et al., 2018; Zsogon et al., 2018). According to Carli et al. (2011) and Foolad (2007), most of the high-lycopene tomato cultigens suffer from adverse pleiotropic effects of the mutated genes such as slow germination and seedling growth, high seedling mortality, low leaf coverage, brittle stems, low yield, low soluble solids content, high susceptibility to various plant pathogens, and premature defoliation. The sum of these negative effects prohibits the widespread commercial employment of these varieties. However, Ilahy et al. (2018) found that mixing the *hp-1* or *hp-2* mutations with non-mutant backgrounds might decrease the negative effects of the *hp* mutations in some high-lycopene tomato cultigens such as HLY13 and HLY18, which are grown commercially. To our best knowledge, these high-lycopene cultigens had never been subject to transcriptional analysis of the carotenoid biosynthesis pathway genes, and little is known about the underlying mechanisms regulating fruit lycopene content in these high-lycopene cultigens.

In the present study, 42 potential high-lycopene tomato cultigens with distinct genetic backgrounds were obtained from many international tomato breeding companies and comparatively assayed. Real-time RT-PCR was used to determine the relative gene expression levels of the 25 carotenoid biosynthetic pathway genes and high-performance liquid chromatography (HPLC) was used to determine the fruit contents of lycopene, phytofluene, and β-carotene. The objectives of this study were to systematically investigate the expression patterns of the complete carotenoid biosynthesis pathway genes at different developmental stages of tomato fruit and the chromoplast size and number per cell, and link the differential gene expression patterns and the variation of chromoplast size and number per cell to the fruit lycopene content. This large-scale analysis of high-lycopene tomato cultigens can enable the

identification of the key pathway genes and the variations in chromoplast size and number affecting fruit lycopene content.

Materials and Methods

Plant materials and growth conditions

Seeds of 42 potential high-lycopene tomato cultigens were obtained globally (Table 1). The wild tomato relative *S. pimpinellifolium* L. (LA2093) was used as a positive control while the cultigens Moneymaker and NC 1Y (Gardner, 2000) were used as the negative controls representing a low-lycopene and non-red tomato line, respectively. The wild tomato produces fruit with a bright red color and contains many interesting and desirable traits that have been lost in domesticated tomatoes (Sharma et al., 2008). Moneymaker has wild-type alleles for *hp-2^{j}*/*hp-2^{j}*. The tomato cultigen NC 1Y has the *tangerine* mutation in the encoding region of *CrtISO* and produces a significant amount of prolycopene at the expense of lycopene synthesis (Isaacson et al., 2002; Panthee et al., 2013).

All seeds were germinated in flat trays and grown in 3-G pots at 22-27°C in a plastic house located at the Plants for Human Health in Kannapolis, NC from September 2018 to February 2019. Natural light was supplemented with Greenpower LED toplighting units (Phillips; Amsterdam, Netherlands) which provided an extra six hours of light per day with photon flux of 520 μmol/s. Three pots, each containing two plants per cultigen, were placed in a randomized complete block design throughout the greenhouse. Tomato fruits were collected from each replicate of each cultigen at four fruit ripeness stages based on the USDA Visual Aid TM-L-1 (1975). These stages consisted of 1) breaker (the beginning of yellow-orange in color covering no more than 10%), 2) orange (orange in color covering 30-60%), 3) pink (pink to red

in color covering 60-90%), and 4) ripe (red in color covering 90-100%). Complete pericarp tissues, roughly 4 × 4 cm, were excised from each of the collected tomato fruit samples using clean scalpel. Half of the collected pericarp tissues (including fruit skin and pericarp tissues) was flash frozen using liquid nitrogen, ground to fine powder using a sterile mortar and pestle and stored at -80°C for RNA extraction. The other half of the collected pericarp tissue was not ground and was immediately placed in -80°C freezer for carotenoid quantification.

RNA extraction and cDNA synthesis

RNA was extracted from 100 mg of the frozen powder of each fruit sample and purified using the Total Plant RNA Kit (Sigma; Burlington, MS, USA) and the On-Column DNase I treatment (Sigma; Burlington, MS, USA) according to manufacturer's instructions. Concentration and purity of each RNA sample were confirmed via Nanodrop ND-1000 spectrophotometer (Thermo Fisher; Wilmington, DE, USA) and 1% agarose gel electrophoresis. RNA was used for cDNA synthesis only if A260/A280 ratio was within the 1.9 – 2.1 range (indicating lack of contaminates) and 2 distinct bands representing 28S and 18S rRNA were shown on agarose gel with minimal streaking (indicating lack of degradation). First strand cDNA was synthesized from 1 µg of purified RNA using the High Capacity cDNA Reverse Transcription Kit (Applied Biosystems; Foster City, CA, USA) according to manufacturer's instructions. The synthesized cDNA was stored at -80°C.

Sequence analysis and primer design

The carotenoid biosynthesis pathway genes plus two internal control (reference) genes *Expressed* (accession number: Solyc07g025390.2.1) and *CAC* (accession number: Solyc08g006960.2.1)

(Exposito-Rodriguez et al., 2008; Gonzalez-Aguilera et al., 2016) were included in the present study (Tables S1; S2). The selection of the two internal control genes was based on their high reference stability and function together when assaying tomato fruit tissues (Exposito-Rodriguez et al., 2008; Gonzalez-Aguilera et al., 2016). The protein sequence of each gene was obtained from Genbank and used as the query sequence to search against the tomato whole genome sequence in the Phytozome database (v12.1; https://phytozome.igi.doe.gov/pz/portal.html) using BLASTN. The deduced protein sequences of all the returned homologs of each gene were used for protein sequence alignment using ClustalX 2.0 (http://www.clustal.org/). After the homologous sequences that obviously lacked sequence homology were removed, the remaining homologous sequences of each gene were used for cDNA sequence alignment by using their cDNA (including 5'- and 3'-UTR) sequences (Fig. S1). The single nucleotide polymorphisms (SNPs) present in the cDNA alignment of each gene with its homologs were used for gene-specific primer design for each gene. Two forward and two reverse primers were designed close to each other so that they formed 4 primer pairs for each of the 27 genes (Tables S1; S2 and Figs. S2-S13). Each primer was 20 – 23 bp in length with 45-50% GC content while the PCR amplicons were 85 – 125 bp in length (including the length of the two primers) if possible (Tables S1; S2).

Optimization of Real-time RT-PCR conditions

Optimization of Real-time RT-PCR conditions included optimization of primer annealing temperature, optimization of primer concentration, and identification of the optimal cDNA concentration range for each primer pair of each gene. The goal was to identify the optimal primer pair, primer annealing temperature, primer concentration and cDNA concentration range

so that $R^2 \geq 0.99$ and Efficiency (E) = 100 ~ 105% could be achieved for the standard cDNA concentration curve with a logarithmic scale (Table S2). The best primer pair with $R^2 \geq 0.99$ and E = 100 ~ 105% for each gene served as the prerequisite for using the $2^{-\Delta Ct}$ and $2^{-\Delta\Delta Ct}$ method (Dorak, 2007; Livak and Schmittgen, 2001; Vandesompele et al., 2002) for data analysis.

Real-time RT-PCR

The relative transcript abundance of each gene was quantified by Real-time RT-PCR using the optimized Real-time RT-PCR conditions for the best primer pair (Tables S1; S2) and *Expressed* and *CAC* as the two internal control genes. Real-time RT-PCR was performed with three technical replicates on clear plastic 96-well plates with optical film (Bio-Rad; Hercules, CA, USA) on a CFX96 Touch Real-Time PCR Detection System (Bio-Rad; Hercules, CA, USA). Each 10 μL reaction volume consisted of 5 μL SYBR Master Mix (#4344463, Thermo Fisher; Waltham, MA, USA), 0.25 – 0.35 μL of forward and reverse primers (10 μM), 1 μL of diluted cDNA, and nuclease-free water. The PCR product was amplified with the best primer pair for each gene at an initial 95°C for 2 minutes, then 39 cycles of 95°C for 5 seconds and 59°C for 30 seconds. Biological replicates were performed in triplicate and their Ct values were averaged. Data analysis for relative expression level of each gene was conducted with the $2^{-\Delta Ct}$ method where the mean Ct value of each gene of interest (GOI) was subtracted from the geometric mean of the two internal control genes: $\Delta Ct = Ct_{GOI} - Ct_{Control}$ where the geometric mean of the control genes was used as $Ct_{Control}$ (Dorak, 2007; Vandesompele et al., 2002). The $2^{-\Delta\Delta Ct}$ method was used for comparative analysis of relative gene expression of each GOI in a cultigen with Moneymaker being used as the negative control: $\Delta\Delta Ct = \Delta Ct_{GOI} - \Delta Ct_{Control}$ (Dorak, 2007; Livak and Schmittgen, 2001; Vandesompele et al., 2002).

HPLC for lycopene quantification

Pericarp samples stored at -80°C were allowed to thaw at room temperature and then pureed with a genogrinder (SPEX; Metuchen, NJ, USA). The purees were assayed for total soluble solids content (SSC) and acid content using digital refractometers (i.e., Pocket Pal and D5 Acid meter. Atago; Bellevue, WA, USA). Total lycopene was assayed using the method of Davis et al. (2003) and an UltraLab Color Scan Pro (Hunter Associates Laboratory; Reston, VA, USA). Carotenoids (i.e., trans-lycopene, beta-carotene, and phytofluene) was extracted using hexane:ethanol:acetone at a ratio of 2:1:1 following the method of Fish et al. (2002). Specifically, purees of red (0.3 g) and pink, orange, and breaker stages (0.6 g) were added to individual 40 mL amber vials. This was followed by the addition of 5 mL of 95% ethanol and vortex for 1 minute, 10 mL of HPLC-grade hexane and vortex for 20 seconds, and 5 mL of acetone and mixing by hand. In a room equipped with orange fluorescent light to eliminate UV light, all vials were capped and sonicated for 20 minutes, shaken by hand half-way through, and then placed back on the shaker at 200 rpm for 15 minutes. After the addition of 4 mL of double distilled water, all vials were shaken well by hand, and then placed back on the shaker for another 5 minutes. Samples were allowed to sit for 15 minutes, and if layer separation did not occur, the vials were cooled at -20°C for 5 minutes until separation occurred.

Five mL of the top organic layer of each sample was transferred to a 10 mL amber vial. Samples were dried under nitrogen for roughly 30 minutes until completely dry, and then stored at -80°C. Samples were thawed at room temperature for 1 hour, followed by the addition of 1 mL of tetrahydrofuran (THF) containing 250 ppM butylated hydroxytoluene (BHT), and 1 mL of HPLC-grade methanol in order to completely dissolve residue in the vials. Samples were mixed by shaking carefully by hand for at least 10 times so as not to get solvent on the caps. One mL

sample was pipetted and rolled down the side of each vial to ensure all residues were dislodged and dissolved before filtering. One mL of top organic layer from each vial was filtered through a 0.2 μM PTFE filter into HPLC vials, packed with N2 and stored at -80°C until all samples had been prepared for HPLC analysis.

Extracts (40 μL) were injected onto a HPLC (Elite; Hitachi High Technologies; Dallas, TX, USA) equipped with a diode array detector (DAD) and carotenoid C_{30} 4.6 × 250-mm column (YMC America; Allentown, PA, USA), controlled temperature auto sampler, and column compartment (35°C). Carotenoids were detected at wavelengths of 345 and 470 nm. The mobile phase consisted of 0.05% triethylamine (TEA) with 50 mM ammonium acetate in methanol (A), 0.05% TEA in 2-propanol (B), and 0.05% TEA with 250 mg/L BHT in THF (C) with a constant flow rate of 1 mL/.min using a step gradient of 0 min, 90% A, 10% B; 24 min, 54% A, 35% B, 11% C; 35 min, 30% A, 35% B, 35% C; and 43–58 min, 90% A, 10% B. Calibration curves were determined using external standards of trans-lycopene, α-carotene, β-carotene, lutein, and zeaxanthin (CaroteNature; Ostermundigen, Munsingen, Switzerland) to identify and quantify carotenoids in samples. The D-2000 software (Hitachi; Kokubunji, Tokoyo, Japan) was used as the system run controller.

Statistical Analysis

Statistical analyses of HPLC, RT-PCR, and chromoplast data were performed via a two-tailed student's t-test with two-sample unequal variance.

Results

Quantification of fruit carotenoid contents at different fruit ripening stages

In order to understand how fruit phytofluene, lycopene, and beta-carotene contents changed during the progression of fruit ripening, tomato fruits were harvested from the 42 potential high-lycopene tomato cultigens, the positive control wild tomato (LA2093) and two negative control cultigens Moneymaker and NC 1Y at the fruit developmental stages of breaker, orange, pink, and ripe, and fruit contents of the three carotenoids were quantified in pericarp tissues using HPLC. These cultigens showed various fruit sizes and shapes at the ripe stage with highly similar bright red color as the wild tomato and Moneymaker but very different from NC 1Y which showed an orange color due to the *tangerine* mutation in the *CrtISO* gene (Figure 2).

Fruit lycopene content relatively steadily increased from the breaker stage to the ripe stage in all of the tomato cultigens (Figure 3). At the breaker stage, only 21 cultigens had any detectable levels of fruit lycopene, ranging from 0.5 μg/g Fresh Weight (FW) in 'Sevance' to 12.07 μg/g FW in 'Lycobol', and an average of 3.48 μg/g FW in all of the 42 cultigens that was significantly higher than that in the negative control Moneymaker (1.84 μg/g lycopene FW; $p < 0.05$). Fruit lycopene content varied from 8.91 μg/g FW in HLY13 to 54.4 μg/g FW in HLY18 at the orange stage, and from 33.57 μg/g FW in SVTD3418 to 121.11 μg/g FW in Lyco 2 at the pink stage. The average lycopene contents were 27.94 and 59.82 μg/g FW in all the 42 cultigens at the orange and pink stages, respectively, which were significantly higher than that in Moneymaker (10.52 and 28.72 μg/g FW, respectively; $p < 0.05$). All of the cultigens produced the maximal amounts of fruit lycopene at the ripe stage except Lyco2 and NC 1Y (0.59 μg/g FW) which reached their maximal levels at the pink stage. At the ripe stage, the highest fruit lycopene content came from the wild tomato, which was 261 μg/g FW, followed by ISI12152 at

168 μg/g FW and HLY18 at 154 μg/g FW, while the least was from LA4026 which was 49 μg/g FW and comparable to that in Moneymaker (47.33 μg/g FW) (Figure 3). We found that the fruit lycopene content in 23 out of the 42 cultigens at the ripe stage was at least two times higher that in Moneymaker, while the remaining 19 cultigens had less than 2 times fruit lycopene content than Moneymaker. The average fruit lycopene content was 96.9 μg/g FW in the 42 cultigens at the ripe stage, which were significantly higher than that in Moneymaker ($p < 0.05$). In addition, the average increase in lycopene content from breaker to orange stages was 11.4-fold, from orange to pink stages was 2.2-fold, and from pink to ripe stages was 1.6-fold.

Unlike lycopene, fruit beta-carotene contents remained relatively constant in many of the cultigens across different fruit developmental stages with the exception of NC 1Y which did not produce beta-carotene in fruits (Figure 4). At the breaker stage, fruit beta-carotene contents ranged from 0.58 μg/g FW in Sevance to 10.78 μg/g FW in Crispino Plum with an average of 2.98 μg/g FW in all the 42 cultigens. Then, fruit beta-carotene contents varied from 0.82 μg/g FW in NC 4Grape to 10.14 μg/g FW in Crispino Plum at the orange stage with an average of 3.60 μg/g FW, from 1.09 μg/g FW in SVTD3418 to 11.58 μg/g FW in HLY18 at the pink stage with an average of 4.63 μg/g FW, and from 0.7 μg/g FW in H7204 to 18.3 μg/g FW in HLY18 at the ripe stage with an average of 4.99 μg/g FW. The average beta-carotene contents in all the 42 cultigens at the orange and ripe stages were significantly higher than that in Moneymaker (i.e., 0.90 and 2.92 μg/g FW, respectively; $p < 0.05$). The average increase in beta-carotene contents from breaker to orange stages was 1.2-fold, from orange to pink stages was 1.4-fold, and from pink to ripe stage was 1.1-fold. Generally speaking, fruit beta-carotene contents were about 8-10 times less than the lycopene contents in almost every cultigen at the ripe stage. Interestingly,

HLY18 produced the highest fruit beta-carotene content and the 3rd highest lycopene content (Figure 4).

Similar to fruit lycopene contents, we observed a gradual increase in fruit phytofluene contents in most cultigens across fruit ripening process even though phytofluene was undetectable in all the cultigens at the breaker stage (Figure 5). Fruit phytofluene contents ranged from 0.04 μg/g FW in Crispino Plum to 0.7 μg/g FW in H9997 at the orange stage, from 0.08 μg/g FW in Amai to 2.55 μg/g FW in Nemacrimson at the pink stage, and from 0.6 μg/g FW in Simba F1 to 6.07 μg/g FW in HM9905 at the ripe stage. The average contents in all the 42 cultigens were 0.33, 1.44, and 2.32 μg/g FW at the three stages, which at the pink and ripe stages were significantly higher than that in Moneymaker (0.65, and 1.07 μg/g FW, respectively; $p < 0.05$) but significantly lower than that in NC 1Y (2.94, and 5.02 μg/g FW at the pink and ripe stages, respectively; $p < 0.05$). The average increase in phytofluene contents from orange to pink was 4.0-fold and from pink to ripe was 1.8-fold. We noticed that fruit phytofluene contents at the ripe stage were almost half of beta-carotene contents in almost every cultigen, and the two highest phytofluene contents came from the HM9905 and wild tomato, which produced the 8th highest and the highest lycopene contents, respectively (Figure 5).

Optimization of real-time RT-PCR conditions

Using individual carotenoid biosynthesis pathway genes as the query sequences, the BLASTN search against the tomato whole genome sequences returned a total of 25 pathway genes with high protein sequence homology (Figure S1). Phylogenetic analysis of the protein sequences of these 25 genes together with the internal control genes *Expressed* and *CAC* grouped them into 12 groups (Figure S1). Based on the cDNA sequence alignment of the genes within each group,

sequence-specific primers were designed for each of the 25 genes (Table S1; Figures S2-S13). Optimization of real-time RT-PCR conditions for each primer pair of each gene was conducted by optimizing primer annealing temperature, primer concentration, and cDNA serial dilution range for each primer pair of each gene as described in Zhao et al. (in preparation). As shown in Table S2, the optimal annealing temperature was 56.8 or 59.0ºC and the primer concentration was 250, 300, 350 nM for most primer pairs of each gene. The best primer pair of each gene had $R^2 > 0.99$ and efficiency (E) = 100 – 105% under the conditions of the optimal annealing temperature and primer concentration and various cDNA serial dilutions (Table S2). The only exceptions came from *GGPPS3*, *TPT1*, *PSY1*, *β-LCY1*, *BCH2*, *NSY* and *CAC* which had E = 94.3 – 98.7%.

Relative expression levels of the upstream genes prior to lycopene biosynthesis in the carotenoid biosynthesis pathway at the breaker and ripe stages

To understand whether and how fruit lycopene contents are transcriptionally regulated, we used real-time RT-PCR to analyze the relative expression levels of the complete carotenoid biosynthesis pathway genes in the pericarp tissues at the breaker and ripe stages that were used for HPLC analysis. Using *Expressed* and *CAC* as the two internal control genes (Exposito-Rodriguez et al., 2008; Gonzalez-Aguilera et al., 2016), the relative gene expression of all the pathway genes showed a general trend of strong expression of most upstream genes and weak expression of most downstream genes in all cultigens at both developmental stages (Figures 6; 7). Among the upstream genes in all cultigens, *PSY1* and *Z-ISO* consistently had the highest and the second highest relative expression levels, respectively, followed by *GGPPS3*, *SSU II*, *PDS*, *ZDS* and *CrtISO*, while *GGPPS2*, *PSY2* and *CrtISO-L1* had the least relative expression levels;

all of these genes had relative expression levels larger than 1, indicating higher relative expression levels than the internal control genes (Tables 2; S3). In contrast, *GGPPS1*, *TPT1*, *TPT2*, *PSY3* and *CrtISO-L2* had relative expression levels less than 1, indicating lower relative expression than the internal control genes (Tables 2; S3). Since the *tangerine* mutation resulted in a non-functional *crtiso* in NC 1Y (Isaacson et al., 2002; Panthee et al., 2013), we compared the relative expression levels of these upstream genes in all the 42 cultigens as a group with that of *crtiso* in NC 1Y at both breaker and ripe stages. We found that most of these upstream genes at either stage as a group had significantly higher relative expression levels than that of *crtiso* in NC 1Y (Table S3). However, the relative expression levels of *TPT2* and *PSY3* at the breaker stage were insignificantly different from that of *crtiso* in NC 1Y (Table S3; Figures 6; S14). Thus, expression of *TPT2* and *PSY3* in all the 42 cultigens at the breaker stage as a group were minimal or silenced, and not included for further analysis.

We grouped the 42 cultigens by stage of ripeness and compared relative expression levels of the remaining upstream genes with positive and negative control cultigens. The expression levels of the 42 cultigens was also analyzed by dividing into 4 and 5 subgroups based on the fruit lycopene content at the ripe stage (as >150, 100-150, 50-100, <50 μg/g FW). As results were very similar statistically, we are displaying results from the one group statistical assay. When compared to Moneymaker, we found that *GGPPS2*, *SSU II*, *PSY2*, and *CrtISO-L1* at both stages, *CrtISO* at the breaker stage, and *GGPPS3*, *TPT1*, and *ZDS* at the ripe stage had significantly higher relative expression levels, while *PSY3* at the ripe stage had significantly lower relative expression levels (Table 2; Figures 6; S14). Thus, higher relative expression of these genes contributed to higher fruit lycopene contents in the 42 cultigens than in Moneymaker. In comparison to wild tomato, *PSY2* and *CrtISO-L1* at both stages, and *TPT1* and *TPT2* at the ripe

stage had significantly higher relative expression levels in the 42 cultigens, while *GGPPS1* and *TPT2* at the breaker stage and *GGPPS2* and *ZDS* at the ripe stage had a significantly lower relative expression levels in the 42 cultigens (Table S4; Figures 6; S14). Therefore, the precise transcriptional regulation of these seven genes contributed to the lower fruit lycopene contents in the 42 cultigens than in the wild tomato. In addition, when the relative expression level of each gene in each cultigen was compared between the two developmental stages, we found all of the upstream genes showed either significantly higher or lower relative expression in various cultigens between the two stages (Figure S14). It is worthwhile to point out that *CrtISO-L2* showed significantly higher relative expression levels in 8 out of the 42 cultigens at the ripe stage than that at the breaker stage (Figure S14).

Surprisingly, *PSY1* and *Z-ISO* in the cultigens at both stages did not show significant difference in relative expression levels from that in either Moneymaker or wild tomato even though they were the highest expressed genes in the whole pathway (Tables 2; S4). At the breaker stage, the relative expression levels of *PSY1* ranged from 221.84 in LA4013 to 1,182.8 in Lycobol with an overall average of 449.90 in the 42 cultigens, and *Z-ISO* varied from 26.58 in Valentine F1 to 313.68 in HLY13 with an overall average of 139.69 in the 42 cultigens (Figure S14). At the ripe stage, the relative expression levels of *PSY1* ranged from 170.87 in H9997 to 1,182.8 in Lycobol with an overall average of 449.90 in the 42 cultigens, and that of *Z-ISO* varied from 26.58 in Valentine F1 to 313.68 in HLY13 with an overall average of 139.69 in the 42 cultigens (Figure S14).

Relative expression levels of the downstream genes in the carotenoid biosynthesis pathway at the breaker and ripe stages

Among the downstream genes in all cultigens, *BCH1*, *ZEP*, and *VDE* at both stages and *CYP97C11* at the breaker stage had relative expression levels larger than 1, indicating higher relative expression than the internal control genes, while the other 6 downstream genes had relative expression levels smaller than 1, thus lower relative expression than the internal control genes (Tables S4; S5; Figure 7). In all the 42 cultigens, the average relative expression levels of *BCH1*, *ZEP*, *VDE* and *CYP97C11* (0.79 – 2.43) were comparable to the upstream genes *GGPPS2*, *PSY2* and *CrtISO-L1* (2.37 – 3.67), while which of *CrtISO-L1* (0.33 – 0.40) was comparable to the upstream genes *TPT1* and *CrtISO-L2* (0.37 – 0.59) (Table S3). When compared to the relative expression levels of the non-functional mutated *crtiso* in NC 1Y, and we found that these 5 downstream genes had significantly higher relative expression levels than the *crtiso* in NC 1Y (Table S3). However, the relative expression levels of *β-LYC1*, *β-LYC2*, and *NSY* at the breaker stage and *ε-LYC* at the ripe stage were insignificantly different from that of *crtiso* in NC 1Y (Table S3; Figures 7; S15). Thus, expression of *β-LYC1*, *β-LYC2*, and *NSY* at the breaker stage and *ε-LYC* at the ripe stage in all the 42 cultigens as a group were minimal or silenced and not included for further analysis.

We compared the relative expression levels of all the remaining downstream genes in all the 42 cultigens at each stage as a group with that of the positive and negative control cultigens at the same stages. We found that *β-LYC1*, *β-LYC2*, *NSY*, *ε-LYC* at the ripe stage, *BCH2*, *VDE*, *CYP97A29* at both stages, and *BCH1* at the breaker stage had significantly higher relative expression levels than their counterparts in Moneymaker (Table 3). In addition, *β-LYC1*, *β-LYC2* and *ZEP* at the ripe stage, *BCH1*, *VDE* and *CYP97C11* at both stages, and *ε-LYC* at the breaker

stage had significantly higher relative expression levels than their counterparts in the wild tomato (Table S5; Figures 7; S15). Thus, transcriptional regulation of these genes contributed to the lower fruit lycopene content in the 42 cultigens than in the wild tomato since higher expression of downstream genes might consume more lycopene. We also noticed that *BCH1* and *BCH2* had significantly increased relative expression levels at the ripe stage than at the breaker stage in 9 and 5 out of the 42 cultigens, respectively. In contrary, *ε-LYC* and *CYP97A29* had significantly decreased relative expression levels at the ripe stage than at the breaker stage in 8 and 7 out of the 42 cultigens, respectively (Figures 7; S15).

Discussion

Here we identified the key carotenoid biosynthesis pathway genes that contributed to fruit lycopene content in the 42 tomato cultigens. These genes showed unique expression patterns prior to and after lycopene biosynthesis when compared to the positive and negative control cultigens. To our best knowledge, this is the first systematic investigation of the relative expression of the complete carotenoid biosynthesis pathway genes in various cultigens, and correlation of their expression patterns with fruit lycopene content.

The wild tomato had the highest amount of lycopene at the ripe stage relative to all the other cultigens (Figure 3). This is in accordance with Razifard et al. (2020) which showed most of the selection pressure in tomato domestication was on fruit size rather than fruit color, leading to decreased fruit lycopene content. Moneymaker had the lowest lycopene content (besides NC 1Y; Figure 3). Thus, these two cultigens were used as the positive and negative controls in the present study, respectively. The mutated *crtiso* gene in NC 1Y was used as a negative control gene so that we found that *TPT2*, *PSY3*, *β-LYC1*, *β-LYC2*, *NSY* at the breaker stage and *ε-LYC* at

the ripe stage in all the 42 cultigens were minimally expressed or silenced (Figures 6; 7; S14; S15). As shown in Figures 3-5, fruit lycopene and phytofluene contents showed a gradual increase across fruit ripening and reached the maximal levels at the ripe stage in most cultigens, while fruit beta-carotene contents remained relatively constant in many cultigens. The average fruit contents of each of the three metabolites in all the cultigens as a group were significantly higher than that in Moneymaker during fruit ripening. Thus, the high fruit lycopene content in these cultigens did not occur at the expense of phytofluene and beta-carotene contents. This indicates that more metabolic flux flows from the upstream MEP pathway into the carotenoid biosynthesis pathway in these cultigens during fruit ripening (Figure S16).

Using real-time RT-PCR, we found a general trend that most upstream genes prior to lycopene biosynthesis were highly expressed and most downstream genes were extremely lowly expressed in all the 42 cultigens plus the wild tomato during fruit ripening, leading to high fruit lycopene content. This general trend has also been reported in low-lycopene cultigens such as Moneymaker, M82, Ailsa Craig, Tangerine 3183, Red Setter, and Rheilands Rhum (Ament et al., 2006; Giorio et al., 2008; Giuliano et al., 1993; Isaacson et al., 2002; Lawrence et al., 1997; Lois et al., 2000; Pecker et al., 1992; Ronen et al., 1999; 2000; Stigliani et al., 2011). When compared to Moneymaker, we found that significant higher expression in upstream genes *GGPPS2*, *GGPPS3*, *TPT1*, *SSU II*, *PSY2*, *ZDS*, *CrtISO* and *CrtISO-L1* at one or two stages. This is the first report of the relative expression levels of *TPT1*, *TPT2*, and *SSU II* in tomato during fruit ripening, while *GGPPS2* had been reported to have an increased expression in the orange fruits of Moneymaker (Ament et al., 2006). During fruit ripening, it was reported that *PSY1* had increased expression in low-lycopene cultigens Ailsa Craig (Lois et al., 2000), M82 and Tangerine 3183 (Isaacson et al., 2002), Rheilands Rhum (Giuliano et al., 1993), and Red Setter

(Giorio et al., 2008; Stigliani et al., 2011). Similarly, it was reported that *PDS* had enhanced expression in M82 and Tangerine 3183 (Isaacson et al., 2002; Ronen et al., 1999; 2000), UC82-B (Pecker et al., 1992) and Rheilands Rhum (Giuliano et al., 1993). However, we found that *PSY1* and *PDS* did not have a significant change in expression in all the 42 cultigens as a group in comparison to Moneymaker (Figure S14). Expression of *PSY2* and *CrtISO* had been reported to be gradually increased during fruit ripening in M82 and Tangerine 3183 (Isaacson et al., 2002), and Red Setter (Giorio et al., 2008; Stigliani et al., 2011), but expression of *CrtISO-L1* and *ZDS* had never been reported during fruit ripening in tomato. In addition, we found the relative expression of downstream genes *β-LYC1*, *β-LYC2*, *BCH1*, *BCH2*, *VDE*, *NSY*, *ε-LYC* and *CYP97A29* at one or two stages was significantly higher than their counterparts in Moneymaker (Table 3). Therefore, the significantly enhanced expression of these upstream and downstream genes contributed to the higher metabolic flux flow into the carotenoid biosynthesis pathway. Moreover, when compared to the wild tomato, we found significant higher expression in downstream genes *β-LYC1*, *β-LYC2*, *BCH1*, *VDE*, *ZEP*, *ε-LYC* and *CYP97C11* in these cultigens at one or two stages. This resulted in higher consumption of lycopene as a substrate for the downstream pathway, leading to lower fruit lycopene content in these cultigens than in the wild tomato. The high-lycopene content in the wild tomato also indicates that overexpression of upstream genes may not be necessarily increasing lycopene content so long as lycopene is exposed to increased pressure from downstream genes. Therefore, both upstream and downstream genes should be the targets for genetic engineering, gene editing and breeding in order to improve fruit lycopene content in crops. Studies on expression of these downstream genes during fruit ripening were mainly conducted on low-lycopene cultigens such as M82

(Ronen et al., 1999; 2000) and Red Setter (Stigliani et al., 2011), which showed different expression patterns from the present study.

The high-lycopene tomato cultigens were developed using various genetic backgrounds, and the underlying mechanism for increased lycopene biosynthesis in most of them is largely unknown. Several cultigens contained the *old-gold* (*og*) and *old gold-crimson* (og^c) mutations in the *β–LCY2* promoter causing lowered expression, which leads to increased lycopene content at the expense of beta-carotene (Mohan et al., 2016, Ronen et al., 2000). For example, LA4025 and LA4026 contained the *og* mutation while NC 4 Grape, Fla. 8153, SVTD3418, and Fla. 7907B harbored the og^c mutation. We found that these cultigens were not different in beta-carotene than the negative control Moneymaker. According to Enfissi et al. (2017), og^c mutation resulted in higher gene expression in *GGPPS1*, *PDS*, *β-LCY1*, and *ε-LCY*, and lowered expression in *GGPPS2*, *PSY1*, *PSY2*, *ZDS*, *CrtISO*, and *β-LCY2* in low-lycopene cultigens, which were not observed in these cultigens (Figures 6; 7; S14; S15). Moreover, the relative expression levels of *β–LCY2* in LA4025, LA4026, NC 4Grape, SVTD3418, and Fla. 7907B at both stages were insignificantly different from Moneymaker, and that in Fla. 8153 was significantly higher at the ripe stage than that in Moneymaker. In addition, a few cultigens such as LA3004 contained the *hp-1* mutation in the *DDB1* gene, and HLY18, HM5235, LA4013, and HLY13 harbored the *hp-2* mutation in *DET1*. *DDB1* and *DET1*, which do not belong to the carotenoid biosynthetic pathway, affect fruit lycopene content through the changes in chromoplast number and/or size (Azari et al., 2010; Kolotilin et al., 2007). Kilambi et al. (2013) found that an *hp-1* mutant had lowered expression in *GGPPS2*, *PSY1*, *PSY2*, *Z-ISO*, *CrtISO*, *β-LCY1*, and *β-LCY2* and increased expression in *PDS*, *ZDS*, and *CYP97A29* at both maturity stages. Kolotilin et al. (2007) reported that an *hp-2* mutant contained decreased expression of *β-LCY2* and enhanced expression in

GGPPS1 and *PDS* at the breaker stage as well as lowered expression of *BCH2* and increased expression of *GGPPS1*, *PSY1*, *PDS*, *ZDS* and *β-LCY2* at the ripe stage. However, all of these were not observed in the *hp-1* mutant LA3004 and the *hp-2* mutants HLY18, HM5235, LA4013, and HLY13 (Figures S14; S15). Therefore, all of these discrepancies in gene expression indicate that crossing of the original mutant cultigens with different breeding backgrounds dramatically changed expression levels of the pathway genes.

Conclusion

We found that higher lycopene content resulted from a combination of significantly higher relative expression levels in upstream genes *GGPPS2*, *SSU II*, *PSY2*, and *CrtISO-L1* at both stages, *CrtISO* at the breaker stage, and *GGPPS3*, *TPT1*, and *ZDS* at the ripe stage, and significantly lower relative expression levels in *PSY3* at the ripe stage in these 42 cultigens when compared to the negative control Moneymaker. We also found that lower lycopene content resulted from a combination of significantly higher relative expression levels in downstream genes *β-LYC1*, *β-LYC2*, *NSY*, *ε-LYC* at the ripe stage, *BCH2*, *VDE*, *CYP97A29* at both stages, and *BCH1* at the breaker stage contributed to lower lycopene content in these 42 cultigens when compared to the positive control the wild tomato. Thus, we identified that a coordinated transcriptional regulation of the upstream and downstream carotenoid biosynthesis pathway genes contributed to significantly higher metabolic flux flow into the pathway in the 42 tomato cultigens than in the negative control cultigen, leading to high fruit lycopene content. These results will provide a highly valuable resources for molecular breeding, genetic engineering, and gene editing for the improvement of tomato fruit lycopene content.

REFERENCES

Ament, K., Van Schie, C.C., Bouwmeester, H.J., Haring, M.A. and Schuurink, R.C. (2006) Induction of a leaf specific geranylgeranyl pyrophosphate synthase and emission of (E,E)-4,8,12-trimethyltrideca-1,3,7,11-tetraene in tomato are dependent on both jasmonic acid and salicylic acid signaling pathways. *Planta* 224, 1197–1208.

Arméndariz, R., Macua, J.I., Lahoz, I., Garnica, J. and Bozal, J.M. (2006) Lycopene content in commercial tomato cultivars for paste in Navarra. *Acta Horticulturae* 724, 259–262.

Azari, R., Reuveni, M., Evenor, D., Nahon, S., Shlomo, H., Chen, L. and Levin, I. (2010) Overexpression of *UV-DAMAGED DNA BINDING PROTEIN 1* links plant development and phytonutrient accumulation in *high pigment-1* tomato. *Journal of Experimental Botany* 61, 3627–3637.

Bai, Y. and Lindhout, P. (2007) Domestication and breeding of tomatoes: What have we gained and what can we gain in the future? *Annals of Botany* 100, 1085–1094.

Bino, R.J., de Vos, C.H.R., Lieberman, M., Hall, R.D., Bovy, A., Jonker, H.H., Tikunov, Y., Lommen, A., Moco, S. and Levin, I. (2004) The light-hyperresponsive *high pigment-2*^{dg} mutation of tomato: alterations in the fruit metabolome. *New Phytologist* 166, 427–438.

Bramley, P.M. (2002) Regulation of carotenoid formation during tomato fruit ripening and development. *Journal of Experimental Botany* 53, 2107–2113.

Burton-Freeman, B.M. and Sesso, H.D. (2014) Whole food versus supplement: Comparing the clinical evidence of tomato intake and lycopene supplementation on cardiovascular risk factors. *Advances in Nutrition* 5, 457–485.

Carli, P., Caruso, G., Fogliano, V., Carputo, D., Frusciante, L. and Ercolano, M.R. (2011) Development of a methodology to forecast the nutritional value of new tomato hybrids. *Euphytica* 180, 291–300.

Cazzonelli, C.I. and Pogson, B.J. (2010) Source to sink: Regulation of carotenoid biosynthesis in plants. *Trends in Plant Science* 15, 266–274.

Chandra, H.M. and Ramalingam, S. (2011) Antioxidant potentials of skin, pulp, and seed fractions of commercially important tomato cultivars. *Food Science and Biotechnology* 20, 15–21.

Cookson, P.J., Kiano, J.W., Shipton, C.A., Fraser, P.D., Romer, S., Schuch, W., Bramley, P.M. and Pyke, K.A. (2003) Increases in cell elongation, plastid compartment size and phytoene synthase activity underlie the phenotype of the *high pigment-1* mutant of tomato. *Planta* 217, 896–903.

Djidonou, D., Simonne, A.H., Koch, K.E., Brecht, J.K. and Zhao, X. (2016) Nutritional quality of field-grown tomato fruit as affected by grafting with interspecific hybrid rootstocks. *HortScience* 51, 1618–1624.

Dorak, M. (2007) Real-time PCR. Taylor & Francis Group, New York.

Egea, I., Bian, W., Barsan, C., Jauneau, A., Pech, J.-C., Latché, A., Li, Z. and Chervin, C. (2011) Chloroplast to chromoplast transition in tomato fruit: Spectral confocal microscopy analyses of carotenoids and chlorophylls in isolated plastids and time-lapse recording on intact live tissue. *Annals of Botany* 108, 291–297.

Enfissi, E.M.A., Nogueira, M., Bramley, P.M. and Fraser, P.D. (2017) The regulation of carotenoid formation in tomato fruit. *The Plant Journal* 89, 774–788.

Expósito-Rodríguez, M., Borges, A.A., Borges-Pérez, A. and Pérez, J.A. (2008) Selection of internal control genes for quantitative real-time RT-PCR studies during tomato development process. *BMC Plant Biology* 8, 131.

Fantini, E., Falcone, G., Frusciante, S., Giliberto, L. and Giuliano, G. (2013) Dissection of tomato lycopene biosynthesis through virus-induced gene silencing. *Plant Physiology* 163, 986–998.

FAOSTAT. Retrieved June 16, 2020, from http://www.fao.org/faostat/en/#home

Fish, W.W., Perkins-Veazie, P. and Collins, J.K. (2002) A quantitative assay for lycopene that utilizes reduced volumes of organic solvents. *Journal of Food Composition and Analysis* 15, 309–317.

Foolad, M.R. (2007) Genome mapping and molecular breeding of tomato. *International Journal of Plant Genomics* 2007, 52.

Foolad, M.R, Merk, H.L. and Ashrafi, H. (2008) Genetics, genomics and breeding of late blight and early blight resistance in tomato. *Critical Reviews in Plant Science* 27, 75-107.

Fraser, P.D., Kiano, J.W., Truesdale, M.R., Schuch, W. and Bramley, P.M. (1999) Phytoene synthase-2 enzyme activity in tomato does not contribute to carotenoid synthesis in ripening fruit. *Plant Molecular Biology* 40, 687–698.

Gallagher, C.E., Matthews, P.D., Li, F. and Wurtzel, E.T. (2004) Gene duplication in the carotenoid biosynthetic pathway preceded evolution of the grasses. *Plant Physiology* 135, 1776–1783.

Galpaz, N., Wang, Q., Menda, N., Zamir, D. and Hirschberg, J. (2008) Abscisic acid deficiency in the tomato mutant *high-pigment 3* leading to increased plastid number and higher fruit lycopene content. *The Plant Journal* 53, 717–730.

Gardner, R.G. (2000) `Carolina Gold', a hybrid tomato, and its parents, NC 1Y and NC 2Y. *HortScience* 35, 966–967.

Giorio, G., Stigliani, A.L. and D'Ambrosio, C. (2008) Phytoene synthase genes in tomato (*Solanum lycopersicum* L.) – new data on the structures, the deduced amino acid sequences and the expression patterns. *The FEBS Journal* 275, 527–35.

Giuliano, G., Bartley, G.E. and Scolnik, P.A. (1993) Regulation of carotenoid biosynthesis during tomato development. *Plant Cell* 5, 379–387.

González-Aguilera, K.L., Saad, C.F., Chávez Montes, R.A., Alves-Ferreira, M. and de Folter, S. (2016) Selection of reference genes for quantitative real-time RT-PCR studies in tomato fruit of the genotype MT-Rg1. *Frontiers in Plant Science* 7, 1386.

Ilahy, R., Siddiqui, M.W., Tlili, I., Montefusco, A., Piro, G., Hdider, C. and Lenucci, M.S. (2018) When color really matters: horticultural performance and functional quality of high-lycopene tomatoes. *Critical Reviews in Plant Sciences* 37, 15–53.

Isaacson, T., Ronen, G., Zamir, D. and Hirschberg, J. (2002) Cloning of tangerine from tomato reveals a carotenoid isomerase essential for the production of β-carotene and xanthophylls in plants. *Plant Cell* 14, 333–342.

Islamian, J.P. and Mehrali, H. (2015) Lycopene as a carotenoid provides radioprotectant and antioxidant effects by quenching radiation-induced free radical singlet oxygen: An overview. *Cell Journal* 16, 386–391.

Jiang, C. (2019) Hybrid tomato plant named HM 5235. US Patent No. US10238050B2.

Kachanovsky, D.E., Filler, S., Isaacson, T. and Hirschberg, J. (2012) Epistasis in tomato color mutations involves regulation of phytoene synthase 1 expression by *cis*-carotenoids. *Proceedings of the National Academy of Sciences* 109, 19021–19026.

Kilambi, H.V., Kumar, R., Sharma, R. and Sreelakshmi, Y. (2013) Chromoplast-specific carotenoid-associated protein appears to be important for enhanced accumulation of carotenoids in *hp1* tomato fruits. *Plant Physiology* 161, 2085–2101.

Kolotilin, I., Koltai, H., Tadmor, Y., Bar-Or, C., Reuveni, M., Meir, A., Nahon, S., Shlomo, H., Chen, L. and Levin, I. (2007) Transcriptional profiling of *high pigment-2*^{dg} tomato mutant links early fruit plastid biogenesis with its overproduction of phytonutrients. *Plant Physiology* 145, 389–401.

Lawrence, S.D., Cline, K. and Moore, G.A. (1997) Chromoplast development in ripening tomato fruit: identification of CDNAs for chromoplast-targeted proteins and characterization of a cDNA encoding a plastid-localized low-molecular-weight heat shock protein. *Plant Molecular Biology* 33, 483–92.

Li, X., Wang, Y., Chen, S., Tian, H., Fu, D., Zhu, B., Luo, Y. and Zhu, H. (2018) Lycopene is enriched in tomato fruit by CRISPR/Cas9-mediated multiplex genome editing. *Frontiers in Plant Science* 9, 559.

Liu, L., Shao, Z., Zhang, M. and Wang, Q. (2015) Regulation of carotenoid metabolism in tomato. *Molecular Plant* 8, 28–39.

Livak, K.J. and Schmittgen, T.D. (2011) Analysis of relative gene expression data using real-time quantitative PCR and the $2^{-\Delta\Delta Ct}$ method. *Methods* 25, 402-408.

Lois, L.M., Rodríguez-Concepción, M., Gallego, F., Campos, N. and Boronat, A. (2000) Carotenoid biosynthesis during tomato fruit development: Regulatory role of 1-deoxy-D-xylulose 5-phosphate synthase. *The Plant Journal* 22, 503–513.

Mascio, P., Kaiser, S. and Sies, H. (1989) Lycopene as the most efficient biological carotenoid singlet oxygen quencher. *Archives of Biochemistry and Biophysics* 274, 532–538.

McQuinn, R.P., Wong, B. and Giovannoni, J.J. (2018) *AtPDS* overexpression in tomato: Exposing unique patterns of carotenoid self-regulation and an alternative strategy for the enhancement of fruit carotenoid content. *Plant Biotechnology Journal* 16, 482–494.

Mohan, V., Pandey, A., Sreelakshmi, Y. and Sharma, R. (2016) Neofunctionalization of chromoplast specific lycopene beta cyclase gene (*CYC-B*) in tomato clade. *PLoS One* 11, e0153333.

Namitha, K.K., Archana, S.N. and Negi, P.S. (2011) Expression of carotenoid biosynthetic pathway genes and changes in carotenoids during ripening in tomato (*Lycopersicon esculentum*). *Food & Function* 2, 168.

Narita, J.O. and Gruissem, W. (1989) Tomato hydroxymethylglutaryl-CoA reductase is required early in fruit development but not during ripening. *The Plant Cell* 1, 181–190.

Oltman, A.E., Jervis, S.M. and Drake, M.A. (2014) Consumer attitudes and preferences for fresh market tomatoes. *Journal of Food Science* 79, S2091–S2097.

Paetzold, H., Garms, S., Bartram, S., Wieczorek, J., Urós-Gracia, E.-M., Rodríguez-Concepción, M., Boland, W., Strack, D., Hause, B. and Walter, M.H. (2010) The isogene 1-Deoxy-D-xylulose 5-phosphate synthase 2 controls isoprenoid profiles, precursor pathway allocation, and density of tomato trichomes. *Molecular Plant* 3, 904–916.

Pandurangaiah, S., Ravishankar, K.V., Shivashankar, K.S., Sadashiva, A.T., Pillakenchappa, K. and Narayanan, S.K. (2016) Differential expression of carotenoid biosynthetic pathway genes in two contrasting tomato genotypes for lycopene content. *Journal of Biosciences* 41, 257–264.

Panthee, D.R., Perkins-Veazie, P., Randall, D. and Brown, A.F. (2013) Lycopene estimation in tomato lines using infrared absorbance and tomato analyzer. *International Journal of Vegetable Science* 19, 240–255.

Pecker, I., Chamovitz, D., Linden, H., Sandmann, G. and Hirschberg, J. (1992) A single polypeptide catalyzing the conversion of phytoene to zeta-carotene is transcriptionally regulated during tomato fruit ripening. *Proceedings of the National Academy of Sciences of the United States of America* 89, 4962–4966.

Rao, A. and Rao, L. (2007) Carotenoids and human health. *Pharmacological Research* 55, 207–216.

Rao, A.V. and Agarwal, S. (1999) Role of lycopene as antioxidant carotenoid in the prevention of chronic diseases: A review. *Nutrition Research* 19, 305–323.

Razifard, H., Ramos, A., Della Valle, A.L., Bodary, C., Goetz, E., Manser, E.J., Li, X., Zhang, L., Visa, S., Tieman, D., van der Knaap, E. and Caicedo, A.L. (2020) Genomic evidence for complex domestication history of the cultivated tomato in Latin America. *Molecular Biology and Evolution* 37, 1118–1132.

Rodríguez-Concepción, M., Ahumada, I., Diez-Juez, E., Sauret-Güeto, S., Lois, L.M., Gallego, F., Carretero-Paulet, L., Campos, N. and Boronat, A. (2001) 1-Deoxy-d-xylulose 5-phosphate reductoisomerase and plastid isoprenoid biosynthesis during tomato fruit ripening. *The Plant Journal* 27, 213–222.

Rodríguez-Concepción, M., Querol, J., Lois, L.M., Imperial, S. and Boronat, A. (2003) Bioinformatic and molecular analysis of hydroxymethylbutenyl diphosphate synthase (GCPE) gene expression during carotenoid accumulation in ripening tomato fruit. *Planta* 217, 476–482.

Ronen, G., Cohen, M., Zamir, D. and Hirschberg, J. (1999) Regulation of carotenoid biosynthesis during tomato fruit development: Expression of the gene for lycopene epsilon-cyclase is down-regulated during ripening and is elevated in the mutant *Delta*. *The Plant Journal* 17, 341–351.

Ronen, G., Carmel-Goren, L., Zamir, D. and Hirschberg, J. (2000) An alternative pathway to β-carotene formation in plant chromoplasts discovered by map-based cloning of *Beta* and *old-gold* color mutations in tomato. *Proceedings of the National Academy of Sciences* 97, 11102–11107.

Rothan, C., Diouf, I. and Causse, M. (2018) Trait discovery and editing in tomato. *The Plant Journal* 97, 73–90.

Sharma, A., Zhang, L., Niño-Liu, D., Ashrafi, H. and Foolad, M.R. (2008) A *Solanum lycopersicum* × *Solanum pimpinellifolium* linkage map of tomato displaying genomic locations of R-genes, RGAs, and candidate resistance/defense-response ESTs. *International Journal of Plant Genomics* 2008, 1–18.

Stigliani, A.L., Giorio, G. and D'Ambrosio, C. (2011) Characterization of P450 carotenoid β- and ε-hydroxylases of tomato and transcriptional regulation of xanthophyll biosynthesis in root, leaf, petal and fruit. *Plant and Cell Physiology* 52, 851–865.

Vandesompele, J., Preter, K.D., Roy, N.V. and Paepe, A.D. (2002) Accurate normalization of real-time quantitative RT-PCR data by geometric averaging of multiple internal control genes. *Genome Biology* 3, RESEARCH0034.

Walter, M.H. and Strack, D. (2011) Carotenoids and their cleavage products: Biosynthesis and functions. *Natural Product Reports* 28, 663.

Whatley, J.M. and Whatley, F.R. (1987) When is a chromoplast? *New Phytologist* 106, 667–678.

Yoo, H., Park, W., Lee, G.-M., Oh, C.-S., Yeam, I., Won, D.-C., Kim, C. and Lee, J. (2017) Inferring the genetic determinants of fruit colors in tomato by carotenoid profiling. *Molecules* 22, 764.

Yuan, H., Zhang, J., Nageswaran, D. and Li, L. (2015) Carotenoid metabolism and regulation in horticultural crops. *Horticulture Research* 2, 15036.

Zhao, F., Maren, N.A., Kosentka, P.Z., Lu, H., Duduit, J.R., Ashrafi, H., Ranney, T.G. and Liu, W. An optimized protocol for real-time RT-PCR analysis: a case study of the characterization of reference genes in the novel bioenergy grass *Tripidium ravennae*. (in preparation)

Zhou, F. and Pichersky, E. (2020) The complete functional characterisation of the terpene synthase family in tomato. *New Phytologist* doi: 10.1111/nph.16431

Zsögön, A., Čermák, T., Naves, E.R., Notini, M.M., Edel, K.H., Weinl, S., Freschi, L., Voytas, D.F., Kudla, J. and Peres, L.E.P. (2018) De novo domestication of wild tomato using genome editing. *Nature Biotechnology* 36, 1211–1216.

Table 1. Tomato cultigens used in the present study.

Cultigen #	Name	Source[a]	Mutation(s)[b]
1	LA2093	TGRC (U.S.)	WT
2	ISI 12152	Isi-Diamond (Italy)	N.A.
3	HLY18	Hazera Genetics (Israel)	*hp-2^{dg}/hp-2^{dg}*
4	Lyco 1	Hazera Genetics (Israel)	N.A.
5	UG 27713	TGRC (U.S.)	N.A.
6	H9997	Heinz Seeds (U.S.)	N.A.
7	H1657	Heinz Seeds (U.S.)	N.A.
8	HM9905	H.M. Clause (France)	N.A.
9	NC 4Grape	NCTBP (U.S.)	*og^{c}*
10	LA3004	TGRC (U.S.)	*hp-1^{w}/hp-1^{w}*
11	Lyco 2	Hazera Genetics (Israel)	N.A.
12	NC 84173	NCTBP (U.S.)	WT
13	Amai	Sakata Seeds (Japan)	N.A.
14	Simba F1	Isi-Diamond (Italy)	N.A.
15	Lycos F1	Isi-Diamond (Italy)	N.A.
16	H7204	Heinz Seeds (U.S.)	N.A.
17	HM5235	H.M. Clause (France)	*hp-2^{dg}/hp-2^{dg}*
18	H1311	Heinz Seeds (U.S.)	N.A.
19	Crispino F1	Esasem (Italy)	N.A.
20	Lycobol	United Genetics (U.S.)	N.A.

Table 1. (continued)

Cultigen #	Name	Source[a]	Mutation(s)[b]
21	AK-TC035	Akira Seeds (Spain)	N.A.
22	Crispino Plum	Esasem (Italy)	N.A.
23	Fla. 8153	UFTBP (U.S.)	*og*^{c}
24	CXD277	H.M. Clause (France)	N.A.
25	Kalvert	Esasem (Italy)	N.A.
26	Valentine F1	Johnny Seeds (U.S.)	N.A.
27	LA4013	TGRC (U.S.)	*hp-2*
28	Nemacrimson	United Genetics (U.S.)	N.A.
29	ISI 44536	Isi-Diamond (Italy)	N.A.
30	BQ400	TGRC (U.S.)	N.A.
31	N 6426	TGRC (U.S.)	N.A.
32	SVTD3418	Seminis (U.S.)	*og*^{c}
33	Fla. 7907B	UFTBP (U.S.)	*og*^{c}
34	LA4025	TGRC (U.S.)	*og*
35	ES-608	Esasem (Italy)	N.A.
36	BOS811	TGRC (U.S.)	N.A.
37	H1175	Heinz Seeds (U.S.)	N.A.
38	HLY13	Hazera Genetics (Israel)	*hp-2*^{dg}/*hp-2*^{dg}
39	Fla. 47	UFTBP (U.S)	N.A.
40	Sevance	De Ruiter-Monsanto (U.S.)	N.A.

Table 1. (continued)

Cultigen #	Name	Source[a]	Mutation(s)[b]
41	Vertigo F1	Isi-Diamond (Italy)	N.A.
42	Tasty-Lee Hybrid	Tasty-Lee (U.S.)	N.A.
43	LA4026	TGRC (U.S.)	*og*
44	Moneymaker	-	WT
45	NC IY	NCTBP (U.S.)	*tangerine*

[a]TGRC, Tomato Genetics Resource Center; NCTBP, NC Tomato Breeding Program; UFTBP, UF Tomato Breeding Program. [b]WT and w, wild-type; *og/og^{c}*, *old-gold*/*old-gold crimson*; *hp-2^{dg}*, *high-pigment-2* dark green. N.A., not available.

Table 2. Comparison of the relative expression levels of the upstream genes leading to lycopene biosynthesis in fruits of 42 tomato cultigens at breaker and ripe stages. Moneymaker was used as a negative control cultigen (* denotes *p*-value < 0.05 using a two-tailed student's t-test with two-sample unequal variance, i.e., significantly different from that in Moneymaker).

Gene	Breaker			Ripe		
	Average	**Standard Deviation**	***p*-value**	**Average**	**Standard Deviation**	***p*-value**
GGPPS1	0.12	0.05	0.10	0.13	0.05	0.42
GGPPS2	3.62	4.20	1.60E-10 *	2.37	2.12	4.85E-15 *
GGPPS3	8.75	4.23	0.05	6.17	2.51	6.46E-4 *
TPT1	0.59	0.27	0.63	0.54	0.27	3.84E-3 *
TPT1	0.03	0.03	0.84	0.01	0.01	0.07
SSU II	14.15	4.59	0.01 *	10.50	3.57	1.76E-20 *
PSY1	473.64	275.73	0.07	391.50	153.12	0.72
PSY2	3.56	4.41	0.01 *	3.67	3.31	8.47E-10 *
PSY3	0.03	0.03	0.57	0.05	0.07	0.01 *
PDS	13.33	7.70	0.18	7.88	3.49	0.13
Z-ISO	144.09	87.95	0.95	120.03	59.71	0.37
ZDS	13.33	7.70	0.15	11.39	6.05	1.31E-3 *
CrtISO	13.90	14.12	0.03 *	8.90	5.24	0.66
CrtISO-L1	3.21	3.12	0.01 *	2.43	2.04	4.59E-3 *
CrtISO-L2	0.37	0.25	0.43	0.68	0.32	0.17

Table 3. Comparison of the relative expression levels of the downstream genes after lycopene biosynthesis in 42 tomato cultigens at breaker and ripe stages. Moneymaker was used as a negative control cultigen (* denotes *p*-value < 0.05 using a two-tailed student's t-test with two-sample unequal variance, i.e., significantly different from that in Moneymaker).

Gene	**Breaker**			**Ripe**		
	Average	**Standard Deviation**	***p*-value**	**Average**	**Standard Deviation**	***p*-value**
β-LCY1	0.06	0.08	9.84E-10 *	0.06	0.06	4.49E-4 *
β-LCY2	0.02	0.03	0.36	0.01	0.01	4.75E-05 *
BCH1	1.08	1.41	0.03E-3 *	1.56	1.22	0.50
BCH2	0.06	0.10	5.81E-05 *	0.04	0.03	0.01 *
ZEP	1.14	0.98	0.22	1.02	0.75	0.30
VDE	2.43	2.25	1.47E-3 *	1.70	1.59	3.96E-4 *
NSY	0.07	0.07	0.16	0.05	0.05	0.05 *
ε-LCY	0.06	0.07	0.89	0.01	0.02	8.06E-4 *
CYP97A29	0.55	0.40	1.09E-14 *	0.33	0.19	4.13E-07 *
CYP97C11	1.60	1.33	0.19	0.79	0.60	0.11

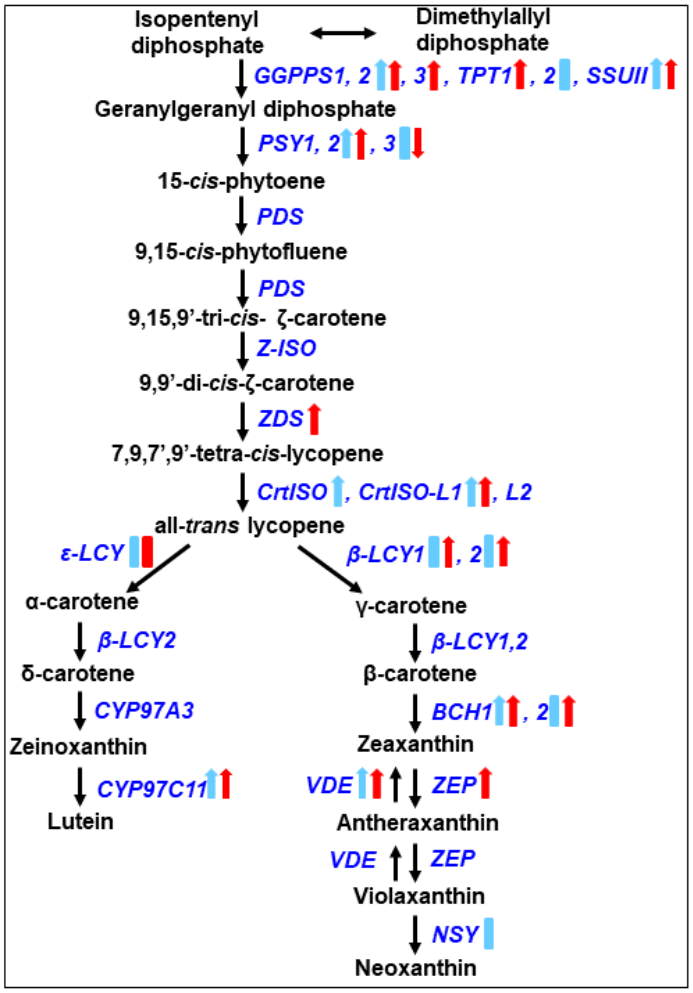

Figure 1. The carotenoid biosynthetic pathway in tomato and the transcriptional regulation of gene expression as tomato fruit moved from initial (breaker) to final (ripe) stages of ripening. Relative expression levels of each pathway gene at the breaker and ripe stages were measured individually by real-time RT-PCR with *Expressed* and *CAC* being the internal control genes. Transcriptional regulation of gene expression was studied by comparing the relative expression levels of each pathway gene in all the cultigens at each stage as a group with that of the negative control Moneymaker or the positive control wild tomato (LA 2093). Light blue, breaker stage. Red, ripe stage. Up-arrow, significantly higher relative expression levels for upstream genes in comparison to Moneymaker or for downstream genes in comparison to wild tomato. Down-arrow, significantly lower relative expression levels for upstream genes in comparison to Moneymaker or for downstream genes in comparison to wild tomato. Bar, insignificantly difference in relative expression in comparison to the *crtiso* mutant in NC 1Y.

Figure 2. Representative tomato fruit images of tomato cultigens at the ripe stage; refer to Table 1 for corresponding cultigen names.

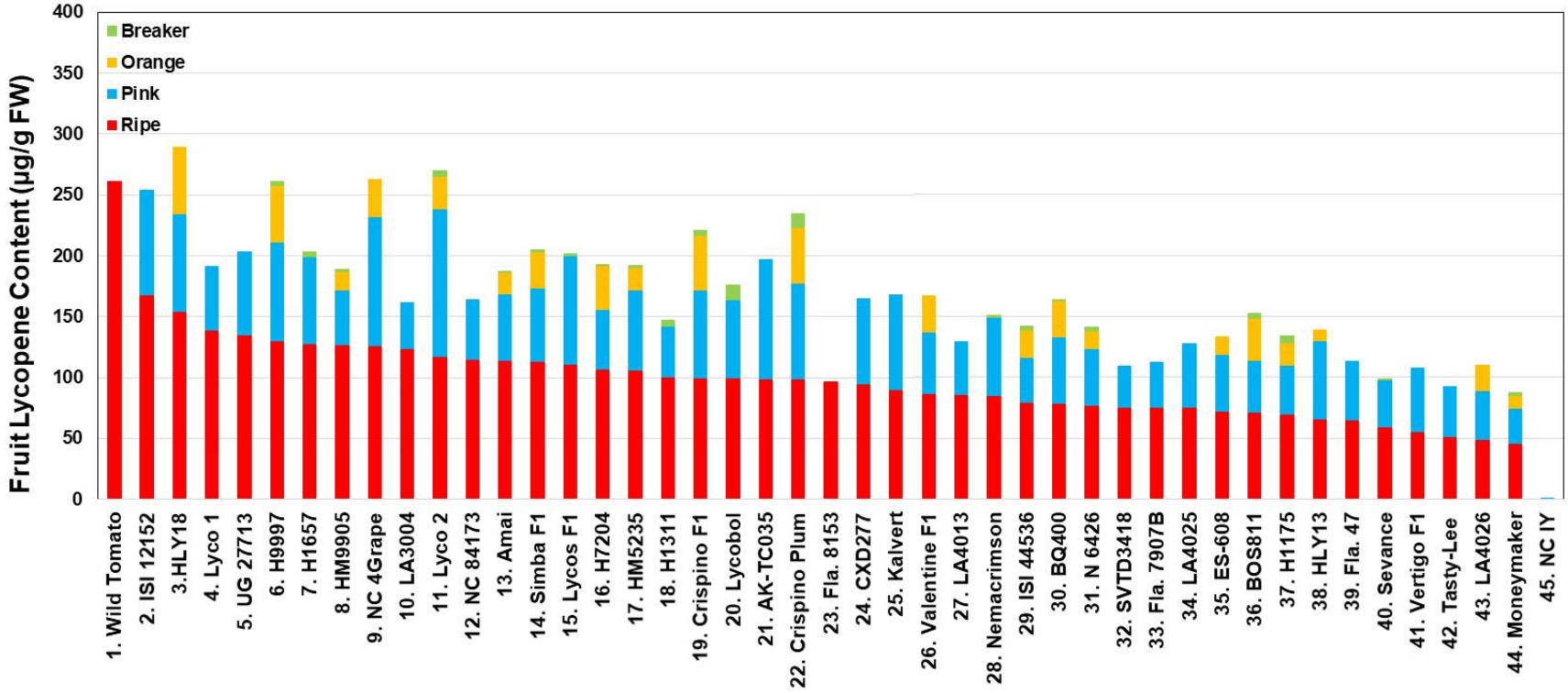

Figure 3. Fruit lycopene contents in the 42 tomato cultigens at breaker, orange, pink and ripe stages of ripeness. The wild tomato (LA 2093) was used as the positive control, and Moneymaker and NC 1Y were used as the negative controls. All cultigens were grown together under the same greenhouse conditions. Trans-lycopene content of pericarp tissue on a fresh weight (FW) was determined using HPLC.

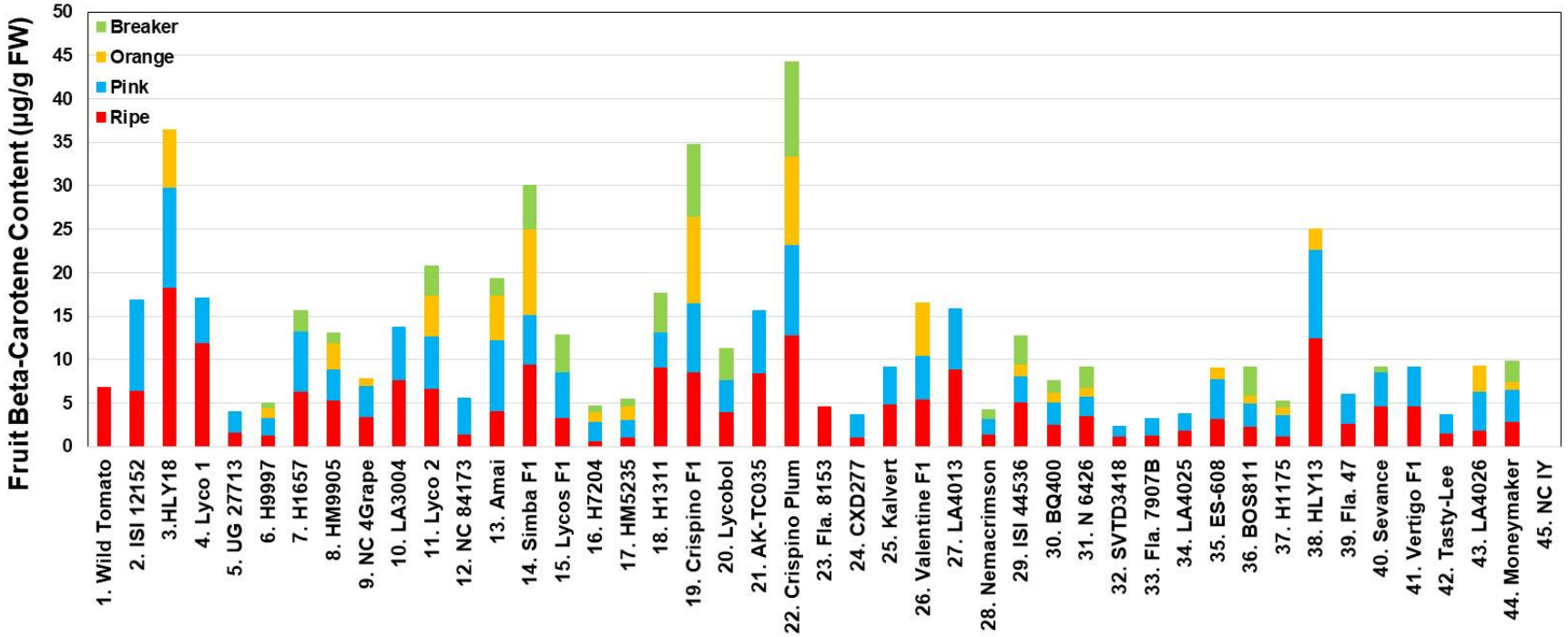

Figure 4. Fruit beta-carotene contents in the 42 tomato cultigens at the fruit developmental stages of breaker, orange, pink and ripe. The wild tomato (LA 2093) was used as the positive control, and Moneymaker and NC 1Y were used as the negative controls. All cultigens were grown together under the same greenhouse conditions. Trans-lycopene content of pericarp tissue on a fresh weight (FW) was determined using HPLC.

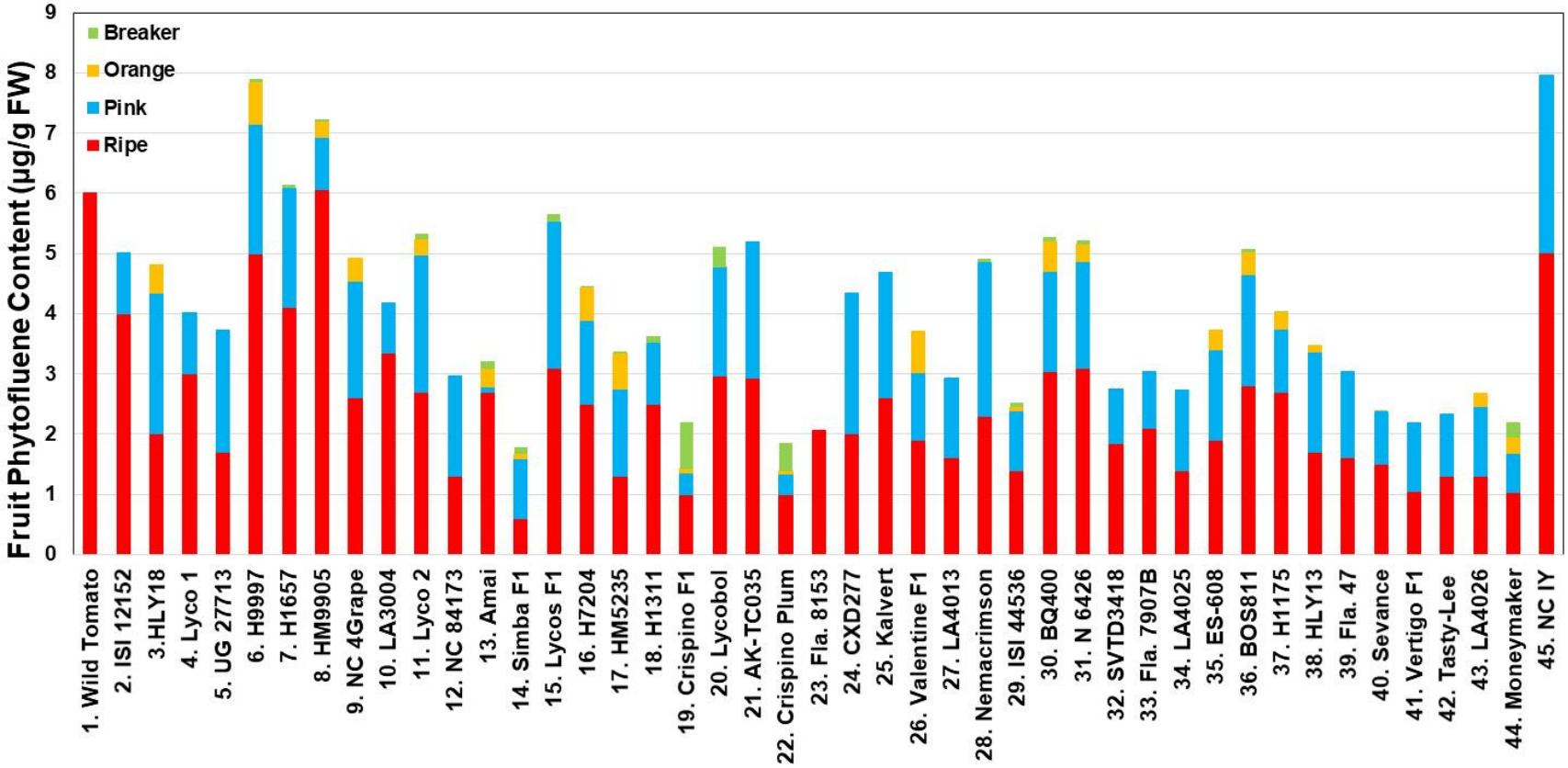

Figure 5. Fruit phytofluene contents in the 42 tomato cultigens at the fruit developmental stages of breaker, orange, pink and ripe. The wild tomato (LA 2093) was used as the positive control, and Moneymaker and NC 1Y were used as the negative controls. All cultigens were grown together under the same greenhouse conditions. Trans-lycopene content of pericarp tissue on a fresh weight (FW) was determined using HPLC.

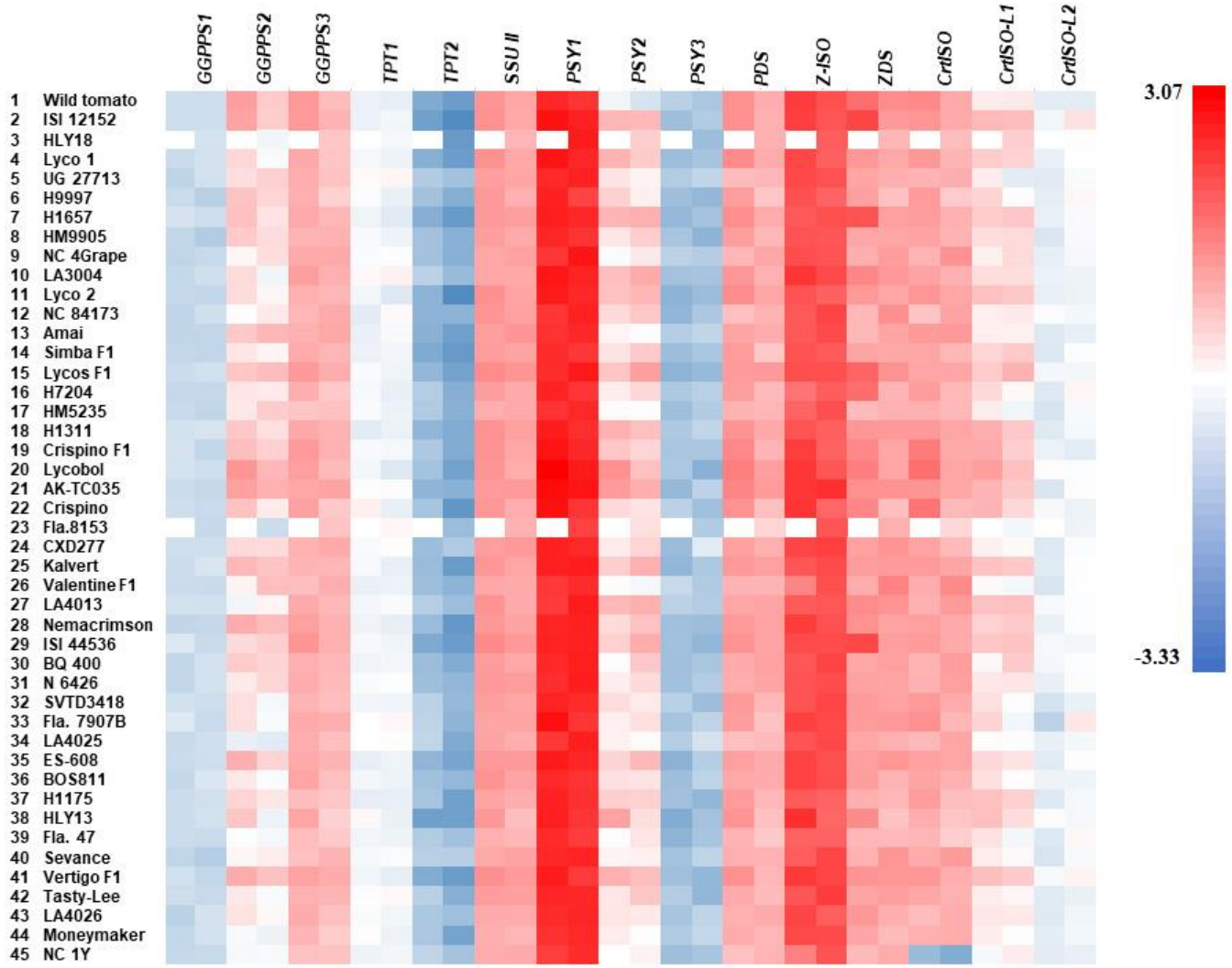

Figure 6. Heat map of relative expression levels of the 15 upstream genes in the carotenoid biosynthesis pathway genes in 42 tomato cultigens at the breaker and ripe stages measured by real-time RT-PCR.

Figure 6. (continued) The relative expression of each gene was measured by real-time RT-PCR, and relative quantification was performed using the standard curve method with the tomato *Expressed* and *CAC* genes as the internal control genes. The mean of the relative expression levels of the three biological replicates were log transformed. The wild tomato (LA2093) was used as the positive control variety while Moneymaker and NC 1Y were used as the negative control varieties. For each gene in each line, left and right boxes represent the breaker and ripe stages, respectively.

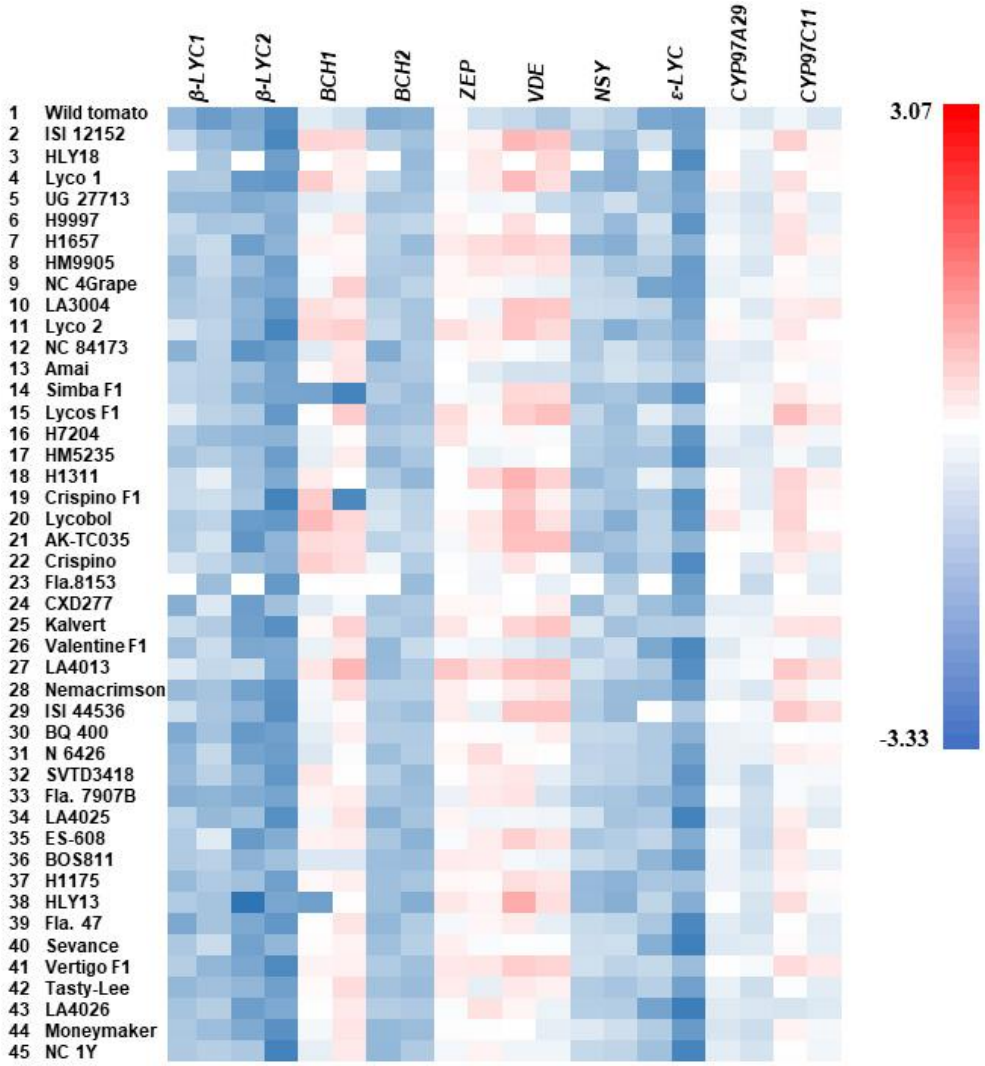

Figure 7. Heat map of relative expression levels of the 10 genes downstream from lycopene biosynthesis. The pathway genes in the 42 tomato cultigens at ripeness stages of breaker and ripe were measured by real-time RT-PCR.

Figure 7. (continued) The relative quantification was performed using the standard curve method with the tomato *Expressed* and *CAC* genes as the internal control genes. The mean of the relative expression levels of the three biological replicates were log transformed. The wild tomato (LA2093) was used as the positive control variety while Moneymaker and NC 1Y were used as the negative control varieties. For each gene in each line, left and right boxes represent the breaker and ripe stages, respectively.

APPENDICES

Appendix A

Supplementary Tables

Appendix B

Supplementary Figures

Appendix A

Table S1. Primer sequences used in the present study.

Gene	Full Name	Accession #	Primer Name[a]	Primer Sequence (5' > 3')
GGPPS1	*Gernanylgeranyl pyrophosphate 1*	Solyc11g011240.1.1	F1	GAAAGACAGCGGGTAAGGAC
			F2	**AAAGACAGCGGGTAAGGACC**
			R1	CATTCATGGCCTTAGCCATC
			R2	**AGCTCATTCATGGCCTTAGCC**
GGPPS2	*Gernanylgeranyl pyrophosphate 2*	Solyc04g079960.1.1	**F1**	**GTTGATAAAACGACGTATCCG**
			F2	AAAACGACGTATCCGAAGCTGC
			R1	GTTGTTTAGCTTCGCCGTTG
			R2	**AGCTGTTGTTTAGCTTCGC**
GGPPS3	*Gernanylgeranyl pyrophosphate 3*	Solyc02g085700.1.1	F1	GAAGGCATTTCTGATGTTGA
			F2	**GAAGGCATTTCTGATGTTGAT**
			R1	**CTCCTAATATAGCCCCTAGC**
			R2	CCTCCTAATATAGCCCCTAG
TPT1	*Geranylgeranyl pyrophosphate 4*	Solyc02g085710.2.1	F1	AGCAATGATTGGTGGTGCG
			F2	**AATGATTGGTGGTGCGTCC**
			R1	ACCTGAAACAGCAGTCCAAG
			R2	**GTCATCCACAACCTGAAACAG**

Table S1. (continued)

Gene	Full Name	Accession #	Primer Name	Primer Sequence (5' > 3')
TPT1	*Geranylgeranyl pyrophosphate 5*	Solyc02g085720.1.1	**F1**	**GTTGACATGCTGTGTGGAGA**
			F2	CATGCTGTGTGGAGATAAATG
			R1	**CCAAGCAATGCTCCTACAAT**
			R2	TCAGATGCACCACCAAGCAA
SSU II	*Gernanylgeranyl pyrophosphate 6*	Solyc09g008920.2.1	F1	TGCTTCAGATGAGGAGATCC
			F2	**CAGATGAGGAGATCCAACAC**
			R1	TCTCCGTCTTCTTTGCTTCC
			R2	**TTCCCCTCAGTTTTGTTCTCC**
PSY1	*Phytoene synthase 1*	Solyc03g031860.2.1	**F1:**	**TATTTGCTGGAAGGGTGACC**
			F2:	CTGGAAGGGTGACCGATAAA
			R1:	**CTGAGCTCAATTCTGTCACG**
			R2:	TAGCTGAGCTCAATTCTGTC
PSY2	*Phytoene synthase 2*	Solyc02g081330.2.1	F1	TGTGAGCAAGCCAAAGAAGC
			F2	**GAGCAAGCCAAAGAAGCTTC**
			R1	**CTAGTGGGGAAGAAGTTGAC**
			R2	TGCTAGTGGGGAAGAAGTTG
PSY3	*Phytoene synthase 3*	Solyc01g005940.2.1	**F1**	**ATGGAGAGAGTTCATGAAGG**
			F2	AGCAGATAAGAAGGGCAAGA
			R1	**TGGCCAACGACTAGCTTTGT**
			R2	GATGACCATACTGGCCAACG

Table S1. (continued)

Gene	Full Name	Accession #	Primer Name	Primer Sequence (5' > 3')
PDS	*Phytoene desaturase*	Solyc03g123760.2.1	**F1**	**AGGAAAGCTTTGTGCTCAAG**
			F2	GGAAAGCTTTGTGCTCAAGC
			R1	**AAACTACGCTTGCTTCCGAC**
			R2	CTAAACTACGCTTGCTTCCG
Z-ISO	*ζ-carotene isomerase*	Solyc12g098710.1.1	F1	TGCAGCCATTCTTGATGGTC
			F2	**AGCCATTCTTGATGGTCGTC**
			R1	**GGAAGTAAGCACCTAATGTC**
			R2	GAGGAAGTAAGCACCTAATG
ZDS	*ζ-carotene desaturase*	Solyc01g097810.2.1	**F1**	**TGTAATGTTGGAGAGCAGCTG**
			F2	AATGTTGGAGAGCAGCTGATG
			R1	**CTCAACTCATCAGATAGGGAC**
			R2	GACTCAACTCATCAGATAGGG
CrtISO	*Carotenoid isomerase*	Solyc10g081650.1.1	**F1**	**GTGTTGGCGATAGTTGCTTC**
			F2	GATAGTTGCTTCCCAGGAC
			R1	CCTAAGTCAGCTGCAACAC
			R2	**TTCAAACCCTAAGTCAGCTG**
CrtISO-L1	*Carotenoid isomerase like 1*	Solyc05g010180.2.1	F1	CTTTTCCTGGCATTGGAGTTC
			F2	**TTTCCTGGCATTGGAGTTCC**
			R1	AAGGCGCGAATGTTCTGAC
			R2	**AGAAGGCGCGAATGTTCTG**

Table S1. (continued)

Gene	Full Name	Accession #	Primer Name	Primer Sequence (5' > 3')
CrtISO-L2	*Carotenoid isomerase like 2*	Solyc02g085250.2.1	F1	ATCGGACTCCAATTGAAGGC
			F2	**CCAATTGAAGGCCTATACTTG**
			R1	**CTCAATGACAACATGCGCAG**
			R2	CTTGAAGTCCTCAATGACAAC
β-LCY1	*Lycopene β-cyclase 1*	Solyc04g040190.1.1	**F1**	**CTTCTGAAGCTTGATTTACCT**
			F2	TACCTGCTACAAGAAGGTTC
			R1	**CAATCGAGACGATAAGAAG**
			R2	CAGGTAGAAACAATCGAGAC
β-LCY2	*Lycopene β-cyclase 2*	Solyc10g079480.1.1	**F1**	**CTTCTGAAGCTTGATTTATCC**
			F2	CTGAAGCTTGATTTATCCGC
			R1	**TGAGTTCAGGAAGAAACAGC**
			R2	CATGAGTTCAGGAAGAAACAG
BCH1	*β-carotene hydroxylase 1*	Solyc06g036260.2.1	**F1**	**CCCATATGGCTTGTTCTTC**
			F2	GTTCTTCGGACCTAAGGAAC
			R1	**CATGATCCTTTCGAAAGTCTC**
			R2	CGTTCATGATCCTTTCGAAAG
BCH2	*β-carotene hydroxylase 2*	Solyc03g007960.2.1	**F1**	**CATAAGAGATTTCCCGTAGGG**
			F2	TAGGGCCTATTGCCAACGTG
			R1	**GGGACACCATCAAATTTGTCC**
			R2	AAGCCATATGGGACACCATC

Table S1. (continued)

Gene	Full Name	Accession #	Primer Name	Primer Sequence (5' > 3')
ZEP	*Zeaxanthin epoxidase*	Solyc02g090890.2.1	F1	CTTCTGAAAGGAAGGAAGAG
			F2	**TCTGAAAGGAAGGAAGAGCG**
			R1	TGCTCAACGCCTGATGTTTG
			R2	**AAATTGCTCAACGCCTGATG**
VDE	*Violaxanthin de-epoxidase*	Solyc04g050930.2.1	**F1**	**GAAAGTGGAAGAAGGAGAGC**
			F2	AAGAAGGAGAGCGGACAATC
			R1	AACCTTCGAACAGTCTACTG
			R2	**GAAACCTTCGAACAGTCTAC**
NSY	*Neoxanthin synthase*	Solyc06g074240.1.1	F1	TCGGACATGGCTCAAACATG
			F2	**CATGGCTCAAACATGACTAGG**
			R1	CTCTCTATTGCTAGATTGCC
			R2	**GCTCTCTATTGCTAGATTGC**
ε-LCY	*Lycopene ε-cyclase*	Solyc12g008980.1.1	F1	CTTGGTTCAAGTCTTTCTTCAG
			F2	**CAAGTCTTTCTTCAGCAGAC**
			R1	GCCTTTTCTCATGTCATTTGG
			R2	**GATCAAGCCTTTTCTCATGTC**
CYP97A29	*Cytochrome P450-type monooxygenase 97A29*	Solyc04g051190.2.1	**F1**	**TCAAATGGCTCTTGGAGCTC**
			F2	AAATGGCTCTTGGAGCTCC
			R1	**TGGAGGTCTTGATCTTCGTG**
			R2	TGGGAACTATTGGAGGTCTTG

Table S1. (continued)

Gene	Full Name	Accession #	Primer Name	Primer Sequence (5' > 3')
CYP97C11	*Cytochrome P450-type monooxygenase 97C11*	Solyc10g083790.1.1	**F1**	**GTTGGAAGCTACAATTGCTC**
			F2	TGGAAGCTACAATTGCTCTC
			R1	GTTGCTCCAGTAGTCATGC
			R2	**TGGTTGCTCCAGTAGTCATG**
CAC (Control)	*Clathrin adaptor complexes medium subunit*	Solyc08g006960.2.1	F1	AAAAGTCCTTGACTCGTCCG
			F2	**TGACTCGTCCGCCAATTCAA**
			R1	**TCTCCCACACCTTGAGAAAC**
			R2	TTGTAGCCACTCTTCTCCCAC
Expressed (Control)	*Expressed sequence*	Solyc07g025390.2.1	**F1**	**CACACCCAAATGCACCAGTT**
			F2	ACACCCAAATGCACCAGTTG
			R1	CACCGTAACACAATGGAAGC
			R2	**ACACCGTAACACAATGGAAG**

[a]The best primer pair for each gene was in bold and used for real-time RT-PCR for the measurement of the relative expression levels of each gene.

Table S2. Optimized real-time RT-PCR conditions for the 25 carotenoid biosynthetic pathway genes and the 2 reference genes (*Expressed* and *CAC*).

Gene	Primer Pair	Amplicon Length (bp)	Optimal Tm (ºC)	Optimal Primer Conc. (nM)	cDNA Dilution	R^2	E (%)
GGPPS1	F1/R1[a]	-	-	-	-	-	-
	F1/R2	115	59.0	350	1 – 1/16	0.9888	101.8
	F2/R1	-	-	-	-	-	-
	F2/R2[b]	**114**	**59.0**	**300**	**1/5 – 1/20**	**0.9955**	**99.7**
GGPPS2	F1/R1	85	59.0	350	1/10 – 1/160	0.9996	93.6
	F1/R2	**89**	**59.0**	**350**	**1/10 – 1/160**	**0.9999**	**99.1**
	F2/R1	79	59.0	300	1/10 – 1/160	0.9963	88.8
	F2/R2	83	59.0	300	1/10 – 1/160	0.9986	95.0
GGPPS3	F1/R1	103	56.8	350	1/10 – 1/160	0.9908	112.8
	F1/R2	104	56.8	350	1/10 – 1/160	0.9998	89.0
	F2/R1	**103**	**59.0**	**350**	**1/10 – 1/160**	**0.9994**	**95.0**
	F2/R2	104	56.8	350	1/10 – 1/160	0.9964	94.5
TPT1	F1/R1	81	56.8	350	1/40 – 1/160	1.000	109.8
	F1/R2	91	56.8	300	1/10 – 1/80	0.9979	93.9
	F2/R1	78	56.8	350	1/20 – 1/160	0.9997	110.7
	F2/R2	**88**	**59.0**	**300**	**1/10 – 1/80**	**0.9995**	**94.3**
TPT2	**F1/R1**	**116**	**59.0**	**350**	**1/5 – 1/80**	**0.9932**	**103.4**
	F1/R2	128	59.0	300	1 – 1/16	0.9919	94.3

Table S2. (continued)

Gene	Primer Pair	Amplicon Length (bp)	Optimal Tm (ºC)	Optimal Primer Conc. (nM)	cDNA Dilution	R^2	E (%)
	F2/R1	111	59.0	350	1 – 1/16	0.9593	80.6
	F2/R2	121	59.0	300	1 – 1/16	0.9953	98.6
SSU II	F1/R1	101	56.8	350	1/100 – 1/1600	0.9654	139.7
	F1/R2	117	56.8	300	1/100 – 1/1600	0.9920	108.8
	F2/R1	96	56.8	350	1/100 – 1/1600	0.9849	111.8
	F2/R2	**112**	**59.0**	**350**	**1/10 – 1/80**	**0.9994**	**99.6**
PSY1	**F1/R1**	**111**	**59.0**	**300**	**1/10 – 1/40**	**0.9977**	**98.2**
	F1/R2	114	59.0	300	1/200 – 1/1600	0.9942	86.3
	F2/R1	105	59.0	300	1/100 – 1/800	0.9998	92.4
	F2/R2	108	59.0	300	1/100 – 1/800	0.9941	96.85
PSY2	F1/R1	86	56.8	350	1/10 – 1/160	0.9967	103.3
	F1/R2	88	56.8	300	1/10 – 1/160	0.9997	85.2
	F2/R1	**83**	**59.0**	**350**	**1/10 – 1/160**	**0.9988**	**102.3**
	F2/R2	85	56.8	300	1/10 – 1/160	0.9978	88.9
PSY3	**F1/R1**	**100**	**59.0**	**300**	**1/20 – 1/80**	**0.9910**	**101.8**
	F1/R2	-	-	-	-	-	-
	F2/R1	80	56.8	350	1/20 – 1/160	0.9833	90.1
	F2/R2	-	-	N/A	-	-	-
PDS	**F1/R1**	**89**	**59.0**	**350**	**1/10 – 1/160**	**0.9955**	**99.2**

Table S2. (continued)

Gene	Primer Pair	Amplicon Length (bp)	Optimal Tm (ºC)	Optimal Primer Conc. (nM)	cDNA Dilution	R^2	E (%)
	F1/R2	91	59.0	350	1/10 – 1/160	0.9998	87.0
	F2/R1	88	59.0	300	1/10 – 1/160	0.9818	90.0
	F2/R2	90	59.0	350	1/10 – 1/160	0.9998	89.1
Z-ISO	F1/R1	107	56.8	350	1/100 - 1/1600	0.9987	105.2
	F1/R2	109	56.8	350	1/100 – 1/1600	0.9974	98.2
	F2/R1	**104**	**59.0**	**350**	**1/5 – 1/80**	**0.9987**	**99.0**
	F2/R2	106	56.8	300	1/100 – 1/1600	0.9928	91.1
ZDS	**F1/R1**	**98**	**59.0**	**300**	**1/10 – 1/160**	**0.9988**	**99.1**
	F1/R2	100	56.8	300	1/10 – 1/160	0.9994	93.3
	F2/R1	95	56.8	300	1/10 – 1/160	0.9995	104.4
	F2/R2	97	56.8	300	1/10 – 1/160	0.9994	94.8
CrtISO	F1/R1	91	59.0	350	1/10 – 1/80	0.9992	111.6
	F1/R2	**98**	**59.0**	**350**	**1/10 – 1/40**	**0.9987**	**105.1**
	F2/R1	83	59.0	350	1/10 – 1/80	0.9971	86.7
	F2/R2	90	59.0	300	1/10 – 1/80	0.9993	110.5
CrtISO-	F1/R1	89	59.0	300	1/10 – 1/160	0.9954	99.3
L1	F1/R2	91	59.0	300	1/10 – 1/160	0.9939	91.9
	F2/R1	87	59.0	350	1/10 – 1/160	0.9972	96.8
	F2/R2	**89**	**59.0**	**350**	**1/10 – 1/160**	**0.9985**	**100.9**

Table S2. (continued)

Gene	Primer Pair	Amplicon Length (bp)	Optimal Tm (ºC)	Optimal Primer Conc. (nM)	cDNA Dilution	R^2	E (%)
CrtISO-L2	F1/R1	104	59.0	300	1/10 – 1/160	0.9902	111.1
	F1/R2	113	59.0	350	1/10 – 1/160	0.9983	90.7
	F2/R1	**96**	**59.0**	**350**	**1/10 – 1/160**	**0.9983**	**100.6**
	F2/R2	105	59.0	350	1/10 – 1/160	0.9992	95.1
β-LCY1	**F1/R1**	**85**	**59.0**	**350**	**1/10 – 1/80**	**0.9987**	**98.7**
	F1/R2	88	56.8	350	1/10 – 1/160	0.9984	93.9
	F2/R1	77	56.8	350	1/10 – 1/160	0.9902	92.3
	F2/R2	80	56.8	350	1/10 – 1/160	0.9989	96.0
β-LCY2	**F1/R1**	**111**	**59.0**	**350**	**1/5 – 1/80**	**0.9954**	**100.1**
	F1/R2	121	56.8	350	1/5 – 1/80	0.9963	90.5
	F2/R1	109	56.8	350	1/5 – 1/80	0.9950	99.7
	F2/R2	119	56.8	350	1/5 – 1/80	0.9988	93.6
BCH1	**F1/R1**	**105**	**59.0**	**300**	**1/10 – 1/320**	**0.9990**	**102.0**
	F1/R2	109	59.0	350	1/10 – 1/160	0.9977	105.5
	F2/R1	93	59.0	350	1/10 – 1/160	0.9859	87.7
	F2/R2	97	59.0	350	1/10 – 1/160	0.9805	104.0
BCH2	**F1/R1**	**101**	**59.0**	**300**	**1/20 – 1/80**	**0.9991**	**97.3**
	F1/R2	110	59.0	300	1/10 – 1/40	0.9971	96.2
	F2/R1	-	-	-	-	-	-

Table S2. (continued)

Gene	Primer Pair	Amplicon Length (bp)	Optimal Tm (ºC)	Optimal Primer Conc. (nM)	cDNA Dilution	R^2	E (%)
	F2/R2	-	-	-	-	-	-
ZEP	F1/R1	-	-	-	-	-	-
	F1/R2	-	-	-	-	-	-
	F2/R1	105	59.0	350	1/10 – 1/160	0.9945	89.5
	F2/R2	**109**	**59.0**	**350**	**1/10 – 1/40**	**0.9991**	**99.7**
VDE	F1/R1	113	56.8	350	1/10 – 1/160	0.9926	117.2
	F1/R2	115	59.0	350	1/5 – 1/80	0.9969	95.5
	F2/R1	**105**	**56.8**	**350**	**1/10 – 1/160**	**0.9965**	**107.4**
	F2/R2	107	56.8	350	1/10 – 1/160	0.9936	95.1
NSY	F1/R1	91	56.8	300	1/5 – 1/80	0.9537	101.76
	F1/R2	92	56.8	300	1/5 - 1/80	0.9894	87.5
	F2/R1	86	56.8	300	1/5 – 1/80	0.9973	111.5
	F2/R2	**87**	**59.0**	**300**	**1/5 – 1/40**	**0.9995**	**97.5**
ε-LCY	F1/R1	84	56.8	300	1/20 – 1/320	0.9537	101.8
	F1/R2	90	56.8	300	1/20 – 1/320	0.9894	87.5
	F2/R1	77	56.8	300	1/20 – 1/320	0.9973	111.5
	F2/R2	**83**	**59.0**	**300**	**1/20 – 1/80**	**0.9995**	**100.8**
CYP97A29	**F1/R1**	**103**	**59.0**	**350**	**1/10 – 1/160**	**0.9986**	**102.7**
	F1/R2	113	59.0	350	1/10 – 1/160	0.9964	89.2

Table S2. (continued)

Gene	Primer Pair	Amplicon Length (bp)	Optimal Tm (ºC)	Optimal Primer Conc. (nM)	cDNA Dilution	R^2	E (%)
	F2/R1	101	59.0	350	1/10 – 1/160	0.9996	107.9
	F2/R2	111	59.0	350	1/10 – 1/160	0.9897	111.1
CYP97C11	F1/R1	93	56.8	350	1/10 – 1/160	0.9863	130.2
	F1/R2	**95**	**59.0**	**300**	**1/10 – 1/160**	**0.9974**	**103.6**
	F2/R1	91	56.8	350	1/10 – 1/160	0.9996	115.5
	F2/R2	93	56.8	300	1/10 – 1/160	0.9974	96.0
CAC	F1/R1	96	56.8, 59.0	350	1/10 - 1/160	0.9994	110.5
(Control)	F1/R2	109	56.8, 59.0	350	1/10 - 1/160	0.9989	95.2
	F2/R1	**87**	**56.8, 59.0**	**350**	**1/10 – 1/160**	**0.9989**	**98.6**
	F2/R2	100	56.8, 59.0	350	1/10 - 1/160	0.9969	97.96
Expressed	F1/R1	110	56.8, 59.0	350	1/10 – 1/160	0.9985	105.6
(Control)	**F1/R2**	**111**	**56.8, 59.0**	**250**	**1/10 – 1/160**	**0.9976**	**100.2**
	F2/R1	109	56.8, 59.0	350	1/10 – 1/160	0.9919	111.5
	F2/R2	110	56.8, 59.0	250	1/10 – 1/160	0.9983	111.2
	F1/R2	113	59.0	350	1/10 – 1/160	0.9964	89.2

[a]The primer pair failed for real-time RT-PCR. [b]The best primer pair for each gene was in bold and used for real-time RT-PCR for the measurement of the relative expression levels of each gene.

Table S3. Comparison of the relative expression levels of the carotenoid biosynthesis pathway genes in all the 42 tomato cultigens at each stage as a group with that of the non-functional *crtiso* gene in NC 1Y (* denotes *p*-value < 0.05 using a two-tailed student's t-test with two-sample unequal variance, i.e., significantly different from *crtiso* in NC 1Y).

Gene	Breaker			Ripe		
	Average	Standard Deviation	*p*-value	Average	Standard Deviation	*p*-value
Upstream genes						
GGPPS1	0.12	0.05	0.03 *	0.13	0.05	4.95E-46 *
GGPPS2	3.62	4.20	1.22E-14 *	2.37	2.12	4.18E-21 *
GGPPS3	8.75	4.23	1.53E-40 *	6.17	2.51	2.00E-49 *
TPT1	0.59	0.27	6.19E-19 *	0.54	0.27	5.80E-41 *
TPT2	0.03	0.03	0.46	0.01	0.01	0.04 *
SSU II	14.15	4.59	3.81E-56 *	10.50	3.57	3.79E-57 *
PSY1	473.64	275.73	5.84E-33 *	391.50	153.12	3.95E-51 *
PSY2	3.56	4.41	6.03E-13 *	3.67	3.31	3.94E-21 *
PSY3	0.03	0.03	0.452236	0.05	0.07	2.70E-09 *
PDS	13.33	7.70	6.8E-32 *	7.88	3.49	6.55E-46 *
Z-ISO	144.09	87.95	3.16E-30 *	120.03	59.71	2.60E-41 *
ZDS	13.33	7.70	1.47E-32 *	11.39	6.05	8.97E-39 *
CrtISO	13.90	14.12	4.62E-17 *	8.90	5.24	6.34E-35 *
CrtISO-L1	3.21	3.12	9.08E-18 *	2.43	2.04	7.55E-23 *
CrtISO-L2	0.37	0.25	1.23E-13 *	0.68	0.32	2.30E-42 *

Table S3. (continued)

Gene	Breaker			Ripe		
	Average	**Standard Deviation**	***p*-value**	**Average**	**Standard Deviation**	***p*-value**
Downstream genes						
β-LCY1	0.06	0.08	0.12	0.06	0.06	3.09E-15 *
β-LCY2	0.02	0.03	0.67	0.01	0.01	1.29E-05 *
BCH1	1.08	1.41	1.61E-11 *	1.56	1.22	4.20E-25 *
BCH2	0.06	0.10	0.07	0.04	0.03	3.08E-23 *
ZEP	1.14	0.98	8.20E-21 *	1.02	0.75	8.56E-27 *
VDE	2.43	2.25	9.77E-19 *	1.70	1.59	7.87E-20 *
NSY	0.07	0.07	0.07	0.05	0.05	2.23E-16 *
ε-LCY	0.06	0.07	0.12	0.01	0.02	0.98
CYP97A29	0.55	0.40	4.68E-21 *	0.33	0.19	6.54E-34 *
CYP97C11	1.60	1.33	5.77E-22 *	0.79	0.60	1.81E-25 *

Table S4. Comparison of the relative expression levels of the upstream genes leading to lycopene biosynthesis in the carotenoid biosynthesis pathway in the 42 tomato cultigens at each stage as a group with that of the positive control wild tomato (* denotes *p*-value < 0.05 using a two-tailed student's t-test with two-sample unequal variance, i.e., significantly different from that in the wild tomato).

Gene	**Breaker**			**Ripe**		
	Average	**Standard Deviation**	***p*-value**	**Average**	**Standard Deviation**	***p*-value**
GGPPS1	0.12	0.05	0.01 *	0.13	0.05	0.76
GGPPS2	3.62	4.20	0.40	2.37	2.12	0.01 *
GGPPS3	8.75	4.23	0.57	6.17	2.51	0.07
TPT1	0.59	0.27	0.26	0.54	0.27	4.83E-3 *
TPT2	0.03	0.03	0.05 *	0.01	0.01	6.59E-06 *
SSU II	14.15	4.59	0.28	10.50	3.57	0.16
PSY1	473.64	275.73	0.13	391.50	153.12	0.12
PSY2	3.56	4.41	1.01E-09 *	3.67	3.31	1.10E-19 *
PSY3	0.03	0.03	0.28	0.05	0.07	0.54
PDS	13.33	7.70	0.47	7.88	3.49	0.71
Z-ISO	144.09	87.95	0.37	120.03	59.71	0.59
ZDS	13.33	7.70	0.34	11.39	6.05	8.03E-06 *
CrtISO	13.90	14.12	0.58	8.90	5.24	0.86
CrtISO-L1	3.21	3.12	2.69E-08 *	2.43	2.04	1.35E-05 *
CrtISO-L2	0.37	0.25	0.48	0.68	0.32	3.81E-4 *

Table S5. Comparison of the relative expression levels of the downstream genes after lycopene biosynthesis in the carotenoid biosynthesis pathway in the fruits of the 42 tomato cultigens at each stage as a group with that of the positive control wild tomato (* denotes *p*-value < 0.05 using a two-tailed student's t-test with two-sample unequal variance, i.e., significantly different from that in the wild tomato).

Gene	**Breaker**			**Ripe**		
	Average	**Standard Deviation**	***p*-value**	**Average**	**Standard Deviation**	***p*-value**
β-LCY1	0.06	0.08	0.13	0.06	0.06	2.46E-17 *
β-LCY2	0.02	0.03	0.54	0.01	0.01	2.47E-07 *
BCH1	1.08	1.41	2.42E-3 *	1.56	1.22	9.81E-18 *
BCH2	0.06	0.10	6.27E-07 *	0.04	0.03	0.02 *
ZEP	1.14	0.98	0.53	1.02	0.75	8.39E-18 *
VDE	2.43	2.25	1.24E-17 *	1.70	1.59	3.13E-19 *
NSY	0.07	0.07	0.07	0.05	0.05	0.21
ε-LCY	0.06	0.07	2.05E-08 *	0.01	0.02	0.29
CYP97A29	0.55	0.40	0.46	0.33	0.19	0.05
CYP97C11	1.60	1.33	0.01 *	0.79	0.60	1.83E-08 *

Appendix B

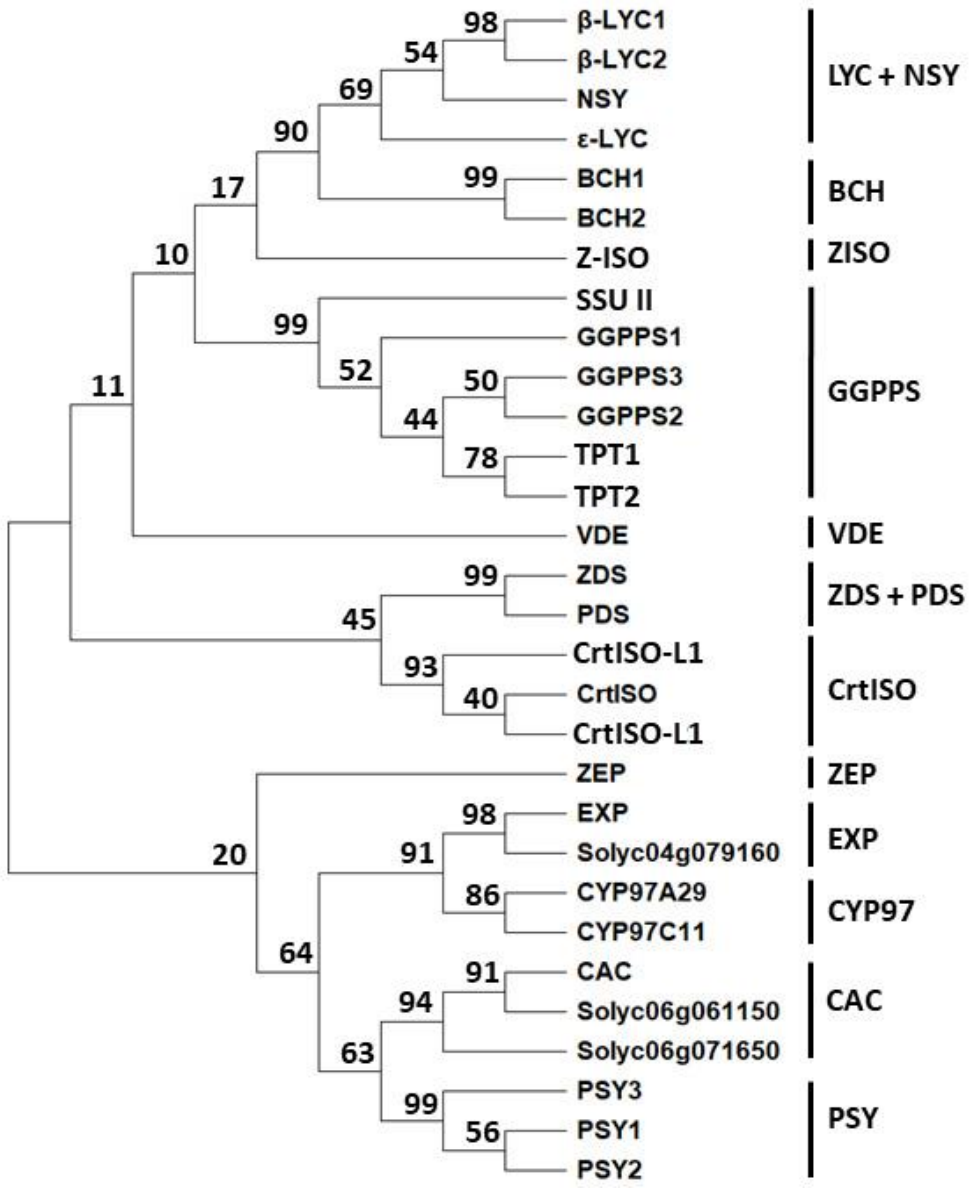

Figure S1. Phylogenetic tree of the carotenoid biosynthesis genes and the internal reference genes in tomato. The tree was constructed using the maximum likelihood method and the full-length protein sequences of those genes and tested with 1,000 bootstrap replications. Bootstrap values are presented at their corresponding nodes. The cDNA sequence alignment of the grouped genes on the right were used for sequence-specific primer design.

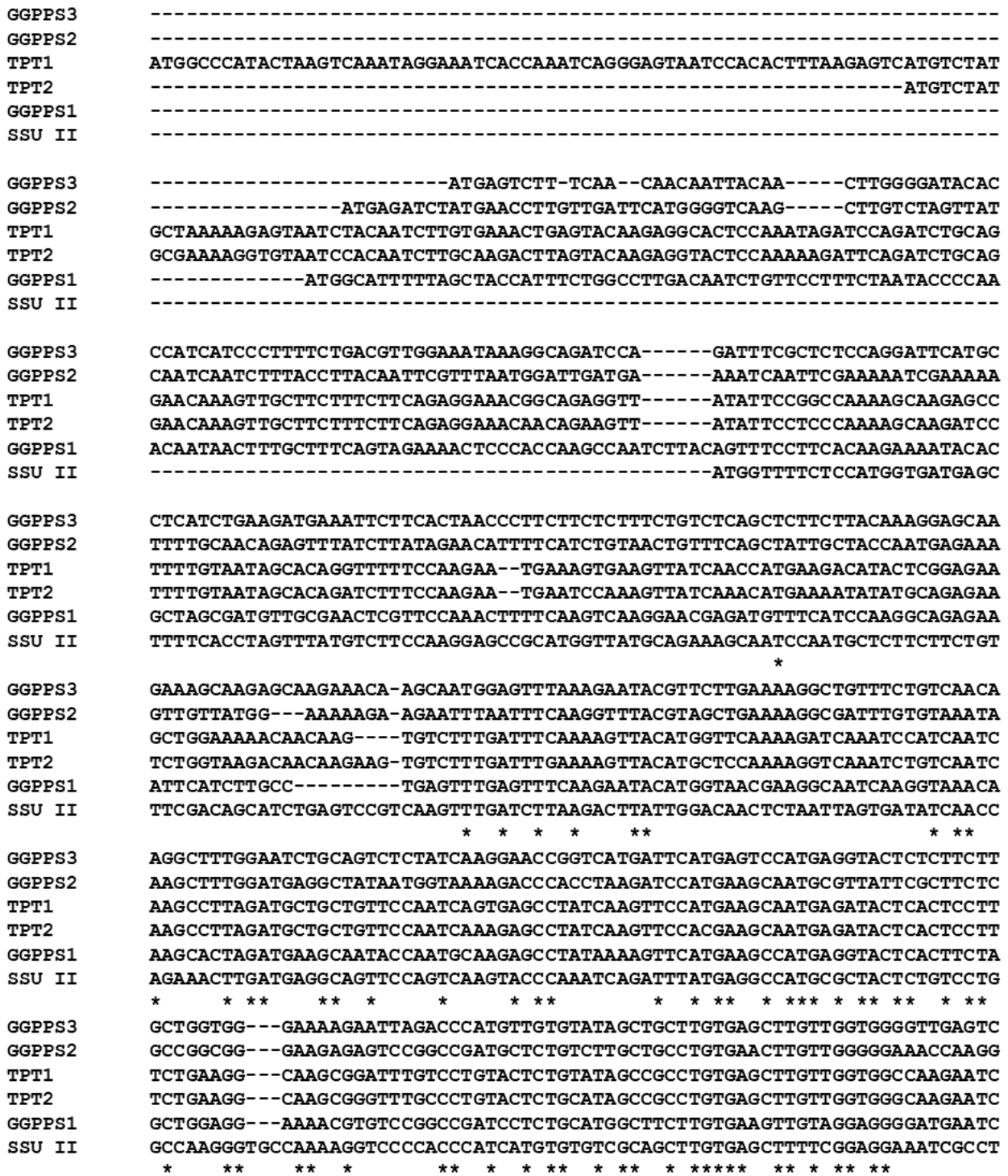

Figure S2. Alignment of the cDNA sequences of the tomato *GGPPS1-3, TPT1, TPT2* and *SSUII* genes for real-time RT-PCR primer design.

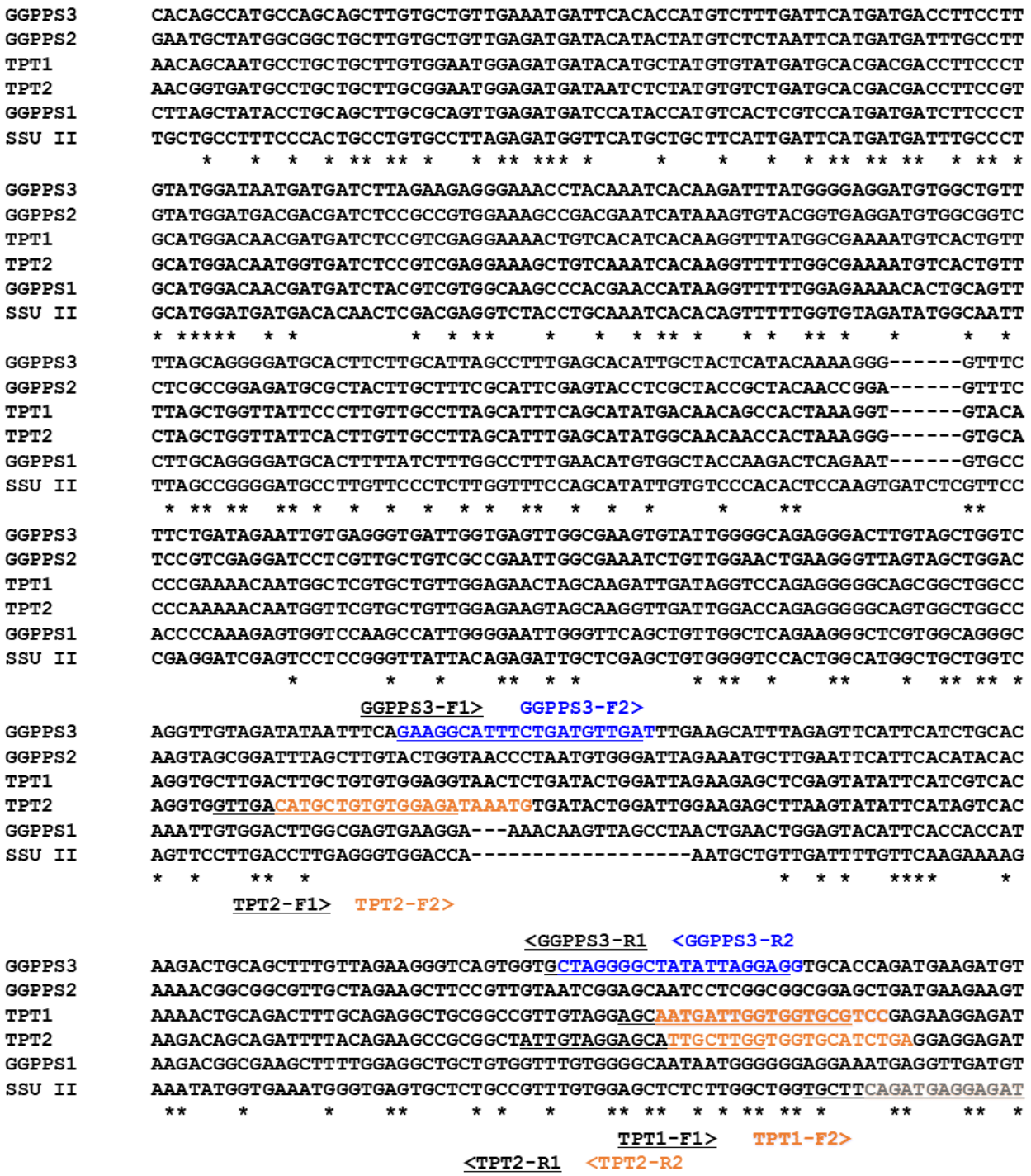

Figure S2. (continued)

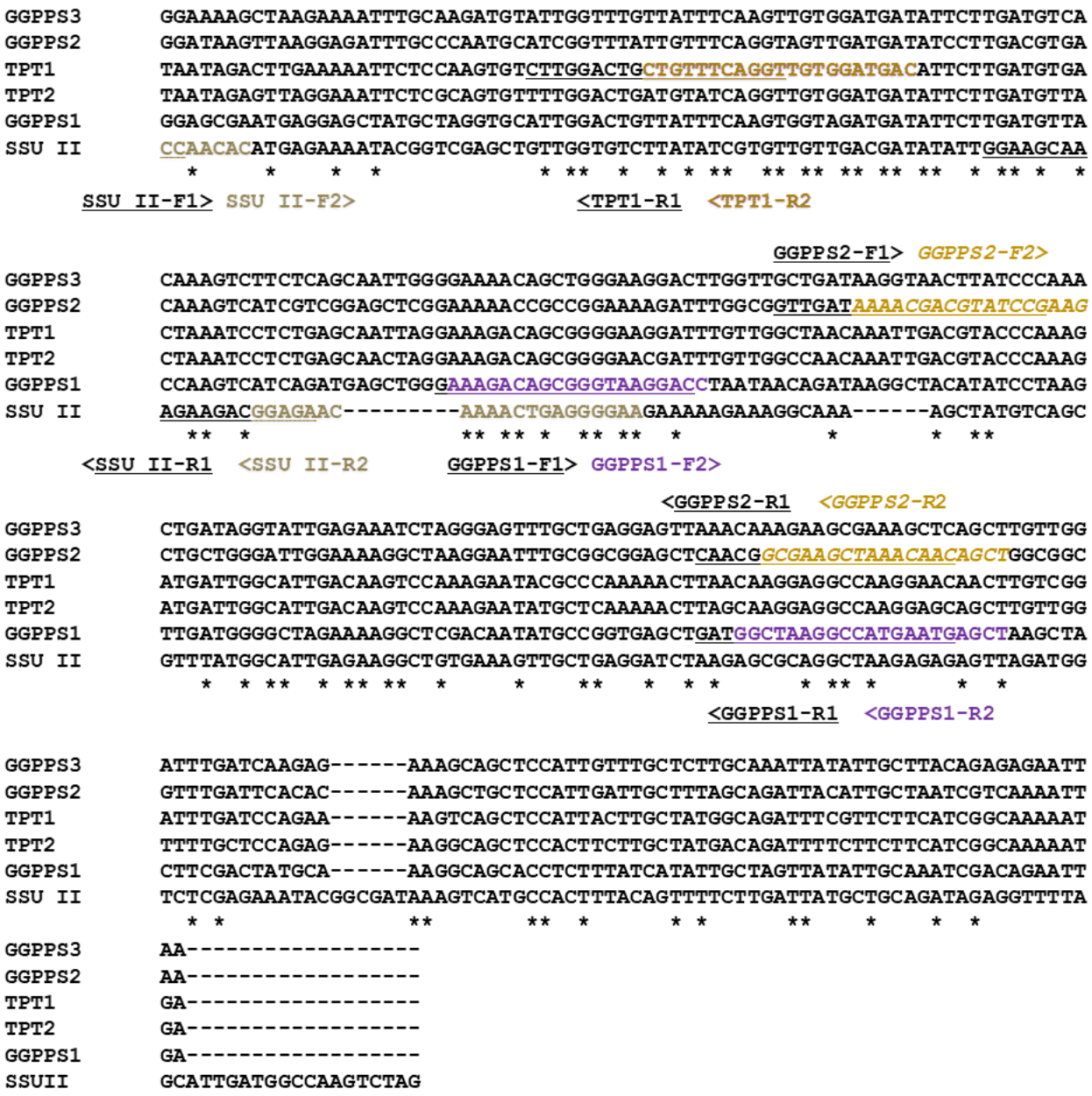

Figure S2. (continued)

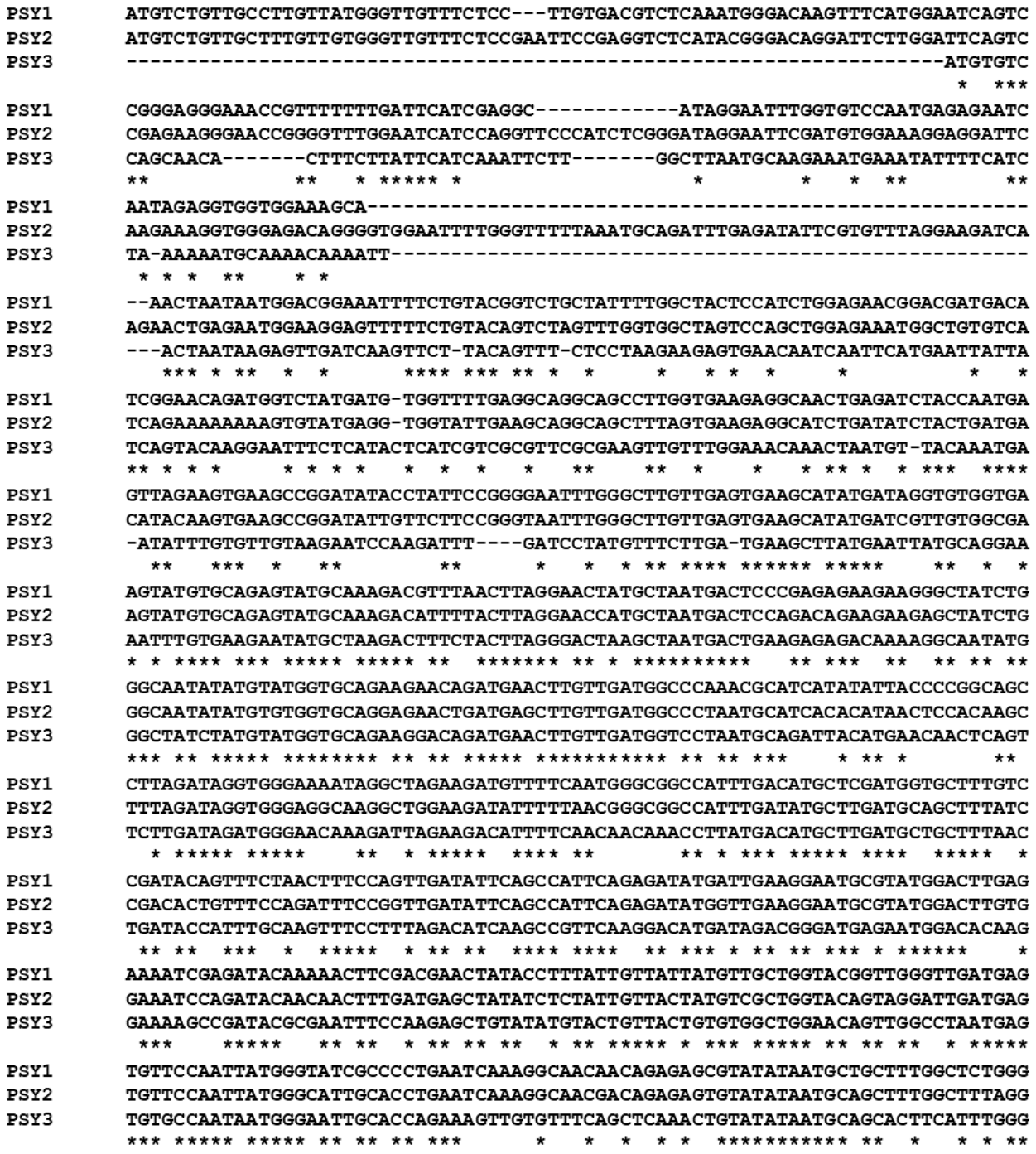

Figure S3. Alignment of the cDNA sequences of the tomato *PSY1-3* genes for real-time RT-PCR primer design.

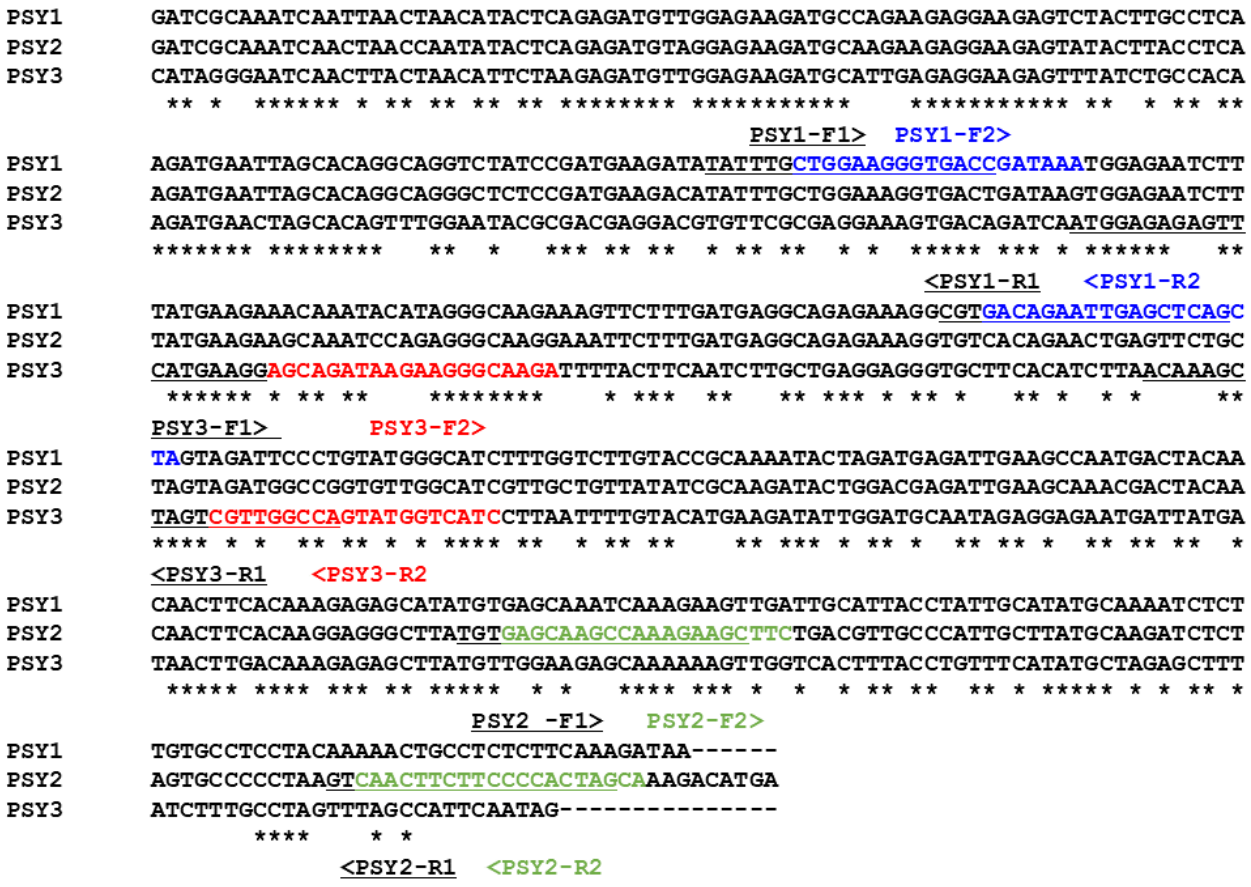

Figure S3. (continued)

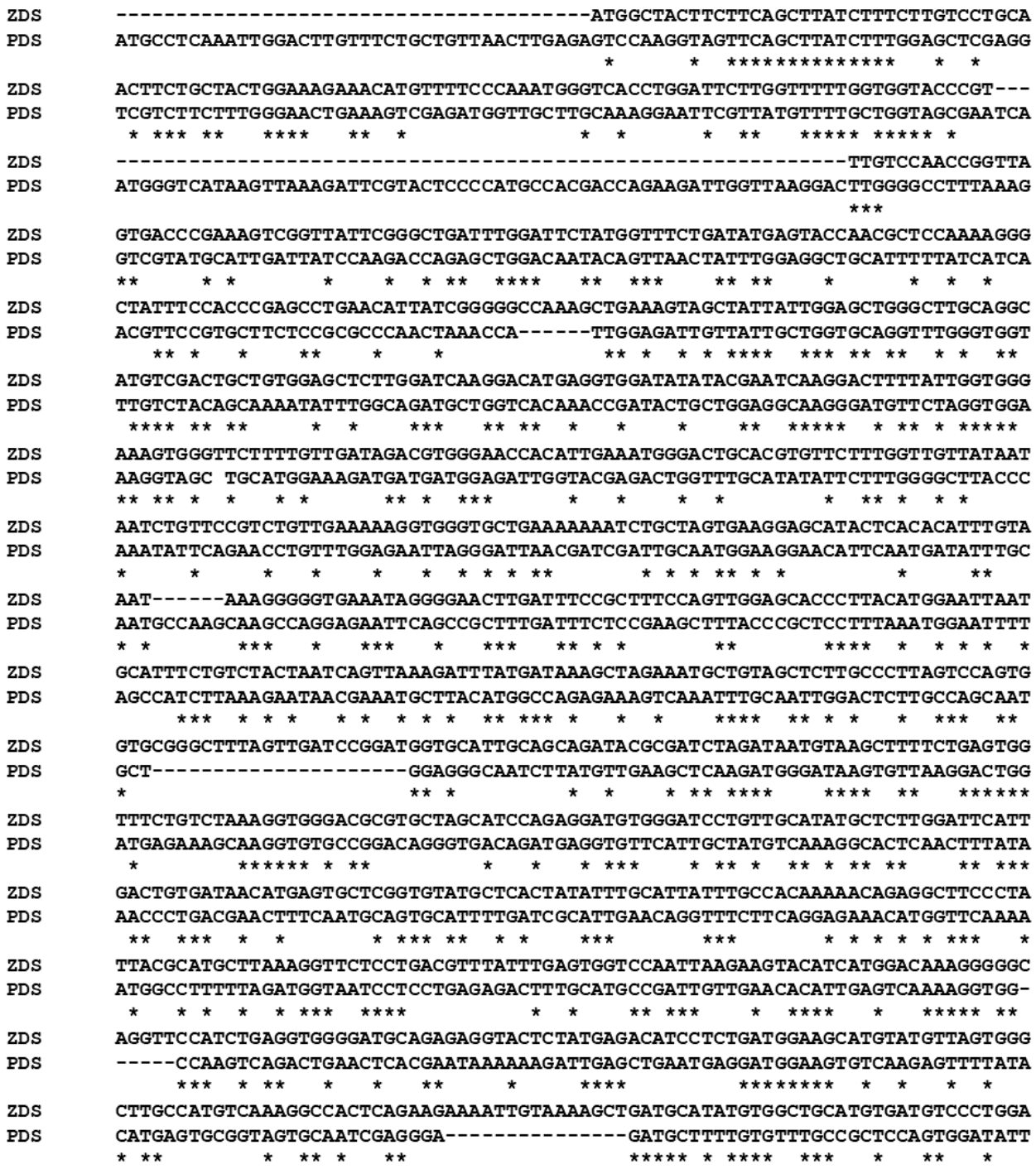

Figure S4. Alignment of the cDNA sequences of the tomato *PDS* and *ZDS* genes for real-time RT-PCR primer design.

Figure S4. (continued)

```
Z-ISO      ATGGCAACTTCAATTTTTCTCTCACACCCTTTTTCTCATTTATTATCAAAACACCATAAAATTCCAAGTCCTA

Z-ISO      AACAAACCATAGCCATAGCATATCACTCCACCAACAAACCCACCACCAAGACTCCATTTTTACCATTACCCAC

Z-ISO      TTCCTTTTTTCCATTTCCCTCAAACCCCAGAAAGGAATTTTGGCCAATTTCAGTGGGAAGAACACAAACAGAT

Z-ISO      GAAAAAGATGAAATCTTGGTGGTGGGTGAAGATTCTGCTGAATTTGAGTTATCCAAACAAAAGATTTCATCTT

Z-ISO      GGGTTTATTTTGCTGGGGTTCTTGGTGTTGTGCTTTATGTTCTTAATGTTGTTTGGATTGACAATTCTACTGG

Z-ISO      ATTTGGAAAATCATTCATTGATTCTGTTTCTAGTATTTCAGATAGCCCTGAAATTGTAATGCTTTCCCTTACC

Z-ISO      TTGATTTTCGCTATAGTCCACAGTGGTCTTGCTAGTCTTAGAGACAAAGGTGAGGAACTCATTGGAGAGCGTG

Z-ISO      CTTTTCGTGTATTGTTTGCTGGGGTATCTCTGCCATTGGCAGTCAGCACAATTGTGTATTTCATTAACCACCG

Z-ISO      ATACGATGGAGTGCAGTTATGGCAATTAAACAGTGTTGCTGGGATTCACGAACTAGTTTGGATTTCTAACTTT

Z-ISO      GTTTCCTTCTTCTTCCTATACCCGTCGACATTCAATTTACTAGAGGTAGCGGCTGTTGACAAGCCCAAGATGC

Z-ISO      ATCTTTGGGAAACTGGGATTATGAGGATTACCAGGCATCCACAGCTGGTCGGGCAGGTTATATGGTGCTTAGC

Z-ISO      TCACACGCTGTGGATTGGGAATTCAGTTGCAGTGGCAGCTTCAGTAGGTTTGATAGGACATCATCTGTTTGGT

Z-ISO      GCCTGGAATGGGGACCGGAGGTTAGCCATACGATATGGTGAGGCTTTTGAAGTCGTGAAGAACAGAACGAGTA
                    ZISO-F1>    ZISO-F2>
Z-ISO      TCATTCCATTTGCAGCCATTCTTGATGGTCGTCAAAAGTTGCCTGAAGATTATTACAAGGAATTTATCAGATT

Z-ISO      GCCATATTTATCGATAACAACATTGACATTAGGTGCTTACTTCCTCCACCCCATTATGCAAGCTGCCAGTTAT
                                  <ZISO-R1    <ZISO-R2
Z-ISO      CGGCTACACTGGTAG
```

Figure S5. The cDNA sequence of the tomato *Z-ISO* gene for real-time RT-PCR primer design.

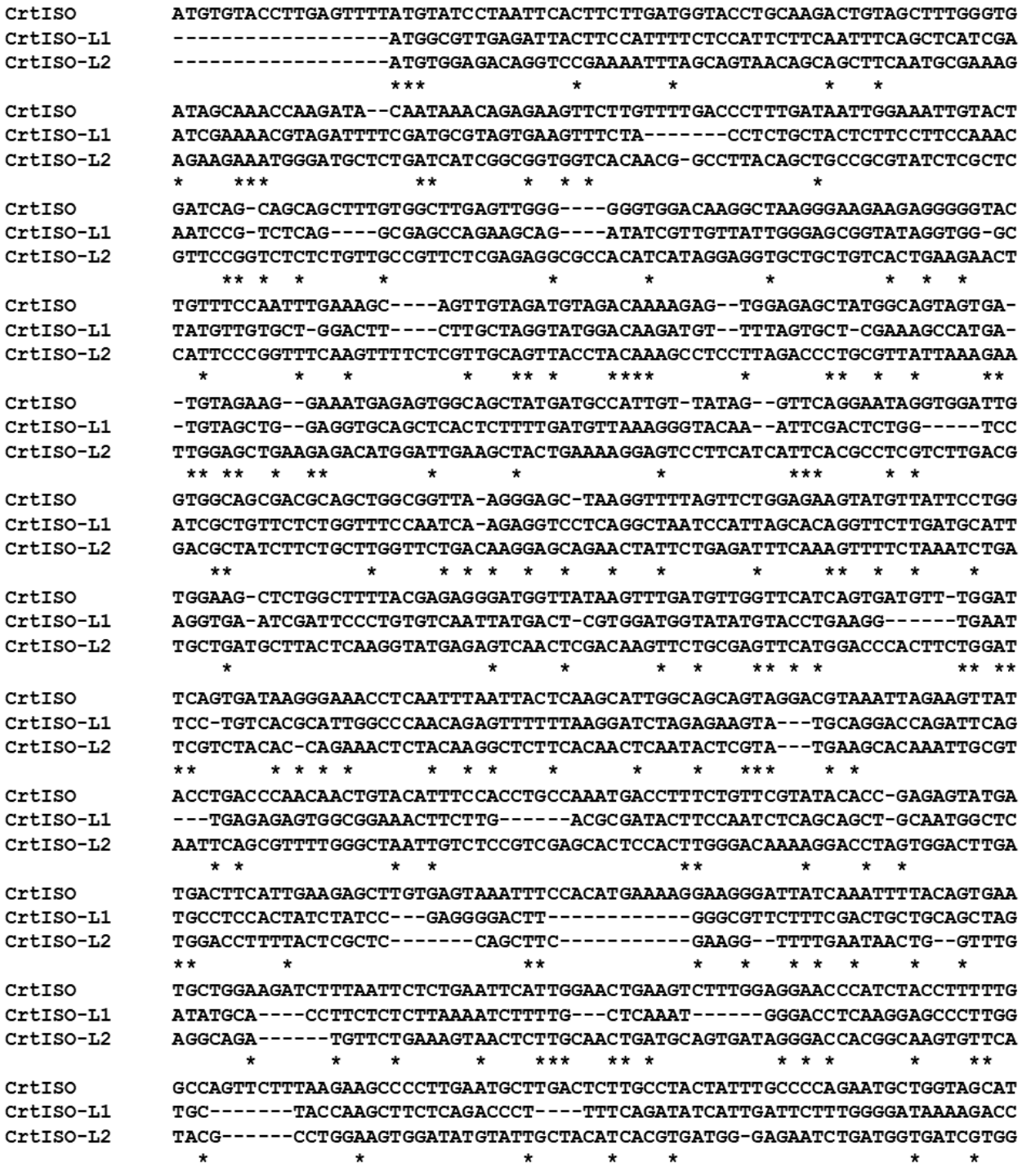

Figure S6. Alignment of the cDNA sequences of the tomato *CrtISO*, *CrtISO-L1* and *CrtISO-L2* genes for real-time RT-PCR primer design.

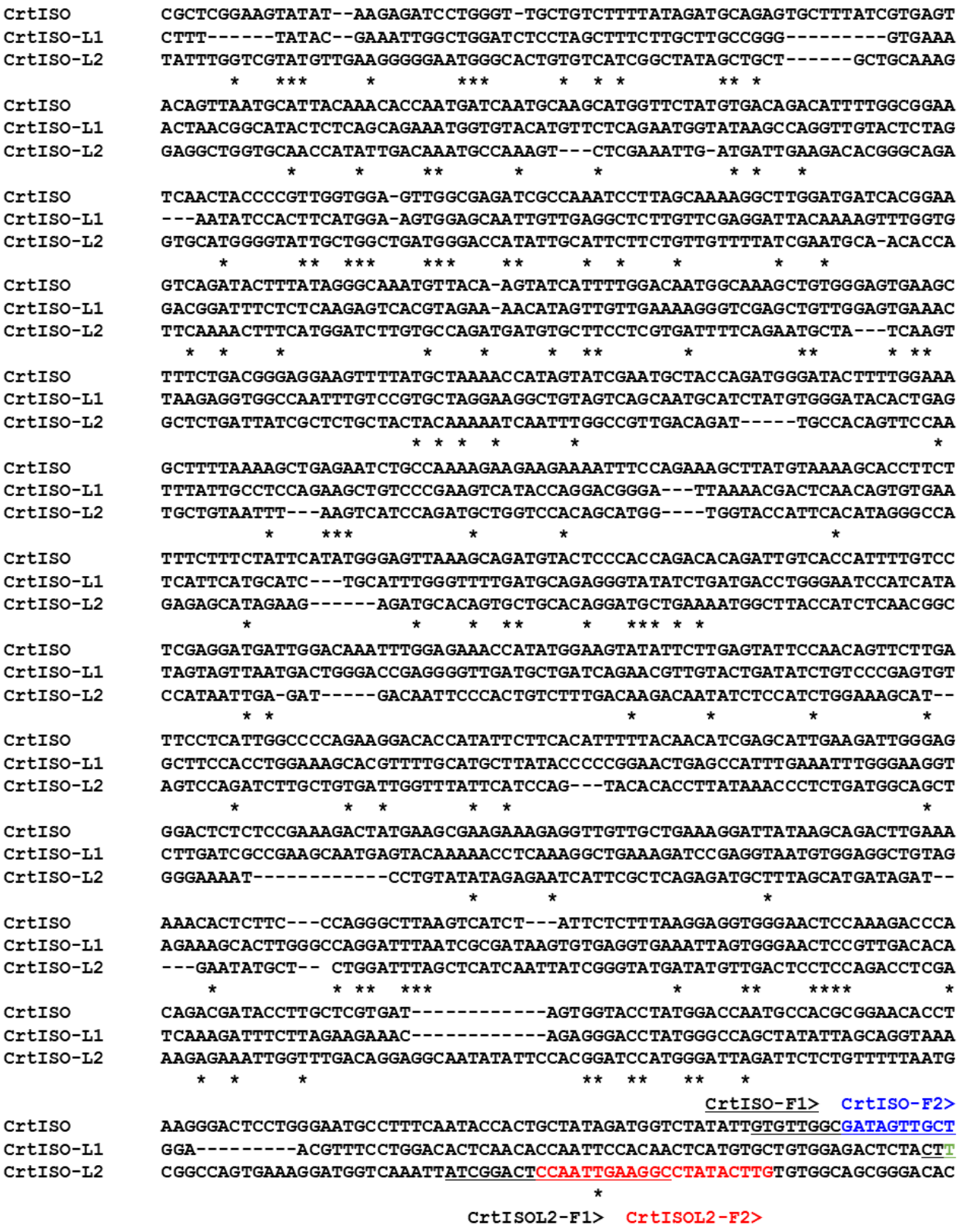

Figure S6. (continued)

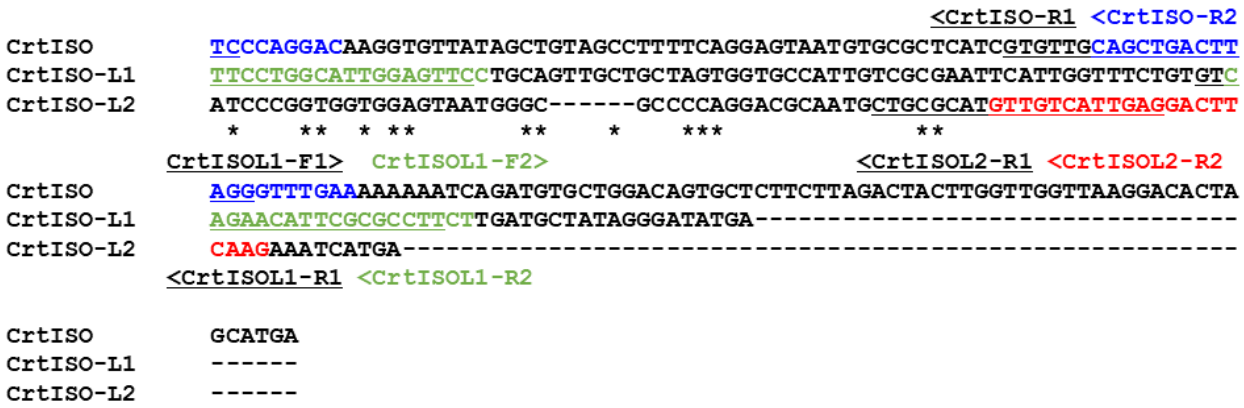

Figure S6. (continued)

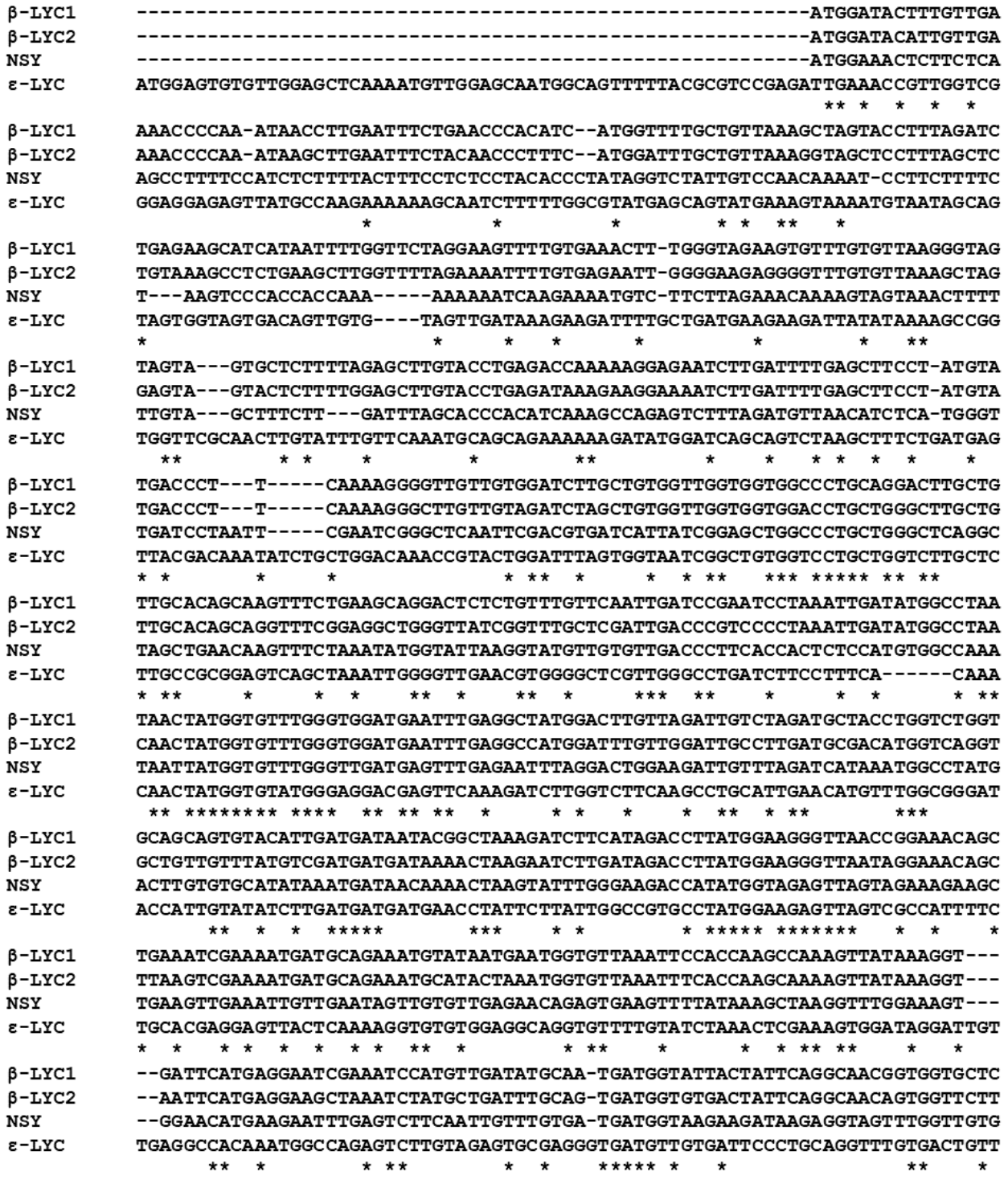

Figure S7. Alignment of the cDNA sequences of the tomato *β-LYC1*, *β-LYC2*, *ε-LCY* and *NSY* genes for real-time RT-PCR primer design.

Figure S7. (continued)

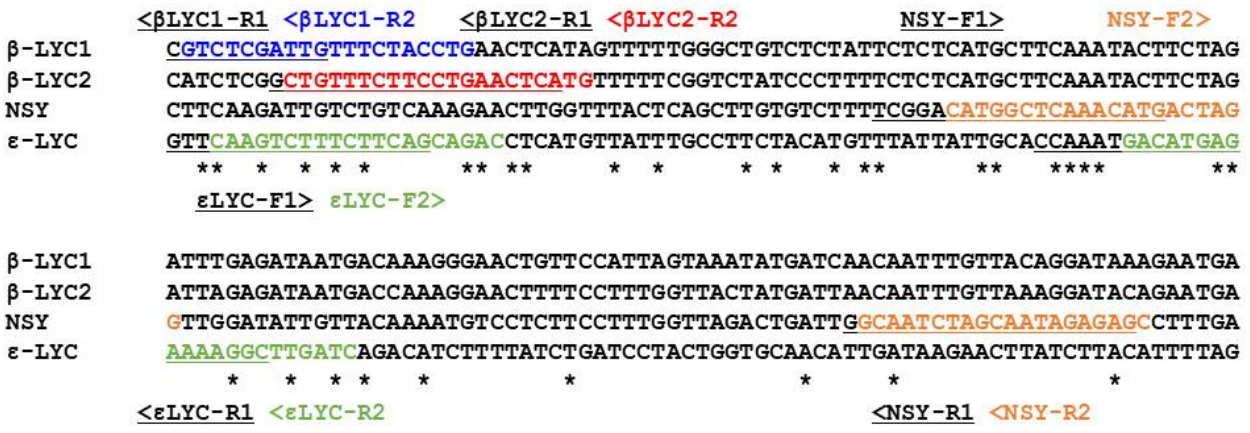

Figure S7. (continued)

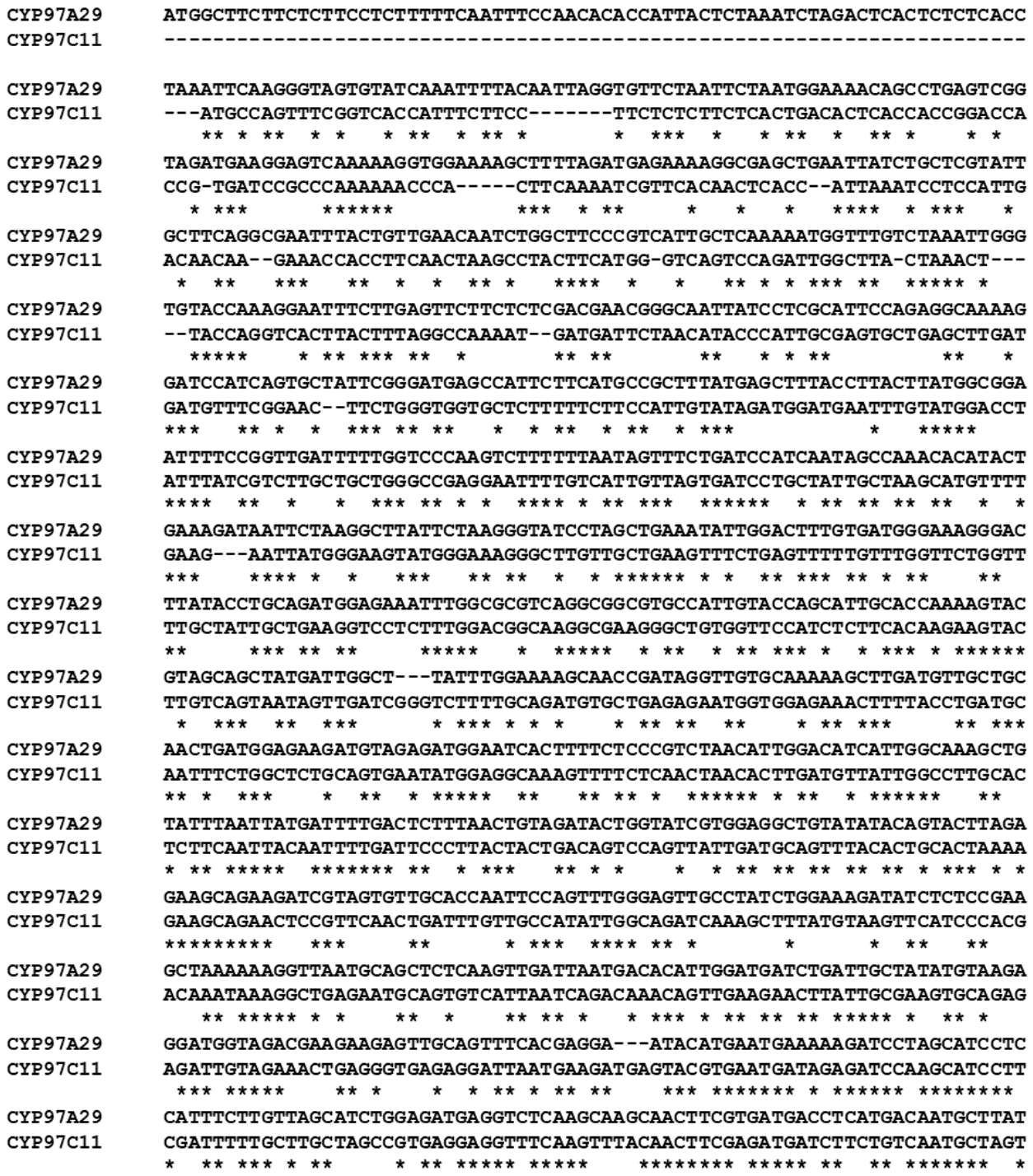

Figure S8. Alignment of the cDNA sequences of the tomato *CYP97A29* and *CYP97C11* genes for real-time RT-PCR primer design.

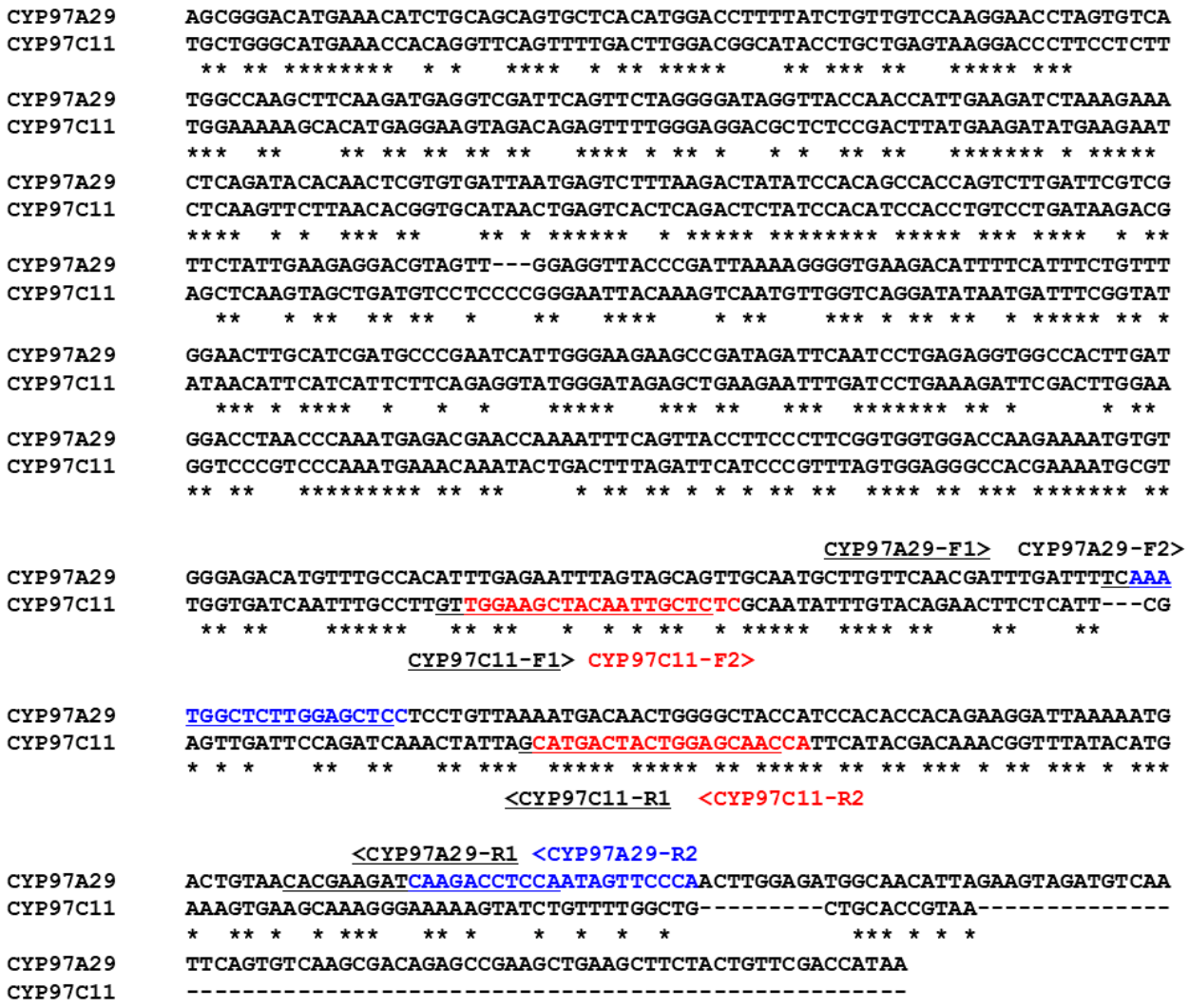

Figure S8. (continued)

Figure S9. Alignment of the cDNA sequences of the tomato *BCH1* and *BCH2* genes for real-time RT-PCR primer design.

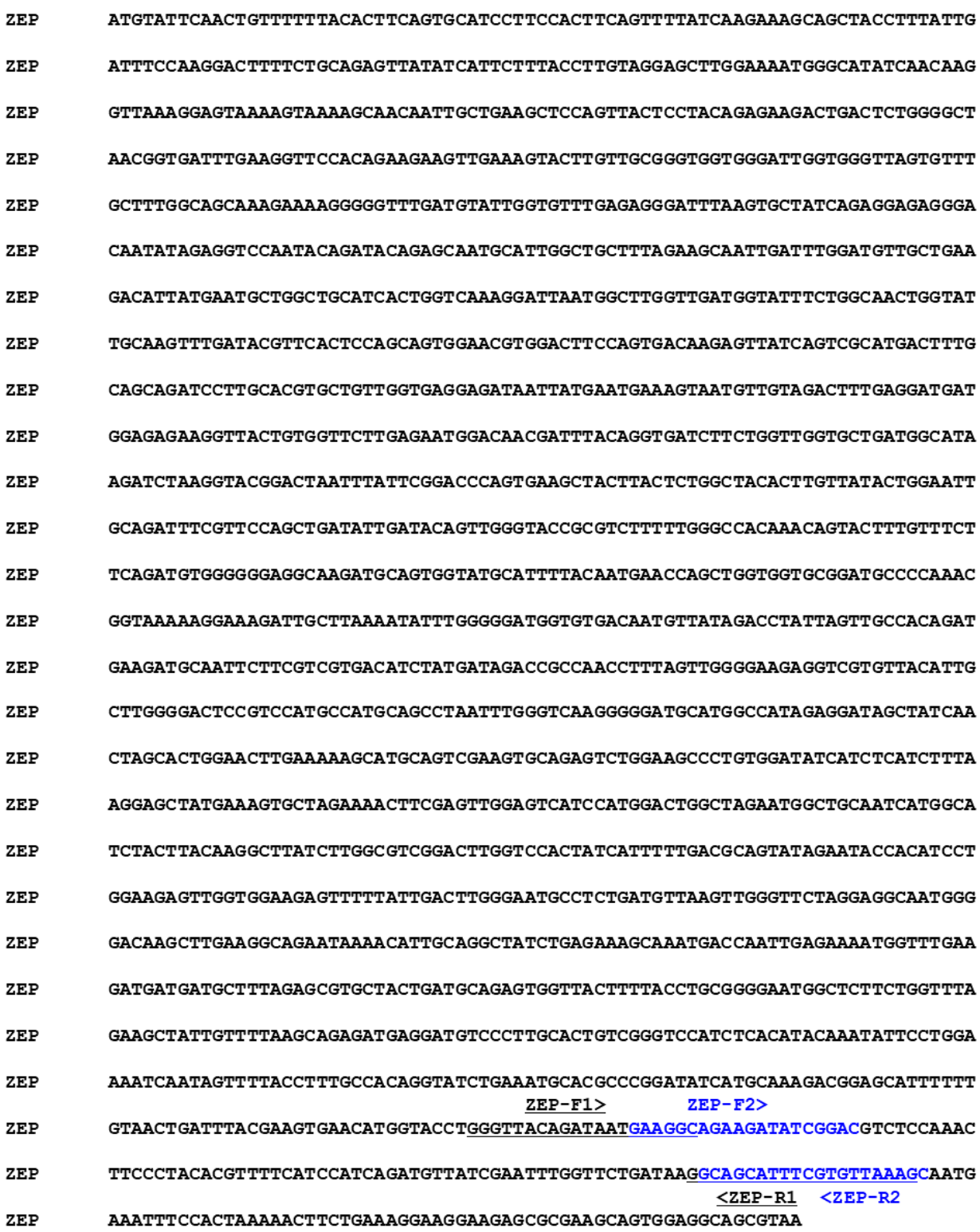

Figure S10. The cDNA sequence of the tomato *ZEP* gene for real-time RT-PCR primer design.

VDE ATGGCGCTTGCCCCTCATTCAAACATTCTGTGCAATCATGAGGCCATCAAATGTCAAGTTGGATCAAGGCTTCAG

VDE AGTCATACAAGATTTAGCTGGGGTAGAGCAGATTACTTTGGTAGTATAGTCCTAGTGAAAATTTGTTCCAGAAGA

VDE CAGATACCTACATACTTGCAGAAATCTTCTAGAATATGTTGTGGTTTGGATTCTAGAAGTCTGCAACTATCATCA

VDE CGGGGGAAACAAAATCTTTCTTCTGCACATAGAATTAACCAGAATGTACCTAAGGGAAATACAATATGGAAATTT

VDE CCAGAAGATGTAGCTTTGATGGTCTTGAAGAAATGGGGCCAATTGGCCAAAACAGCAATTGTAACTATATTTATT

VDE TTGTCAGTTGCTTCAAAGGCTGATGCCGTTGATGCTCTCAAAACTTGTACTTGCTTACTGAAAGAGTGCAGGATA

VDE GAGCTTGCGAAGTGCATCTCAAACCCTGCATGTGCAGCTAATGTTGCCTGTCTCCAAACATGCAACAATAGACCT

VDE GATGAAACGGAATGTCAGATAAAATGTGGTGATTTGTTTGAAAACAGTGTTGTAGACGAGTTCAATGAGTGTGCA

VDE GTCTCCCGGAAGAAATGTGTACCTCGTAAATCTGATGTTGGTGACTTTCCTGTGCCTGATCCCAGTGTTCTCGTC

VDE CAAAAGTTTGACATGAATGATTTTATTGGAAAATGGTACATCACTCGCGGTTTGAATCCCACATTTGATGTTTTT

VDE GATTGTCAATTGCATGAGTTCCATACAGAAGGAAACAAACTTGTGGGAAGTCTGACTTGGAGAATAGGGACACCT

VDE GATGGAGGATTTTTCACTCGATCCGCAGTGCAAAAATTCGTGCAAGATCCAAAGTATCCCGGGATACTCTACAAT

VDE CATGATAATGAGTATCTTCACTACCAAGATGACTGGTATATTTTGTCATCCAAAGTTGAAAACAGTCCAGATGAT

VDE TACATATTTGTGTACTATAAGGGCAGAAATGATGCATGGGATGGATATGGTGGTTCTGTACTTTATACTAGAAGC

VDE TCCGTTTTGCCTGAAACGATTATACCTGAGTTGCAAATTGCAGCTCAAAAAGTTGGTCGTGATTTCAACACTTTC

VDE ATAAAAACAGACAATACTTGTGGCCCTGAGCCACCCCTTGTTGAACGGTTAGAGAAGAAAGTGGAAGAAGGAGAG

VDE CGGACAATCATAAAAGAAGTCGAGGAAATAGAAGAAGAAGTCGAGAAGGTGAAGGAAAAAGAAGTCAGCTTATTC

VDE AGTAGACTGTTCGAAGGTTTCAAAGAGCTGCAACAAGATGAAGAAAACTTTATAAGAGAGCTCAGCAAAGAAGAA

VDE ATGGATATTTTGGATGGACTTAAAATGGAAGCAACTGAAGTAGAAAAACTCTTTGGAAATGCATTACCAATAAGG

VDE AAATTAAGGTAA

VDE-F1> VDE-F2>

<VDE-R1 <VDE-R2

Figure S11. The cDNA sequence of the tomato *VDE* gene for real-time RT-PCR primer design.

Figure S12. Alignment of the cDNA sequences of the tomato *Expressed (EXP)* gene and its homologous sequence for real-time RT-PCR primer design.

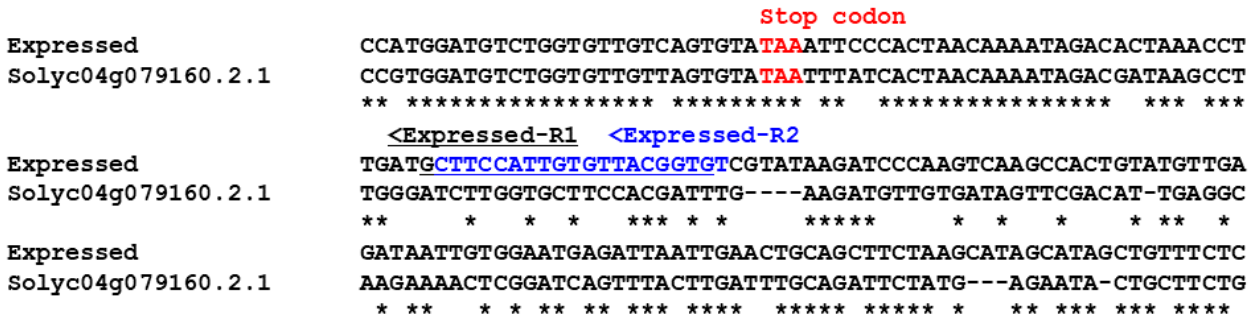

Figure S12. (continued)

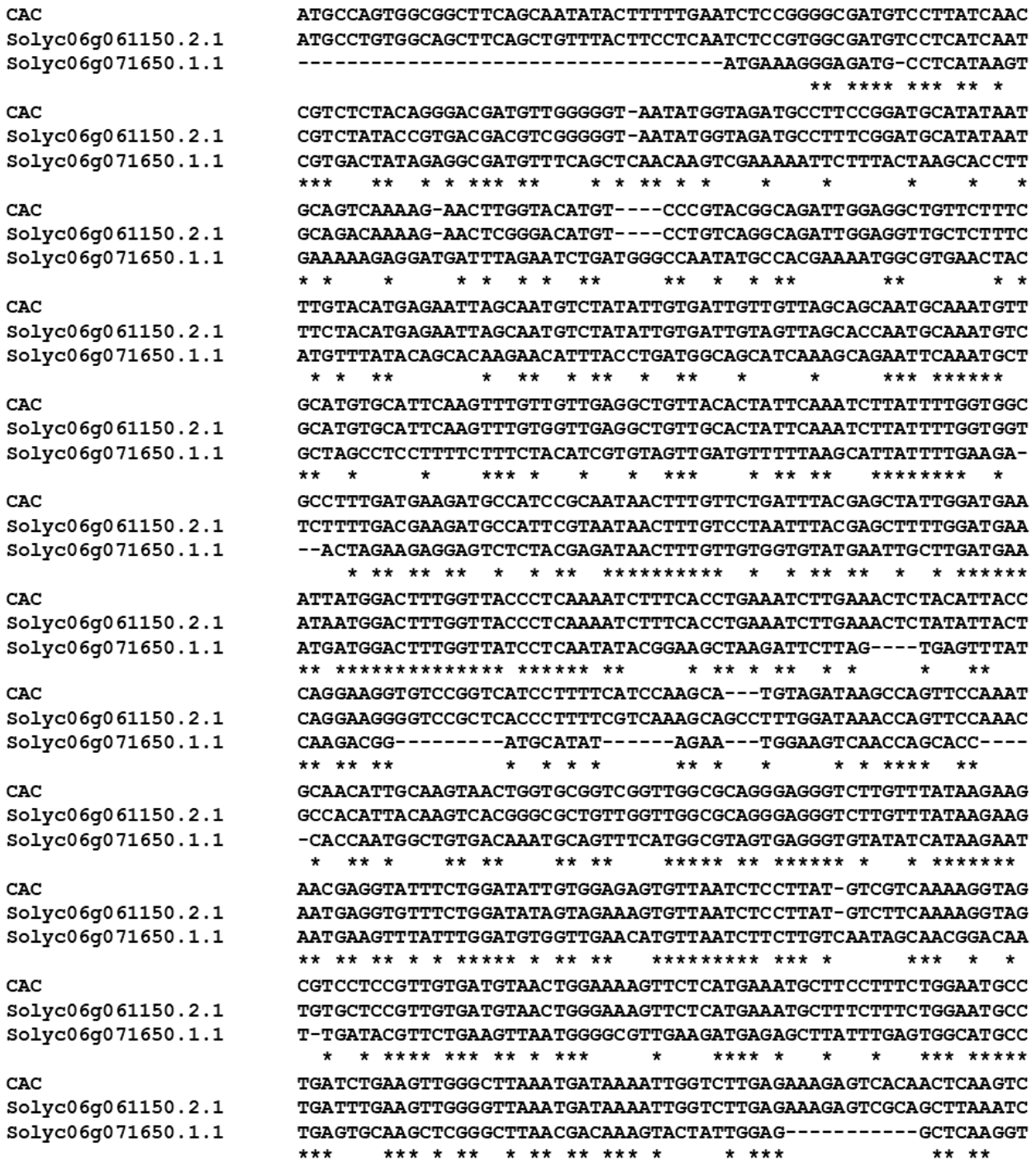

Figure S13. Alignment of the cDNA sequences of the tomato *CAC* gene and its homologous sequences for real-time RT-PCR primer design.

Figure S13. (continued)

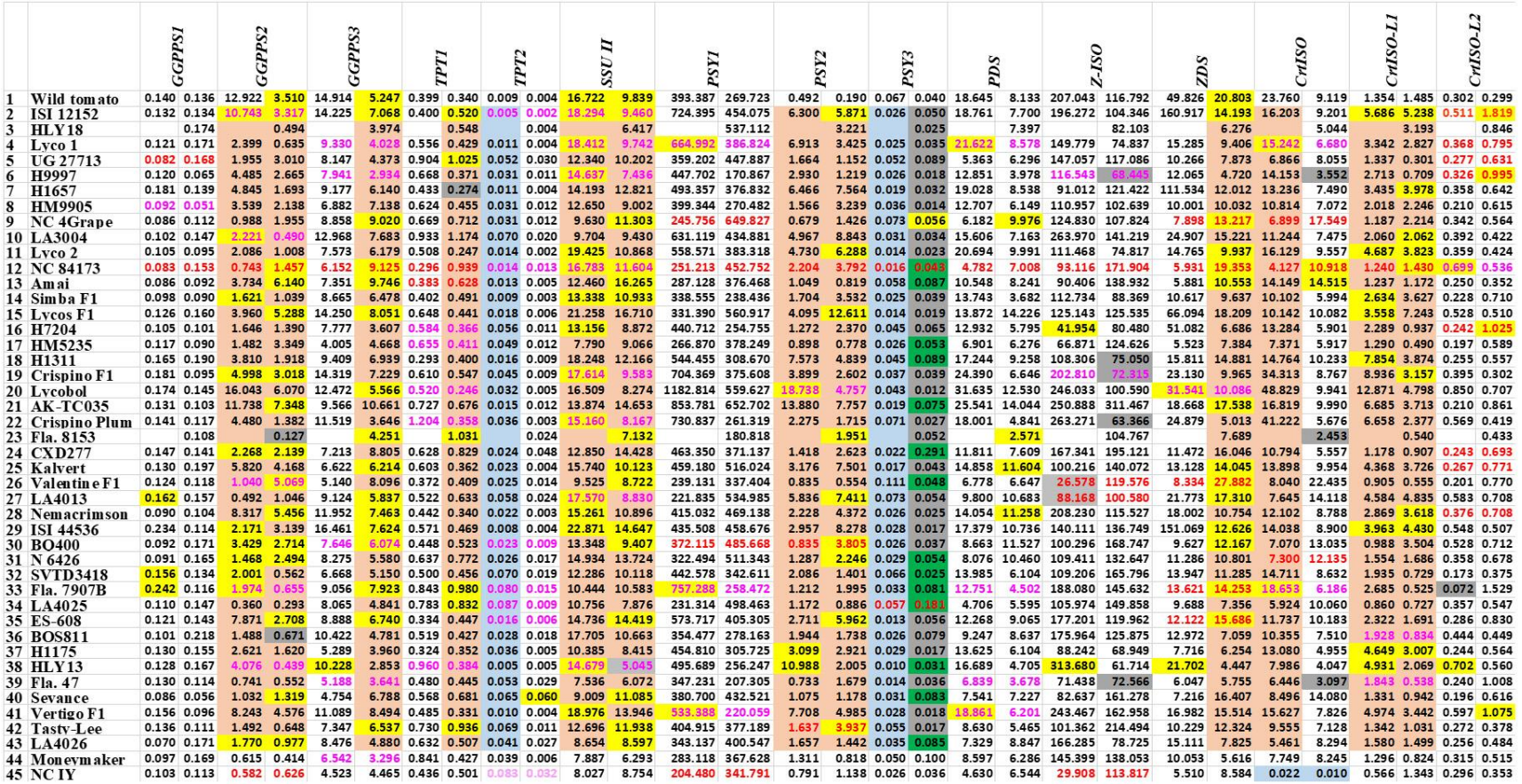

		GGPPS1		GGPPS2		GGPPS3		TPT1		TPT2		SSU II		PSY1		PSY2		PSY3		PDS		Z-ISO		ZDS		CrtISO		CrtISO-L1		CrtISO-L2	
1	Wild tomato	0.140	0.136	12.922	3.510	14.914	5.247	0.399	0.340	0.009	0.004	16.722	9.839	393.387	269.723	0.492	0.190	0.067	0.040	18.645	8.133	207.043	116.792	49.826	20.803	23.760	9.119	1.354	1.485	0.302	0.299
2	ISI 12152	0.132	0.134	10.743	3.317	14.225	7.068	0.400	0.520	0.005	0.002	18.294	9.460	724.395	454.075	6.300	5.871	0.026	0.050	18.761	7.700	196.272	104.346	160.917	14.193	16.203	9.201	5.686	5.238	0.511	1.819
3	HLY18		0.174		0.494		3.974		0.548		0.004		6.417		537.112		3.221		0.025		7.397		82.103		6.276		5.044		3.193		0.846
4	Lyco 1	0.121	0.171	2.399	0.635	9.330	4.028	0.556	0.429	0.011	0.004	18.412	9.742	664.992	386.824	6.913	3.425	0.025	0.035	21.622	8.578	149.779	74.837	15.285	9.406	15.242	6.680	3.342	2.827	0.368	0.795
5	UG 27713	0.082	0.168	1.955	3.010	8.147	4.373	0.904	1.025	0.052	0.030	12.340	10.202	359.202	447.887	1.664	1.152	0.052	0.089	5.363	6.296	147.057	117.086	10.266	7.873	6.866	8.055	1.337	0.301	0.277	0.631
6	H9997	0.120	0.065	4.485	2.665	7.941	2.934	0.668	0.371	0.031	0.011	14.637	7.436	447.702	170.867	2.930	1.219	0.026	0.018	12.851	3.978	116.543	68.445	12.065	4.720	14.153	3.552	2.713	0.709	0.326	0.995
7	H1657	0.181	0.139	4.845	1.693	9.177	6.140	0.433	0.274	0.011	0.004	14.193	12.821	493.357	376.832	6.466	7.564	0.019	0.032	19.028	8.538	91.012	121.422	111.534	12.012	13.236	7.490	3.435	3.978	0.358	0.642
8	HM9905	0.092	0.051	3.539	2.138	6.882	7.138	0.624	0.455	0.031	0.012	12.650	9.002	399.344	270.482	1.566	3.239	0.036	0.014	12.707	6.149	110.957	102.639	10.001	10.032	10.814	7.072	2.018	2.246	0.210	0.615
9	NC 4Grape	0.086	0.112	0.988	1.955	8.858	9.020	0.669	0.712	0.031	0.012	9.630	11.303	245.756	649.827	0.679	1.426	0.073	0.056	6.182	9.976	124.830	107.824	7.898	13.217	6.899	17.549	1.187	2.214	0.342	0.564
10	LA3004	0.102	0.147	2.221	0.490	12.968	7.683	0.933	1.174	0.070	0.020	9.704	9.430	631.119	434.881	4.967	8.843	0.031	0.034	15.606	7.163	263.970	141.219	24.907	15.221	11.244	7.475	2.060	2.062	0.392	0.422
11	Lyco 2	0.105	0.095	2.086	1.008	7.573	6.179	0.508	0.247	0.014	0.002	19.425	10.868	558.571	383.318	4.730	6.288	0.014	0.023	20.694	9.991	111.468	74.817	14.765	9.937	16.129	9.557	4.687	3.823	0.359	0.424
12	NC 84173	0.083	0.153	0.743	1.457	6.152	9.125	0.296	0.939	0.014	0.013	16.783	11.604	251.213	452.752	2.204	3.792	0.016	0.043	4.782	7.008	93.116	171.904	5.931	19.353	4.127	10.918	1.240	1.430	0.699	0.536
13	Amai	0.086	0.092	3.734	6.140	7.351	9.746	0.383	0.628	0.013	0.005	12.460	16.265	287.128	376.468	1.049	0.819	0.058	0.087	10.548	8.241	90.406	138.932	5.881	10.553	14.149	14.515	1.237	1.172	0.250	0.352
14	Simba F1	0.098	0.090	1.621	1.039	8.665	6.478	0.402	0.491	0.009	0.003	13.338	10.933	338.555	238.436	1.704	3.532	0.025	0.039	13.743	3.682	112.734	88.369	10.617	9.637	10.102	5.994	2.634	3.627	0.228	0.710
15	Lycos F1	0.126	0.160	3.960	5.288	14.250	8.051	0.648	0.441	0.018	0.006	21.258	16.710	331.390	560.917	4.095	12.611	0.014	0.019	13.872	14.226	125.143	125.535	66.094	18.209	10.142	10.082	3.558	7.243	0.528	0.510
16	H7204	0.105	0.101	1.646	1.390	7.777	3.607	0.584	0.366	0.056	0.011	13.156	8.872	440.712	254.755	1.272	2.370	0.045	0.065	12.932	5.795	41.954	80.480	51.082	6.686	13.284	5.901	2.289	0.937	0.242	1.025
17	HM5235	0.117	0.090	1.482	3.349	4.005	4.668	0.655	0.411	0.049	0.012	7.790	9.066	266.870	378.249	0.898	0.778	0.026	0.053	6.901	6.276	66.871	124.626	5.523	7.384	7.371	5.917	1.290	0.490	0.197	0.589
18	H1311	0.165	0.190	3.810	1.918	9.409	6.939	0.293	0.400	0.016	0.009	18.248	12.166	544.455	308.670	7.573	4.839	0.045	0.089	17.244	9.258	108.306	75.050	15.811	14.881	14.764	10.233	7.854	3.874	0.255	0.557
19	Crispino F1	0.181	0.095	4.998	3.018	14.319	7.229	0.610	0.547	0.045	0.009	17.614	9.583	704.369	375.608	3.899	2.602	0.037	0.039	24.390	6.646	202.810	72.315	23.130	9.965	34.313	8.767	8.936	3.157	0.395	0.302
20	Lycobol	0.174	0.145	16.043	6.070	12.472	5.566	0.520	0.246	0.032	0.005	16.509	8.274	1182.814	559.627	18.738	4.757	0.043	0.012	31.635	12.530	246.033	100.590	31.541	10.086	48.829	9.941	12.871	4.798	0.850	0.707
21	AK-TC035	0.131	0.103	11.738	7.348	9.566	10.661	0.727	0.676	0.015	0.012	13.874	14.653	853.781	652.702	13.880	7.757	0.019	0.075	25.541	14.044	250.888	311.467	18.668	17.538	16.819	9.990	6.685	3.713	0.210	0.861
22	Crispino Plum	0.141	0.117	4.480	1.382	11.519	3.646	1.204	0.358	0.036	0.003	15.160	8.167	730.837	261.319	2.275	1.715	0.071	0.027	18.001	4.841	263.271	63.366	24.879	5.013	41.222	5.676	6.658	2.377	0.569	0.419
23	Fla. 8153		0.108		0.127		4.251		1.031		0.024		7.132		180.818		1.951		0.052		2.571		104.767		7.689		2.453		0.540		0.433
24	CXD277	0.147	0.141	2.268	2.139	7.213	8.805	0.628	0.829	0.024	0.048	12.850	14.428	463.350	371.137	1.418	2.623	0.022	0.291	11.811	7.609	167.341	195.121	11.472	16.046	10.794	5.557	1.178	0.907	0.243	0.693
25	Kalvert	0.130	0.197	5.820	4.168	6.622	6.214	0.603	0.362	0.023	0.004	15.740	10.123	459.180	516.024	3.176	7.501	0.017	0.043	14.858	11.604	100.216	140.072	13.128	14.045	13.898	9.954	4.368	3.726	0.267	0.771
26	Valentine F1	0.124	0.118	1.040	5.069	5.140	8.096	0.372	0.409	0.025	0.014	9.525	8.722	239.131	337.404	0.835	0.554	0.111	0.048	6.778	6.647	26.578	119.576	8.334	27.882	8.040	22.435	0.905	0.555	0.201	0.770
27	LA4013	0.162	0.157	0.492	1.046	9.124	5.837	0.522	0.633	0.058	0.024	17.570	8.830	221.835	534.985	5.836	7.411	0.073	0.054	9.800	10.683	88.168	100.580	21.773	17.310	7.645	14.118	4.584	4.835	0.583	0.708
28	Nemacrimson	0.090	0.104	8.317	5.456	11.952	7.463	0.442	0.340	0.022	0.003	15.261	10.896	415.032	469.138	2.228	4.372	0.026	0.025	14.054	11.258	208.230	115.527	18.002	10.754	12.102	8.788	2.869	3.618	0.376	0.708
29	ISI 44536	0.234	0.114	2.171	3.139	16.461	7.624	0.571	0.469	0.008	0.004	22.871	14.647	435.508	458.676	2.957	8.278	0.028	0.017	17.379	10.736	140.111	136.749	151.069	12.626	14.038	8.900	3.963	4.430	0.548	0.507
30	BQ400	0.092	0.171	3.429	2.714	7.646	6.074	0.448	0.523	0.023	0.009	13.348	9.407	372.115	485.668	0.835	3.805	0.026	0.037	8.663	11.527	100.296	168.747	9.627	12.167	7.070	13.035	0.988	3.504	0.528	0.712
31	N 6426	0.091	0.165	1.468	2.494	8.275	5.580	0.637	0.772	0.026	0.017	14.934	13.724	322.494	511.343	1.287	2.246	0.029	0.054	8.076	10.460	109.411	132.647	11.286	10.801	7.300	12.135	1.554	1.686	0.358	0.678
32	SVTD3418	0.156	0.134	2.001	0.562	6.668	5.150	0.500	0.456	0.070	0.019	12.286	10.118	442.578	342.611	2.086	1.401	0.066	0.025	13.985	6.104	109.206	165.796	13.947	11.285	14.711	8.632	1.935	0.729	0.173	0.375
33	Fla. 7907B	0.242	0.116	1.974	0.655	9.056	7.923	0.843	0.980	0.080	0.015	10.444	10.583	757.288	258.472	1.212	1.995	0.033	0.081	12.751	4.502	188.080	145.632	13.621	14.253	18.653	6.186	2.685	0.525	0.072	1.529
34	LA4025	0.110	0.147	0.360	0.293	8.065	4.841	0.783	0.832	0.087	0.009	10.756	7.876	231.314	498.463	1.172	0.886	0.057	0.181	4.706	5.595	105.974	149.858	9.688	7.356	5.924	10.060	0.860	0.727	0.357	0.547
35	ES-608	0.121	0.143	7.871	2.708	8.888	6.740	0.334	0.447	0.016	0.006	14.736	14.419	573.717	405.305	2.711	5.962	0.013	0.056	12.268	9.065	177.201	119.962	12.122	15.686	11.737	10.183	2.322	1.691	0.286	0.830
36	BOS811	0.101	0.218	1.488	0.671	10.422	4.781	0.519	0.427	0.028	0.018	17.705	10.663	354.477	278.163	1.944	1.738	0.026	0.079	9.247	8.637	175.964	125.875	12.972	7.059	10.355	7.510	1.928	0.834	0.444	0.449
37	H1175	0.130	0.155	2.621	1.620	5.289	3.960	0.324	0.352	0.036	0.005	10.385	8.415	454.810	305.725	3.099	2.921	0.029	0.017	13.625	6.104	88.242	68.949	7.716	6.254	13.080	4.955	4.649	3.007	0.244	0.564
38	HLY13	0.128	0.167	4.076	0.439	10.228	2.853	0.960	0.384	0.005	0.005	14.679	5.045	495.689	256.247	10.988	2.005	0.010	0.031	16.689	4.705	313.680	61.714	21.702	4.447	7.986	4.047	4.931	2.069	0.702	0.560
39	Fla. 47	0.130	0.114	0.741	0.552	5.188	3.641	0.480	0.445	0.053	0.029	7.536	6.072	347.231	207.305	0.733	1.679	0.014	0.036	6.839	3.678	71.438	72.566	6.047	5.755	6.446	3.097	1.843	0.538	0.240	1.008
40	Sevance	0.086	0.056	1.032	1.319	4.754	6.788	0.568	0.681	0.065	0.060	9.009	11.085	380.700	432.521	1.075	1.178	0.031	0.083	7.541	7.227	82.637	161.278	7.216	16.407	8.496	14.080	1.331	0.942	0.196	0.616
41	Vertigo F1	0.156	0.096	8.243	4.576	11.089	8.494	0.485	0.331	0.010	0.004	18.976	13.946	533.388	220.059	7.708	4.985	0.028	0.018	18.861	6.201	243.467	162.958	16.982	15.514	15.627	7.826	4.974	3.442	0.597	1.075
42	Tasty-Lee	0.136	0.111	1.492	0.648	7.347	6.537	0.730	0.936	0.069	0.011	12.696	11.938	404.915	377.189	1.637	3.937	0.055	0.017	8.630	5.465	101.362	214.494	10.229	12.324	9.555	7.128	1.342	1.031	0.272	0.378
43	LA4026	0.070	0.171	1.770	0.977	8.476	4.880	0.632	0.507	0.041	0.027	8.654	8.597	343.137	400.547	1.657	1.442	0.035	0.085	7.329	8.847	166.285	78.725	15.111	7.825	5.461	8.294	1.580	1.499	0.256	0.484
44	Moneymaker	0.097	0.169	0.615	0.414	6.542	3.296	0.841	0.427	0.039	0.006	7.887	6.293	283.118	367.628	1.311	0.818	0.050	0.100	8.597	6.286	145.399	138.053	10.053	5.616	7.749	8.245	1.296	0.824	0.315	0.515
45	NC IY	0.103	0.113	0.582	0.626	4.523	4.465	0.436	0.501	0.083	0.032	8.027	8.754	204.480	341.791	0.791	1.138	0.026	0.036	4.630	6.544	29.908	113.817	5.510	8.584	0.022	0.010	0.566	1.343	0.296	0.353

Figure S14. The relative expression levels of the upstream genes before lycopene biosynthesis in the carotenoid biosynthesis pathway in the 42 tomato cultigens measured by real-time RT-PCR. The left and right columns of each gene represent the relative expression levels of that gene in the breaker and ripe stages, respectively. Orange, the genes had significantly higher relative expression levels in the 42 cultigens at each stage as a group than that in Moneymaker at that stage.

Figure S14. (continued) Green, the gene had significantly lower relative expression levels in the 42 cultigens at each stage as a group (i.e., *PSY3* at the ripe stage) than that in Moneymaker at that stage. Light blue, the genes had insignificantly different relative expression levels in the 42 cultigens at each stage as a group when compared to the non-functional *crtiso* in NC 1Y. Yellow, the genes had significantly higher relative expression levels in individual cultigens at each stage than that in Moneymaker at that stage. Grey, the genes had significantly lower relative expression levels in individual cultigens at each stage than that in Moneymaker at that stage. Pink, the genes had significantly lower relative expression levels in the ripe stage than in the breaker stage of the same cultigens. Red, the genes had significantly higher relative expression levels in the ripe stage than in the breaker stage of the same cultigens.

		β-LYC1		β-LYC2		BCH1		BCH2		ZEP		VDE		NSY		ε-LYC		CYP97A29		CYP97C11	
1	Wild tomato	0.018	0.004	0.009	0.002	0.284	0.157	0.010	0.013	0.825	0.156	0.101	0.042	0.120	0.064	0.007	0.005	0.476	0.231	0.489	0.208
2	ISI 12152	0.116	0.024	0.011	0.001	2.605	2.439	0.061	0.029	0.954	1.143	6.119	4.071	0.052	0.025	0.161	0.005	0.836	0.513	2.987	0.961
3	HLY18		0.038		0.005		1.296		0.019		1.489		2.473		0.013		0.002		0.308		0.903
4	Lyco 1	0.042	0.047	0.004	0.003	3.245	1.259	0.091	0.025	0.603	1.393	5.360	1.993	0.022	0.012	0.033	0.006	1.092	0.293	1.909	0.843
5	UG 27713	0.020	0.019	0.009	0.013	0.292	0.359	0.034	0.038	0.891	0.498	0.548	0.112	0.060	0.139	0.030	0.008	0.320	0.177	1.150	0.319
6	H9997	0.093	0.035	0.041	0.010	0.556	1.656	0.069	0.088	1.107	0.704	1.916	0.748	0.069	0.020	0.149	0.003	0.402	0.231	1.695	0.397
7	H1657	0.061	0.113	0.005	0.014	1.146	0.964	0.059	0.022	1.391	2.011	2.961	2.294	0.016	0.011	0.094	0.012	0.593	0.288	1.868	1.113
8	HM9905	0.019	0.101	0.020	0.005	0.645	1.061	0.049	0.043	1.035	1.568	1.383	1.707	0.090	0.036	0.050	0.004	0.428	0.213	0.924	0.466
9	NC 4Grape	0.033	0.067	0.009	0.007	0.509	3.062	0.038	0.076	1.009	0.976	0.502	0.380	0.111	0.084	0.006	0.004	0.367	0.482	1.027	0.550
10	LA3004	0.045	0.062	0.016	0.003	1.947	1.505	0.069	0.036	0.863	0.448	4.046	3.663	0.127	0.111	0.082	0.006	0.633	0.260	1.368	1.565
11	Lyco 2	0.202	0.080	0.013	0.001	2.406	3.020	0.102	0.037	1.941	1.238	3.933	2.314	0.046	0.011	0.030	0.011	1.022	0.480	1.573	0.762
12	NC 84173	0.012	0.067	0.003	0.004	0.269	1.610	0.009	0.050	0.690	1.109	0.654	0.453	0.051	0.152	0.059	0.019	0.346	0.254	1.053	0.975
13	Amai	0.083	0.062	0.025	0.006	0.951	1.730	0.034	0.042	0.780	0.302	0.169	0.162	0.079	0.167	0.108	0.036	0.310	0.374	0.829	0.587
14	Simba F1	0.079	0.059	0.011	0.006	0.006	0.001	0.053	0.026	0.649	0.520	2.393	2.209	0.030	0.035	0.016	0.002	0.770	0.487	1.587	0.977
15	Lycos F1	0.260	0.073	0.046	0.003	0.759	3.365	0.024	0.032	2.098	0.953	3.241	4.769	0.089	0.026	0.301	0.043	0.628	0.508	5.064	1.756
16	H7204	0.052	0.023	0.015	0.014	0.400	0.889	0.042	0.058	1.689	0.646	0.962	0.641	0.056	0.034	0.075	0.003	0.382	0.196	1.134	0.499
17	HM5235	0.030	0.058	0.027	0.004	0.342	1.313	0.017	0.039	0.767	0.418	0.541	0.814	0.045	0.029	0.032	0.002	0.235	0.256	0.575	0.229
18	H1311	0.105	0.321	0.031	0.008	1.363	0.800	0.046	0.017	0.745	2.337	7.040	2.852	0.021	0.037	0.381	0.031	0.892	0.310	2.682	1.227
19	Crispino F1	0.107	0.140	0.042	0.001	3.293	0.001	0.151	0.070	0.750	0.676	3.878	1.169	0.064	0.032	0.052	0.002	1.012	0.304	2.450	0.934
20	Lycobol	0.043	0.079	0.004	0.003	5.548	2.419	0.198	0.077	0.954	1.602	5.380	1.820	0.040	0.010	0.076	0.003	1.592	0.576	2.717	0.750
21	AK-TC035	0.051	0.165	0.003	0.015	2.151	1.947	0.076	0.110	0.558	1.427	4.702	4.569	0.021	0.029	0.078	0.014	0.790	0.688	1.943	1.384
22	Crispino	0.182	0.087	0.022	0.013	3.042	2.066	0.459	0.054	0.712	0.493	1.717	0.857	0.106	0.017	0.054	0.002	0.773	0.238	1.340	0.354
23	Fla. 8153		0.023		0.003		0.836		0.022		0.477		0.364		0.055		0.005		0.110		0.302
24	CXD277	0.011	0.237	0.004	0.027	0.294	0.581	0.038	0.050	0.997	1.003	0.758	1.338	0.025	0.111	0.026	0.008	0.309	0.328	0.882	0.875
25	Kalvert	0.113	0.052	0.005	0.002	1.005	2.886	0.060	0.040	1.625	0.858	2.587	4.023	0.208	0.031	0.053	0.053	0.488	0.427	1.703	1.828
26	Valentine F1	0.028	0.123	0.008	0.008	0.393	1.475	0.018	0.113	0.583	0.455	0.299	0.167	0.062	0.119	0.008	0.001	0.272	0.557	0.651	0.323
27	LA4013	0.237	0.097	0.119	0.007	1.574	6.111	0.020	0.048	3.834	1.902	4.063	4.545	0.166	0.081	0.042	0.002	0.485	0.610	3.592	1.945
28	Nemacrimso	0.021	0.033	0.006	0.002	0.527	1.996	0.061	0.058	1.280	0.849	1.345	1.896	0.060	0.021	0.020	0.005	0.385	0.227	1.514	0.603
29	ISI 44536	0.133	0.038	0.014	0.002	0.462	0.901	0.041	0.028	1.316	0.382	3.894	4.050	0.055	0.021	0.730	0.043	0.802	0.524	3.752	1.987
30	BO400	0.008	0.032	0.003	0.005	0.314	1.242	0.052	0.049	0.839	0.861	0.660	1.299	0.105	0.093	0.047	0.013	0.397	0.449	0.816	0.687
31	N 6426	0.016	0.104	0.006	0.004	0.238	0.697	0.025	0.053	1.000	2.066	0.898	0.772	0.080	0.072	0.047	0.005	0.384	0.352	1.300	1.073
32	SVTD3418	0.021	0.069	0.015	0.003	1.597	0.763	0.062	0.021	0.840	1.297	1.565	0.326	0.099	0.069	0.048	0.003	0.350	0.099	0.600	0.559
33	Fla. 7907B	0.011	0.015	0.009	0.006	1.124	1.316	0.034	0.025	0.403	1.386	1.706	0.174	0.043	0.036	0.020	0.005	0.603	0.145	0.607	0.370
34	LA4025	0.071	0.019	0.029	0.002	0.489	1.774	0.013	0.033	1.060	0.474	0.508	0.467	0.162	0.033	0.043	0.001	0.260	0.135	1.288	0.267
35	ES-608	0.049	0.267	0.004	0.010	1.147	1.277	0.038	0.013	0.651	1.327	3.059	1.712	0.039	0.054	0.084	0.009	0.486	0.112	1.686	0.850
36	BOS811	0.047	0.068	0.013	0.028	0.238	0.237	0.024	0.022	1.378	1.276	0.552	0.439	0.109	0.064	0.016	0.003	0.400	0.179	1.382	0.389
37	H1175	0.020	0.047	0.028	0.005	0.952	1.252	0.026	0.035	0.987	0.936	1.959	1.557	0.020	0.013	0.038	0.029	0.403	0.271	1.090	0.894
38	HLY13	0.050	0.034	0.000	0.007	0.005	0.830	0.025	0.010	1.512	1.125	8.610	1.956	0.021	0.011	0.083	0.011	0.712	0.190	2.095	0.574
39	Fla. 47	0.008	0.033	0.008	0.003	0.750	1.646	0.018	0.051	0.557	1.011	1.359	0.347	0.113	0.086	0.040	0.001	0.290	0.166	0.774	0.324
40	Sevance	0.041	0.124	0.005	0.017	0.851	1.109	0.027	0.064	1.220	0.650	0.820	0.721	0.128	0.140	0.011	0.001	0.246	0.272	0.890	0.344
41	Vertigo F1	0.057	0.016	0.007	0.001	1.144	1.196	0.049	0.027	1.543	1.593	3.198	2.608	0.148	0.074	0.104	0.023	0.756	0.582	2.141	1.433
42	Tasty-Lee	0.018	0.028	0.016	0.005	0.877	2.072	0.030	0.021	1.382	0.335	1.471	1.186	0.053	0.035	0.062	0.005	0.367	0.138	0.711	0.304
43	LA4026	0.034	0.056	0.004	0.008	0.750	1.446	0.056	0.044	0.688	1.831	1.043	0.410	0.060	0.055	0.006	0.001	0.258	0.213	0.190	0.253
44	Moneymaker	0.041	0.024	0.008	0.002	0.542	1.680	0.018	0.023	0.702	0.729	0.800	0.325	0.247	0.142	0.051	0.004	0.195	0.128	1.115	0.542
45	NC 1Y	0.045	0.062	0.042	0.001	0.335	1.462	0.018	0.048	0.533	1.108	0.465	0.460	0.102	0.085	0.028	0.001	0.304	0.176	0.754	0.488

Figure S15. The relative expression levels of the downstream genes after lycopene biosynthesis in the carotenoid biosynthesis pathway in the 42 tomato cultigens measured by real-time RT-PCR. The left and right columns of each gene represent the relative expression levels of that gene in the breaker and ripe stages, respectively. Blue, the genes had significantly higher relative expression levels in the 42 cultigens at each stage as a group than that in the wild tomato at that stage. Light blue, the genes had insignificantly different relative expression levels in the 42 cultigens at each stage as a group when compared to the non-functional *crtiso* in NC 1Y.

Figure S15. (continued) Yellow, the genes had significantly higher relative expression levels in individual cultigens at each stage than that in the wild tomato at that stage. Grey, the genes had significantly lower relative expression levels in individual cultigens at each stage than that in in the wild tomato at that stage. Pink, the genes had significantly lower relative expression levels in the ripe stage than in the breaker stage of the same cultigens. Red, the genes had significantly higher relative expression levels in the ripe stage than in the breaker stage of the same cultigens.

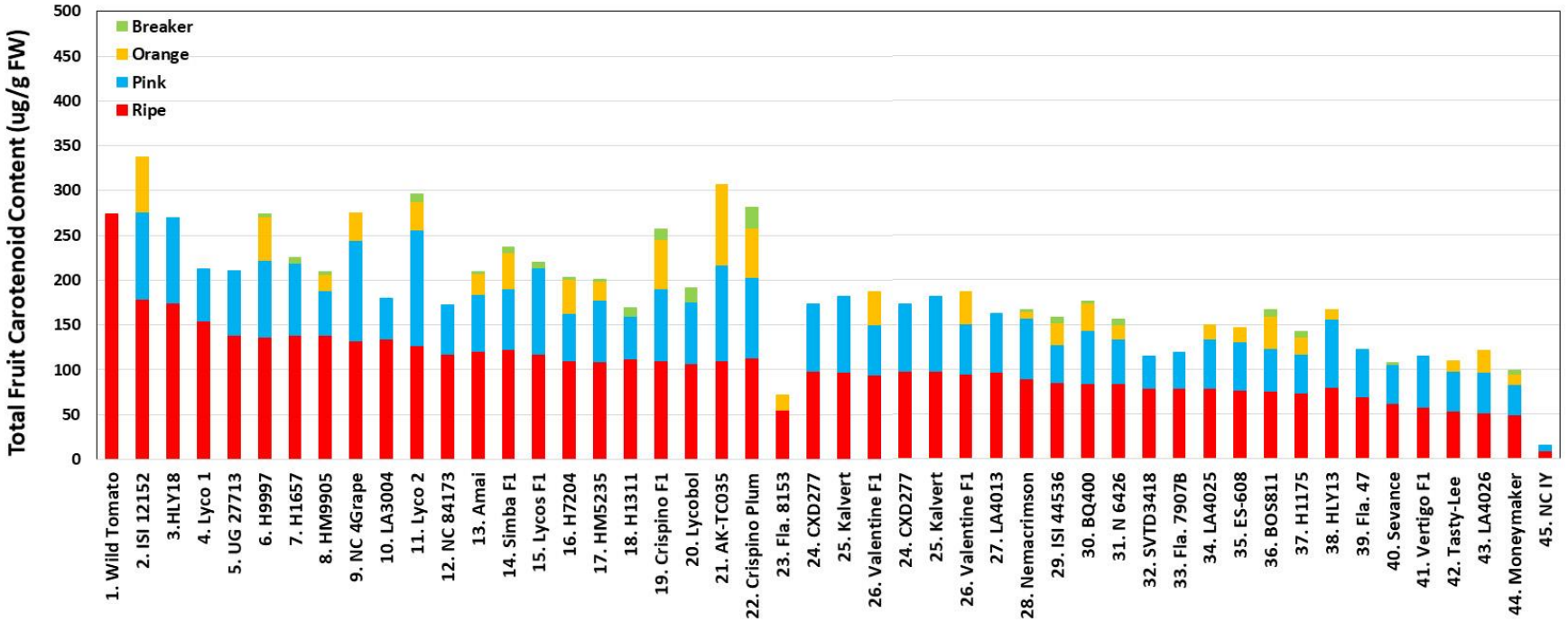

Figure S16. Total fruit carotenoid (phytofluene, lycopene and beta-carotene) contents in the 42 tomato cultigens at the fruit developmental stages of breaker, orange, pink and ripe. The wild tomato (LA 2093) was used as the positive control, and Moneymaker and NC 1Y were used as the negative controls. All of the cultigens were grown under the same greenhouse conditions at the same time, and HPLC was used to quantify fruit phytofluene, lycopene and beta-carotene contents in pericarp tissues. FW, fresh weight